Odor Coding and Memory Traces in the Antennal Lobe of Honeybee

Computational Studies of Neural Dynamics
based on Calcium-Imaging Data

D I S S E R T A T I O N

zur Erlangung des akademischen Grades
doctor rerum naturalium
(Dr. rer. nat.)
im Fach Biophysik

eingereicht an der
Mathematisch-Naturwissenschaftlichen Fakultät I
Humboldt-Universität zu Berlin

von
Herrn Dipl.-Phys. Roberto Fernández Galán
geboren am 26. März 1975 in Madrid

Präsident der Humboldt-Universität zu Berlin:
Prof. Dr. Jürgen Mlynek

Dekan der Mathematisch-Naturwissenschaftlichen Fakultät I:
Prof. Dr. Michael Linscheid

Gutachter:

1. Prof. Dr. Andreas V.M. Herz
2. Prof. Dr. Hanspeter Herzel
3. Prof. Dr. Klaus Obermayer

eingereicht am: 6. Oktober 2003
Tag der mündlichen Prüfung: 17. Dezember 2003

Für Elke,

Todo hombre puede ser, si se lo propone, escultor de su propio cerebro.

Santiago Ramón y Cajal

Contents

List of Figures

Chapter 1

Introduction

1.1 On the questions addressed in this work

Although a full understanding of brain function is still far from being achieved, remarkable headway has been made on specific outstanding questions by combining the approaches of different disciplines. This work focuses on two of those questions:

- how external stimuli are transformed into neural activity (sensory coding), and

- how this information is transiently stored for posterior retrieval (sensory memory).

Our investigations are based on the olfactory system of the honeybee. The striking similarities of the olfactory system across different species suggest that universal computational strategies are used to encode, process and store chemosensory information. We analyze the neural dynamics in this system with calcium-imaging data recorded by Dr. Silke Sachse and Dipl.-Biol. Marcel Weidert at the Institute of Neurobiology of the Free University in Berlin.

1.1.1 On odor coding

Two major matters of controversy in neuroscience are: i) whether neurons use single spikes or the average firing rate of a spike train to encode and transmit information; ii) whether a single neuron or a neural population constitutes the functional encoding unit. The final answers to these questions probably depend on the system under study and also on the approach used to analyze neural responses.

In the second chapter of this thesis we demonstrate how neural-population dynamics in a firing-rate time-scale can encode odor-infomation in a quite simple manner. This contrasts with the complexity of other hypotheses about odor-coding that rely on faster events of the neural dynamics. In addition, we show how a perceptron-based decoder can explain several features of odor recognition like odor discriminability, existence of minimal reaction times and concentration invariances of odor perception.

1.1.2 On memory traces

Great effort has been devoted in the last few decades to find physiological correlates of memory. Most of this work has been inspired by the hypothesis on memory formation of the psychologist Donald Hebb [Hebb, 1949]: that neurons encoding a given stimulus "reverberate" after stimulation and that this reverberation leads to the reinforcement of their connections, thereby consolidating a memory of the stimulus.

Two major experimental findings have supported so far the Hebbian hypothesis (see short review in [Seung, 2000]): i) the existence of persistent activity after stimulation (delay activity) in the prefontal cortex of monkeys during experiments on working memory (originally reported in [Fuster and Alexander, 1971] and [Kubota and Niki, 1971]); ii) the discovery of synaptic long-term potentiation through sustained electrical stimulation of connected neurons (firstly observed by [Bliss and Lomo, 1973] in hippocampal slices).

Most of the work focused on synapses generally involves two neurons. The experiments in the prefontal cortex involve a single, or at most a few, neurons. In the third chapter of this thesis, we provide the first experimental evidence to our knowledge, that a Hebbian mechanism occurs at the network level: we show that the neural units that respond to a given stimulus (odor) change their pairwise correlations. By analyzing the change of correlation across the network, we can retrieve the last stimulus presented.

1.2 Olfaction in neuroscience

1.2.1 The olfactory system as a prototype neural network

The design of the olfactory system is similar across several phyla even when they lack a recent common ancestor, like mammals and insects. This convergence suggests that different species evolved analogous mechanisms to

acquire, encode and process chemosensory information (see, e.g., review by [Hildebrand and Shepherd, 1997]). The study of these mechanisms therefore provides insight into widespread strategies of neural computation.

Common design features are found at each level of organization, from molecules to network modules (see also [Eisthen, 2002]):

- Odor-binding proteins: The mucus and lymph overlying the sensory epithelium of vertebrates and the sensillum of insects contain specialized proteins that bind odor molecules (Fig. 1.1). The proteins are not tied to receptor neurons but are freely dissolved in the mucus or lymph and have a narrow odor affinity. Odor-binding proteins have been found in mammals and insects but not in fish and amphibia. This suggests that mammals and insects independently developed the same strategy to capture odor molecules from the air and transport them through the fluid mucus or lymph to the receptors.

- Odor receptors: Odor receptors are proteins located at the membrane of the receptor neurons (Fig. 1.1) with seven membrane-spanning domains. All odor receptors found belong to the large family of G-protein-coupled receptors. Odor-receptor genes have been identified in more than 20 mammalian species and also in birds, fish, amphibians, lampreys, Drosophila and C. Elegans. Odor molecules couple to the receptors in a lock and key fashion. Receptors of the same type specialize in detecting a given molecular feature called odotope, which is not yet fully determined. It has been proposed that this feature is a band in the inelastic-tunneling spectrum [Turin, 1996]: The receptor protein in combination with an electron donor (NADPH) can be physically described as a two-level system with an energy gap within the spectral range of inelastic-tunneling (from infrared to microwaves). If the odor molecule has a vibration mode with dipolar energy similar to the gap, it will transfer energy to the electrons of the receptor protein inducing the reduction of the disulfide bridge between the receptor protein and the G-protein. For interesting predictions of this model on the odor character of molecules and their mixtures, see [Turin, 2002].

- Signal transduction: Odor binding causes an increase of cAMP (or of IP_3, or of both, depending on the species) in the cytosol of the receptor neuron via activation of the G-protein. This increase opens cation channels permeable mainly to calcium. The incoming calcium in turn depolarizes the cell and gates calcium-dependent chloride channels. Following a concentration gradient, the chloride ions flow outwards depolarizing the cell beyond firing threshold. (Fig. 1.1).
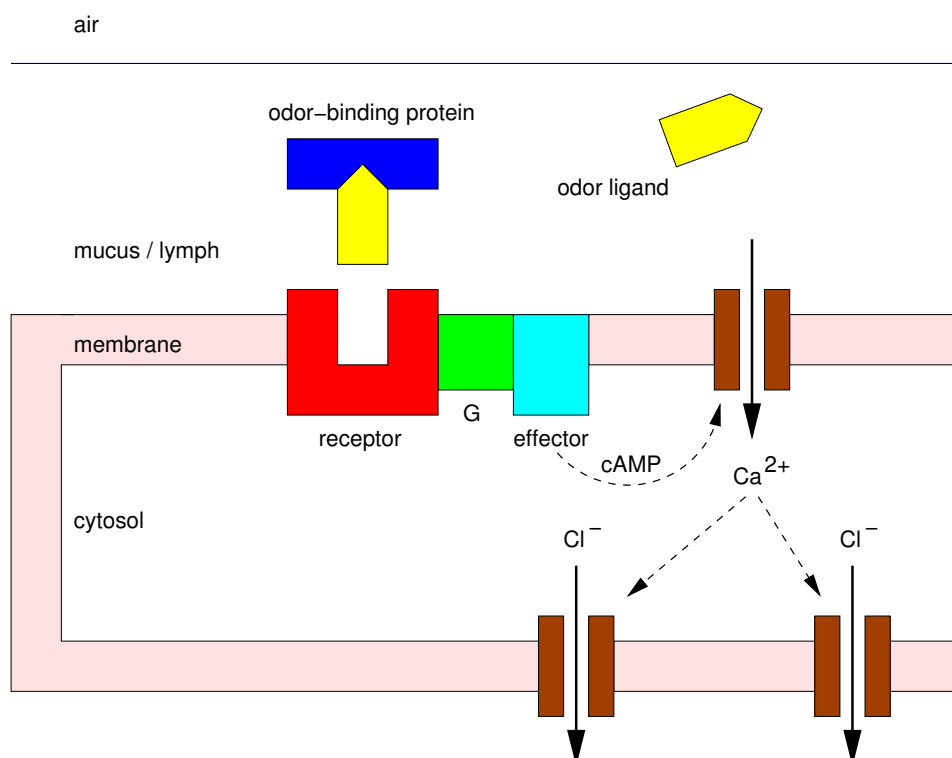
Figure 1.1: Odor transduction: The odor binding-proteins diffused in the mucus (vertebrates) or lymph (invertebrates) capture the odor molecules and transport them to the receptors. Odor locking activates the associated G-protein, stimulating an effector (adenylyl cyclase or phospholipase C). This leads to an increase of cAMP (or of IP_3, or of both, depending on the animal) in the cytosol of the receptor neuron. The increase induces calcium inflow, which in turn gates calcium-dependent chloride channels. The outwards flow of chloride ions depolarizes the receptor neuron beyond the firing threshold.

- Glomerular structures in the primary network of the olfactory pathway: Receptor neurons relay information into a network (olfactory bulb in vertebrates/antennal lobe in invertebrates) of excitatory and inhibitory neurons. The dendrites of these neurons are arranged into clusters called glomeruli (Fig. 1.2). The glomeruli, discovered by Ramón y Cajal in mammals [Ramón y Cajal, 1890], are more than anatomical structures: They are functional units, as a given odor activates a specific set of glomeruli (see e.g. [Korsching, 2002]). The output neurons of the glomeruli project onto multimodal higher processing areas.
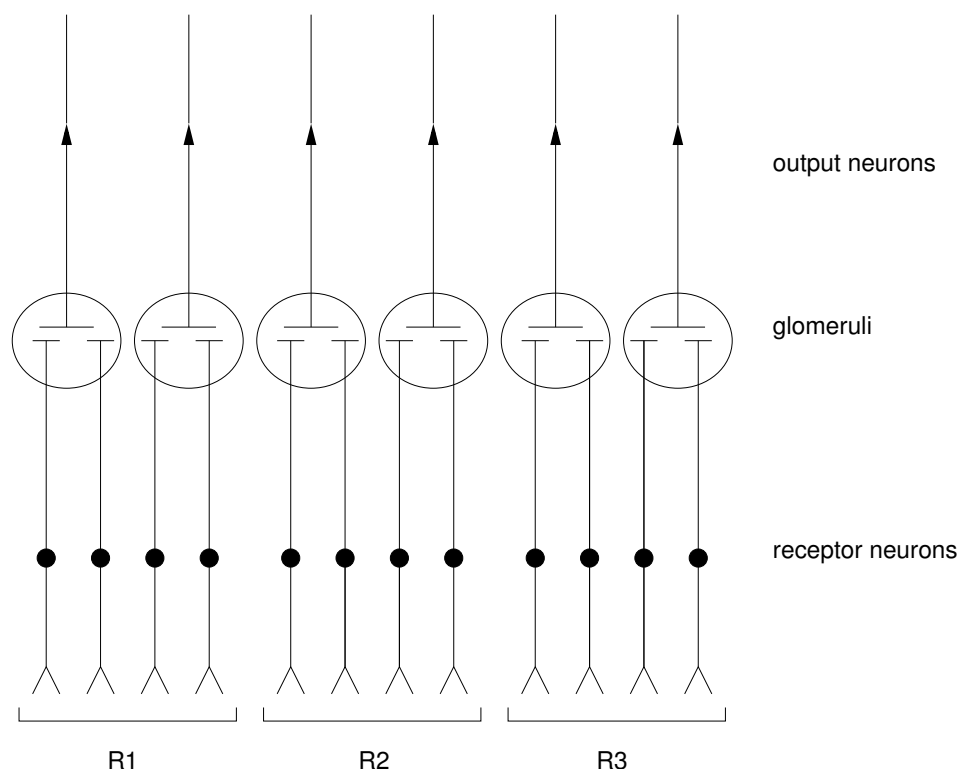
Figure 1.2: Primary Structures of the Olfactory System. Each receptor neuron contains only one receptor-protein type (R). Receptor neurons possessing the same receptor type converge to the same glomeruli. So far there is no evidence of a glomerulus receiving input from receptor neurons with different receptor types (counter-examples are being sought in Drosophila with the tools of molecular genetics that made possible to show receptor-type convergence [Gao et al., 2000]). The receptor neurons transmit odor information into a network (olfactory bulb in vertebrates and antennal lobe in insects) of excitatory and inhibitory neurons (not drawn) whose dendrites are packed forming clusters (glomeruli). The output neurons of the glomeruli (mitral cells in vertebrates/projection neurons in insects) relay information to higher processing areas.

- Modular Analogy: The modular structure of the olfactory system also shows remarkable similarities in animals as disparate as insects and mammals. The analogy is functional rather than anatomical, as the olfactory system of mammals contains more neural layers. Beyond the antennal lobe/olfactory bulb, views on the correspondence between

network modules in insects and mammals have changed over time (see [Strausfeld et al., 1998]). Early work on the mushroom body (Fig. 1.3) proposed this neural network as the place of the insects' "intelligence" [Dujardin, 1850]; it would therefore correspond to the mammalian cortex. More recent findings, however, showed that the mushroom body integrates sensory information and is necessary for learning and memory as well as for spatial orientation (see e.g. [Heisenberg, 1998]), therefore corresponding to the mammalian hippocampus. The analog of the mammalian cortex is the lateral protocerebrum (Fig. 1.3), a diffuse network receiving processed sensory input and steering motor output.
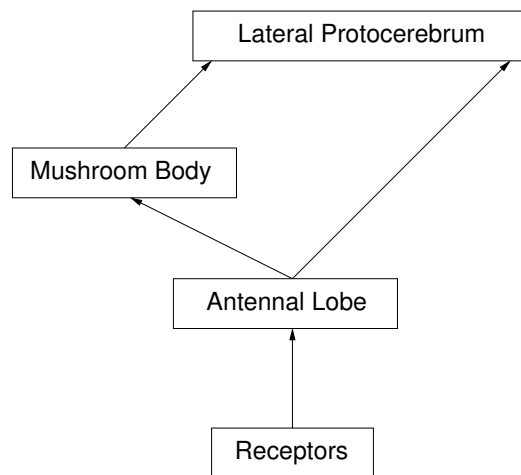
Figure 1.3: Modular architecture of the insect's olfactory system. The olfactory system is structured in modules with functional similarites in insects and vertebrates. The insect's antennal lobe corresponds to the olfactory bulb in vertebrates. The projection neurons of the antennal lobe relay odor information to the mushroom body (analogous to the hippocampus) and the lateral protocerebrum (analogous to the cortex). Only one brain hemisphere is drawn, since this design is bilaterally symmetric.

1.2.2 The honeybee as model system in neuroscience.

Since the olfactory systems of different animals are similar, the choice of a particular species for biological studies is determined by additional advantages of that species against the others in the current research context.

Honeybees are frequently chosen as a model system in neuroscience for several reasons: in comparison with vertebrates, bees are relatively easy to

handle in the laboratory and can also be used in physiological and behavioral experiments; bees are capable of learning visual and olfactory stimuli [von Frisch, 1993]; the anatomy of the bee brain, and especially of its olfactory system, is well characterized (Fig. 1.4); a functional atlas of the honeybee's antennal lobe in terms of glomerular maps is currently available (see example in Fig. 1.5), which enables the systematic study of neural coding in the antennal lobe [Joerges et al., 1997, Galizia et al., 1999]. The antennal lobe of honeybee is therefore an ideal biological neural network in which to study the role of neural interactions in sensory coding and memory formation.

In the following chapters we will focus on odor-coding and short-term memory in the olfactory system of the honeybee. In particular, we will study how odors are mapped onto dynamic neural activity in the antennal lobe and how this neural code may be interpreted by the mushroom body or the lateral protocerebrum. We will also provide evidence of Hebbian mechanisms of a sensory memory in the antennal lobe.
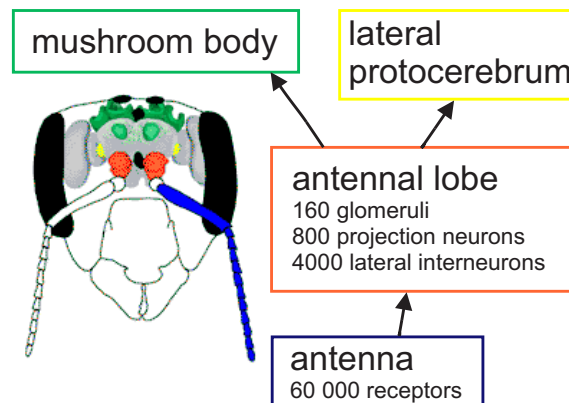
Figure 1.4: The brain of the honeybee. The antenna contains approximately 60,000 receptor neurons that project into the glomeruli of the antennal lobe. There are around 160 glomeruli. Each glomerulus contains no more than 5 projection neurons that relay encoded olfactory information to the mushroom body and the lateral protocerebrum. In the antennal lobe there are also local interneurons (around five times more than projection neurons). Figure downloaded from http://www.neurobiologie.fu-berlin.de/galizia.

1-octanol

1-hexanol

1-nonanol
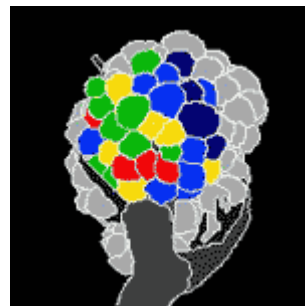
isoamylacetate

Figure 1.5: Odor maps in the antennal lobe of the honeybee. The glomerular arrangement is preserved across animals, permitting glomerulus identification and comparison of odor responses. The comparison reveals odor-specific patterns of glomerular activation. The patterns shown in the figure are responses averaged during stimulation. In the next chapter we will study the temporal evolution of these patterns. Figures downloaded from http://www.neurobiologie.fu-berlin.de/galizia/bee_physiol/default.html.

Chapter 2

Neural Dynamics and
Odor Coding

Relevant hypotheses about odor coding in the olfactory bulb and the antennal lobe are reviewed and discussed. A novel way of studying neural dynamics is presented that reveals a simple mechanism to encode odors in the neural activity of the antennal lobe. It is also shown that the perceptron provides a realistic and biological model of interaction between the antennal lobe (coder) and the mushroom body (decoder). The robustness of this model against changes of odor concentration is studied. With our model it is possible to explain findings of behavioral experiments like concentration-invariance of odor perception and the existence of reaction times in few hundreds of miliseconds.

The data analyzed in this chapter were recorded by Dr. Silke Sachse during her PhD-work at the Institute for Neurobiology of the Free University in Berlin. I am very thankful to her for sharing her data with me.

2.1 Current hypotheses about the olfactory code

Each model on olfaction is biased by the nature of the experimental data it intends to explain. Until the advent of imaging techniques in the early 1990's, electrophysiology was the only experimental procedure available to investigate neural dynamics. The electrophysiology provides us with large amounts of complex data. At higher temporal and spatial resolution olfactory neurons behave as nonlinear oscillators. At lower spatial resolution, one can observe oscillating field potentials that are randomly modulated and reflect the coordinated activity of hundreds (thousands) of neurons.

In an attempt to explain the complexity of the field potentials in the olfactory bulb of rats, Walter Freeman proposed an hypothesis on the olfactory code in the 1980s that applied theoretical concepts to the interpretation of experimental data. He claimed that the neural dynamics in the olfactory system is chaotic [Freeman, 1991]. This would explain why several repetitions of the same odorant evoke different spatial patterns of the field potentials recorded with extracellular multielectrodes [Freeman, 1994]: the initial state of the network would be different before each stimulation and the chaotic dynamics would drive the network through increasingly diverging states (butterfly effect). However, if the neural dynamics were truly chaotic, it would be possible to reconstruct the strange attractor [Packard et al., 1979, Takens, 1981] from the local field potentials as well as its fractal dimension [Grassberger and Procaccia, 1983]. But this was possible only under exceptional conditions like an induced epileptic seizure [Freeman, 1988]. It could be argued that the chaotic attractors of the olfactory system cannot be properly reconstructed in normal conditions because they are high dimensional. In practice, however, there is no way to distinguish between high-dimensional chaotic systems and noisy systems [Hegger et al., 1998]. In other words, the field potentials can simply be noisy but not chaotic signals.

Another caveat to Freeman's hypothesis is the lack of a reliable mapping between sensory input and neural activity. As mentioned above, the same odor evokes different extended field potentials in different presentations. Instead of thinking of deterministic chaos as the essence of neural dynamics, perhaps we should admit that field potentials cannot resolve neural activity that is odor specific. Freeman's work has nevertheless inspired other models that provide a deeper insight into the problem of odor recognition. One of those models has been proposed more recently by Li and Hertz [Li and Hertz, 2000].

Li and Hertz model the olfactory bulb through the interaction between an ensemble of excitatory neurons with an ensemble of inhibitory neurons. The neurons are described as oscillators with saturation similar to the Wilson-Cowan type [Wilson and Cowan, 1972]. The network has no chaotic behavior but converges to oscillating modes. Different odors are encoded in modes of similar frequencies (chosen around 40 Hz) with different phases. In this model, the storage of new patterns changes the old odor-specific modes. Biologically, this implies that each odor quality we perceive would change every time we learn a new odor. According to the model, each odor is encoded in a network eigenmode of similar but different frequency. Biologically this means that one should find odor-specific peaks in the spectrum of the field potentials. This has not been observed in mammals and is definitely not the case in the antennal lobe of insects where any odor enhance the

same frequency peak (around 20 Hz in locusta and honeybees). In fact, the existence of such a robust network oscillation in insects has motivated several experiments in the last few years that led to another hypothesis on the olfactory code: the encoding of odors in oscillating neural assemblies [Laurent and Davidowitz, 1994, Laurent, 1996].

It has been reported that the odor-induced 20 Hz oscillation emerges from the transient synchrony between projection neurons during stimulation [Laurent et al., 1996]. At each maximum of the field potential oscillation a different set of neurons fire together (synchronized assembly). A certain assembly may contain neurons belonging to the former and the next assembly. For a given odor at a given concentration the sequence of active assemblies is the same up to small variations [Wehr, 1999]. Therefore this phenomenon has been proposed to be the basis of the olfactory code [Wehr and Laurent, 1996, Laurent et al., 2001].

A neural code relying on such a dynamical process, that lasts as long as the stimulation itself, has difficulties explaining duration-invariance in odor perception: a given odorant presented during two seconds should be perceived as a different odor when presented for just one second, since in this case one half of the synchronized assemblies are left. Electrophysiological findings in the olfactory bulb of the zebrafish provide a possible solution to this problem [Friedrich and Laurent, 2001]: although the oscillating neural assemblies transiently synchronize until the end of stimulation, a clustering analysis of the neural firing reveals that the population responses to different odors become less and less correlated and after 800 ms they are totally declustered.

It has been reported that projection neurons change their response with concentration [Laurent and Davidowitz, 1994]. This also represents a problem for a neural code that has to cope with intensity invariance, like the olfactory code. However, recent work in locusta reveals that the variations of the sequence of synchronized neural assemblies due to odor concentration are not as pronounced as the differences due to odor identity [Stopfer et al., 2003].

The network oscillation around 20 Hz may have another origin than transiently synchronized neural assemblies, at least in honeybees. The field-potential oscillation does not exclusively appear during stimulation but is usually present during the spontaneous activity in honeybees and may even decrease during stimulation [Szyszka, 1999]. This means that either there are synchronized neural assemblies during the spontaneous activity too, or the field potential does not arise from synchronized spikes. In fact, the membrane potential of the projection neurons oscillates with exactly the same frequency as the field potential [Wehr and Laurent, 1996, Wehr, 1999]. Thus, one cannot exclude that the origin of the field-potential resides in the sub-

threshold dynamics of the projection neurons instead of in the synchrony between spikes.

The experimental findings reported by Laurent *et al.* have been modeled as a "winnerless competion network" [Rabinovich et al., 2001]. This network has no stable state except the origin. As long as the network is stimulated it generates a sequence of synchronized neural assemblies that correspond to heteroclinic trajectories of the dynamics. The model captures the main features of the experimental observations reported [Laurent et al., 2001]. However, an encoding process based on transiently synchronized neural assemblies requires a downstream network to develop a readout mechanism capable of recognizing endless trajectories. To understand the difficulty of this problem consider the decoding mechanism recently proposed in [Laurent, 2002] and [Pérez-Orive et al., 2002]. The authors propose that for every first half of a cycle of the field potential there are Kenyon cells (KC) in the mushroom body that respond to the active synchronized neural assembly. During the second half of the cycle the KC are shut down by the inhibitory input coming from the lateral protocerebrum that was also excited by the active synchronized assembly. Thus, the sequence of synchronized neural assemblies in the antennal lobe is transformed into a sequence of active KC in the mushroom body. Although this mechanism is feasible biologically, it just shifts the problem of interpreting a sequence of active neurons to another layer.

A readout mechanism would be much easier to implement if the trajectories converged to odor-specific stable states that correspond to stable spatial patterns of neural activity. Since the development of imaging techniques increasing attention has been devoted to the purely spatial component of the neural response [Hildebrand and Shepherd, 1997, Korsching, 2002]. The reason for this is that a purely spatial pattern of active glomeruli suffices to identify an odor in the antennal lobe and in the olfactory bulb [Korsching, 2002].

In the next section the neural dynamics in the antennal lobe of honeybee is studied using calcium imaging data. We will then consider the compatibility of our observations with the hypotheses about the olfactory code presented in this section.

2.2 Neural dynamics in the antennal-lobe: Analysis of calcium-imaging data

At the current state of the art, imaging techniques have to trade off temporal versus spatial resolution. In order to have a much broader view of the network activity, one has to tolerate a lower temporal resolution than with

electrophysiology. In contrast, although electrophysiology is faster, it fails to provide a global picture of the network dynamics, since simultaneous in vivo recordings in more than two cells are extremely difficult.

In the experiments we analyze below, our temporal resolution was 6 Hz. Thus, we cannot observe single spikes nor the 20 Hz network oscillation. However, we do resolve the slow modulations of the membrane potential in projection neurons reported by Wehr, which strongly correlate with their instantaneous firing rate [Wehr, 1999, Laurent et al., 2001]. Our spatial resolution permits us to identify several glomeruli (typically between 10 and 20). Each glomerulus contains between 3 and 5 projection neurons.

A novel experimental technique to exclusively stain projection neurons (see Methods in [Sachse and Galizia, 2002] and Appendix A) permits us to specifically study the evolution of those odor-evoked responses that are transmitted to higher processing areas. This is of great importance for understanding the readout mechanism of a downstream network like the mushroom body, as we will see below.

2.2.1 Multidimensional representation of neural activity

Network dynamics are by nature multidimensional. Using a suitable representation of the spatiotemporal activity patterns is the first step to elucidating properties of the neural dynamics. The easiest way to represent network activity is to consider each unit of the network (neuron or glomerulus) as a dimension of a multidimensional space. The degree of activity can be estimated as the instantaneous firing rate for neurons or the instantaneous increase/decrease of calcium concentration for glomeruli. Thus, a spatial activity pattern is mapped onto a point and the dynamics of the network is mapped onto a trajectory. This is an intuitive way of representing the temporal evolution of a system. It is commonly used in mathematics and physics to represent solutions of differential equations. In that context the multidimensional space is referred to as the phase portrait or phase space of the system.

Since a display of the phase space in more than three dimensions (three neurons or three glomeruli) is impossible, it is useful to project the space onto the two or three dimensions that account for the largest portion of variance in the data: the principal components (PC). Each PC is determined by a linear combination of all units in the network. The projection onto the three first principal components is only for visualization purposes. All dynamical and statistical quantities shown below have been computed in the original eight-

dimensional space that corresponds to the eight common glomeruli identified in all bees studied (n = 7).

Figure 2.1 shows the trajectories described by the antennal-lobe network during two repetitions of four different odors in a single bee. We first note that the repetition of the same stimulus yields similar trajectories and trajectories of different odors aim in different directions. They are open and slightly bent at some locations. The crosses on the trajectories indicate the recording of an activity pattern with a sampling frequency of 6 Hz. We see that the trajectories do not evolve at a constant speed but start to slow down after approximately half a second. These features are incompatible with chaotic dynamics [Freeman, 1991] and the features of heteroclinic trajectories in a winnerless competition network [Rabinovich et al., 2001], which show a complex structure (loops and bendings) and do not decrease their velocity asymptotically.

After stimulation the network returns slowly to the resting state (Fig. 2.2). This relaxation follows a turning path that is different from the trajectory during stimulation.

2.2.2 Neural dynamics converge to odor-specific attractors

The observations based upon Figs. 2.1 and 2.2 can be quantified by computing the velocity and the acceleration (see Appendix A) not only in one bee but in all bees investigated (n = 7). The velocity increases rapidly in the first half second of stimulation, reaches a maximum and then slows down. After approximately one second only small fluctuations in the trajectories remain, which are of the same order as those during ongoing activity (Fig. 3a). When the stimulation ceases there is a second peak in the velocity which is smaller than the first one. This means that the relaxation to the resting state is slower than the excitation during stimulation.

In addition to the velocity, one can calculate the acceleration of the trajectories (Fig. 2.3b and 2.3c). As in physics, the acceleration measures the effect of the forces applied to the system that describes a trajectory. In particular, the component of the acceleration vector tangent to the trajectory measures the force that pulls the system in the direction of movement, whereas the normal component measures the force that bends the trajectory.

Only during odor presentation is the tangential component substantially different from zero. At the beginning it is positive, indicating an increase of velocity. After approximately half a second it becomes negative, which means that the velocity slows down. During the spontaneous activity the tangential
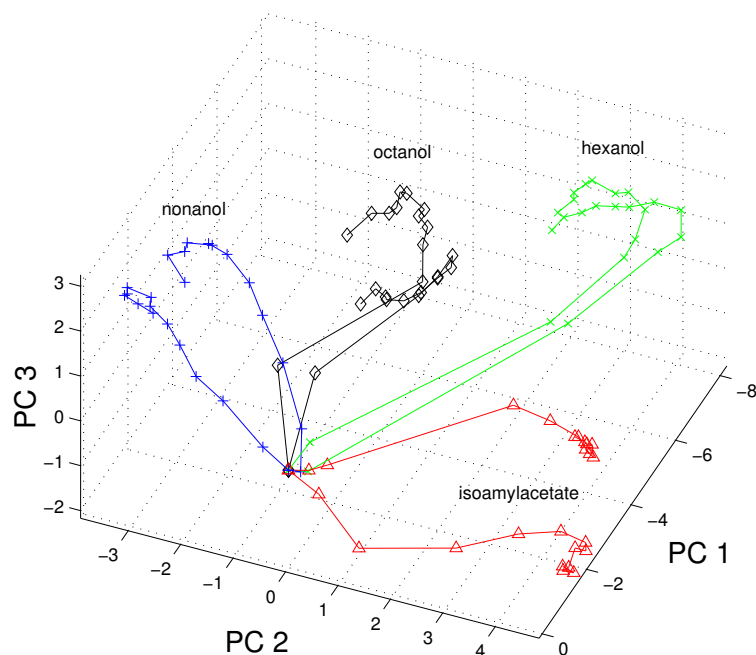
Figure 2.1: Multidimensional representation of the antennal-lobe dynamics during stimulation. Several odors were presented twice to the same bee and the neural activity of the antennal lobe was recorded with calcium imaging at fixed time intervals (167 ms). Thus, the distance between successive data points represents the speed of activity changes. The trajectories depart rapidly from the origin and slow down when they approach odor-specific regions. For visualization purposes the original 21-dimensional space has been projected down onto the three first principal components (PC). These three components account for more than 58% of the variance of the trajectories.

acceleration fluctuates around zero. In contrast, the normal component of the acceleration vector, responsible for changes in the direction of the trajectory, has a bias during the spontaneous activity and increases during stimulation. However, the largest contribution to the total acceleration during stimulation comes from the tangential component.

We thus conclude that odors represent forces that pull and smoothly bend trajectories of neural activity whereas the background activity represents a stochastic force that primarily causes random changes in the direction of the trajectories. The effect of the force applied by the odor is not constant but decreases in time and becomes minimal when the network settles down into regions that represent stable activity patterns. But how odor specific are the
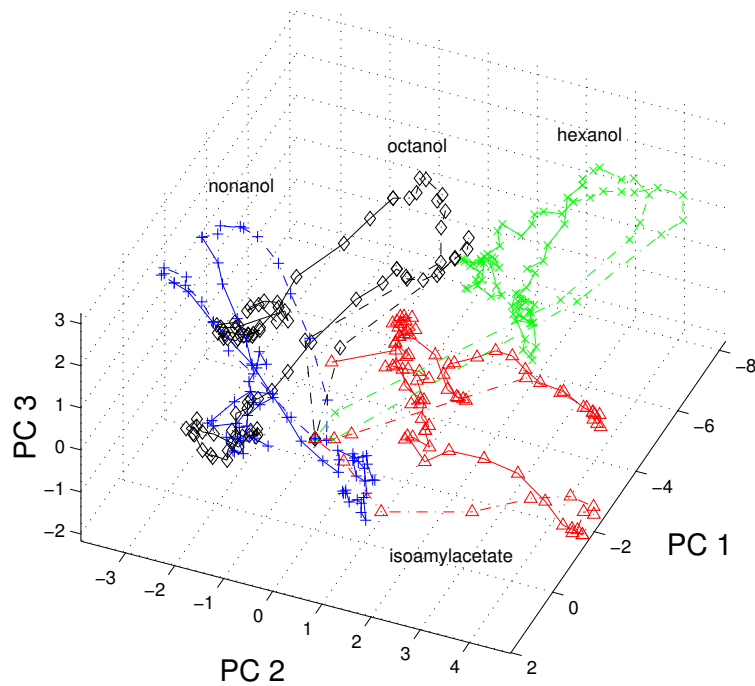
Figure 2.2: Antennal-lobe relaxation dynamics. The trajectories of the antennal-lobe dynamics during post-stimulus relaxation are plotted as a continuation of Fig. 2.1 displayed here again with dashed lines. The solid lines represent the evolution of the trajectories five seconds after stimulation. The trajectories during stimulation and relaxation do not coincide: the latter are slower and more irregular.

stable activity patterns to which the trajectories converge?

The "separability" index provides an answer to this question, as it quantifies how reliable a partition of the phase space into odor-specific regions is. For the mathematical details, see Appendix A. Here we will only consider its geometrical interpretation.

An intuitive way of testing whether two clouds of points do not overlap is to calculate the hyperplane (generalization of a plane in many dimensions) which is maximally distant from both clouds. If that hyperplane exists, the clouds do not overlap. Otherwise they do. In this case, the maximization criterion can be relaxed to allow some degree of overlap. The number of points the plane assigns to the correct cloud yields the classification performance of the hyperplane, and is expressed as a percentage (100% means no overlap at all or perfect separation of both clouds).
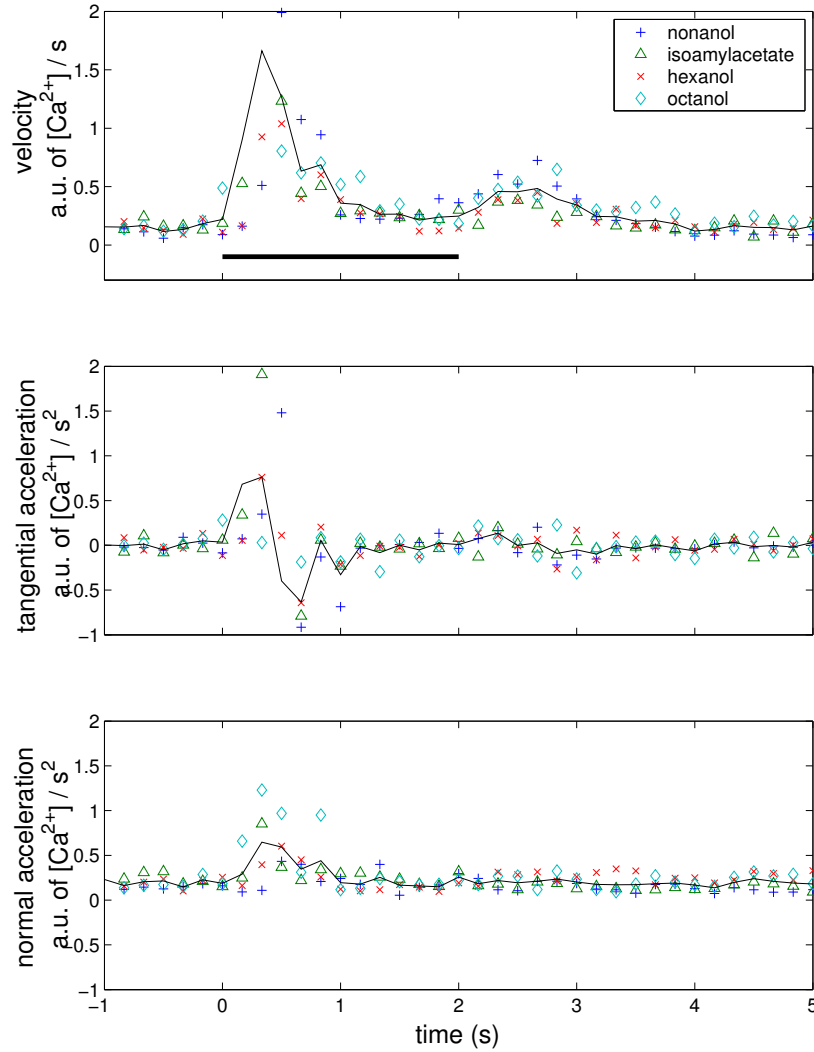
Figure 2.3: Kinematics of the antennal-lobe activity. The symbols represent the mean values of the velocity and acceleration of activity changes at each point in time for a given odor. The arbitrary units of Ca^{2+} are determined with optical imaging (see Appendix A). The continous line denotes the mean computed from all odors. The black bar illustrates the duration of the stimulus presentation. The whole data set, pooled over trials with seven bees, was used for the calculation. See text for details.

Although the classification performance is itself a proper measure of "separability", when the clouds overlap one can improve it with the so called generalization performance (see details in Appendix A), which quantifies the sta-
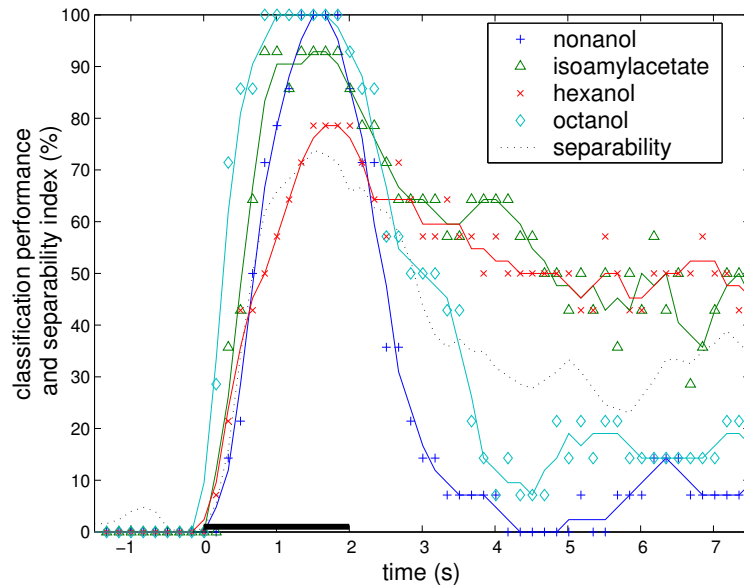
Figure 2.4: Separability and classification performance as a function of time. For the calculations all data collected across trials with seven bees were used. During stimulation (black bar) the partition of the antennal lobe space into odor-specific regions becomes possible, as the increase of the separability (dotted lines) shows. At the point in time of highest separability one support-vector machine (SVM) is trained for each odor. Then, the SVMs are tested over time. The classification performance of a given odor (solid lines) is the fraction of points of that odor, that are recognized as such by the respective SVM. Note that except for hexanol, the odors can be very well discriminated even before the trajectories reach the attractors.

bility of the separating hyperplane under perturbations due to finite-sample effects. The generalization performance averaged for all clouds of points considered quantifies the reliability of the partition of the space into different clouds of points. Therefore we called this quantity "separability".

In the data pooled across bees (n = 7) each odor at each point in time defines a cloud of points. We then study the temporal evolution of the separability of odor-clouds in the network dynamics. The separability at each point in time (Fig. 2.4) shows that the trajectories become more and more odor specific during stimulation. The separability reaches a maximum approximately one second after stimulus onset, when the activity patterns are stationary (velocity trough, see Fig. 2.3a).

At this point in time an optimal separating hyperplane for each odor is

calculated (see Appendix A). The classification performance was for our data: 100% for octanol and nonanol, 93% for isoamylacetate and 79% for hexanol. These values are substantially larger than chance limit (50%) and contrast with the fact that all odors tested evoke similar, overlapping patterns. The result supports the hypothesis that odors are encoded in the antennal-lobe as stable spatial patterns of neural activity [Hildebrand and Shepherd, 1997, Korsching, 2002].

From the results above we conclude that the trajectories reach odor-specific regions (attractors) in approximately one second. The attractors, or equivalently, the associated stable calcium patterns, are a reliable mapping of the input odor onto the antennal lobe and they provide a reliable output to the next neural structures: the mushroom body and the lateral protocerebrum. This suggests that the stable activity patterns can be the basis of the olfactory code in the antennal-lobe. However, such a straightforward interpretation of the calcium-imaging data may be misleading if we are not able to show that a downstream network can decode the antennal-lobe attractors in a feasible way.

2.3 Does the olfactory system work like a perceptron?

Neurons of a network downstream of the antennal lobe have to carry out the same task we have done in order to interpret the network activity: they have to explore the phase space and look at which region the stimulus converges to. Perceptrons [Rosenblatt, 1962] provide an efficient implementation of such a decoding mechanism. For mathematical details see Appendix A (see also [Rumelhart and McClelland, 1986]). Here we simply remark that the algorithm that classifies data points with respect to a hyperplane is mathematically equivalent to a simple artificial neural network: the perceptron. The equation of a hyperplane is

$$\vec{w} \cdot \vec{x}_P = \sum_i w_i \cdot x_{Pi} = b \tag{2.1}$$

where $\vec{x}_P$ are the points belonging to the hyperplane, $\vec{w}$ is a unitary vector normal to the plane and b is the distance to the origin. The hyperplane divides the space into two regions A and B with all points $\vec{x}_A$ in A satisfying

$$y = \vec{w} \cdot \vec{x}_A \geq b \tag{2.2}$$

and all points in B satisfying

$$y = \vec{w} \cdot \vec{x}_B < b. \tag{2.3}$$

Alternatively we can think of x_i as the input from the x_i neuron with synaptic weight w_i into a neuron y with firing threshold b. Then, every input vector $\vec{x}_A$ makes the neuron y fire. The rest of the input space $\vec{x}_B$ does not.

2.3.1 How the mushroom body may interpret the trajectories

Figure 2.5 represents the mapping of a hyperplane in the phase space onto a network that models part of the olfactory system. Some (or all) units x_{An} of a bottom layer (the antennal lobe) synapse with strength w_n to a given unit in an upper layer (e.g. a Kenyon cell of the mushroom body). If the activation threshold of this unit is set to b, it fires in response to odor A.

Within the theory of artificial neural networks [Hertz et al., 1991] it has been shown how synaptic weights can adapt through Hebbian learning to the vector $\vec{w}$, which together with the threshold b determines the optimal separating plane in the phase space for a given odor. Note however, that no learning process is necessary to identify odors with such a network: Suppose that the threshold b is set constant for all units in the upper layer. By connecting each upper unit with random synaptic weights $\vec{w}$ to the units of the bottom layer, each upper unit will look at a random direction of the phase space. If the number of units in the upper layer is large enough, eventually all directions of the phase space will be covered and hence, for any given odor-specific attractor there will always be at least one upper unit that reacts to it. This readout mechanism is consistent with the anatomy of the olfactory system [Strausfeld, 1976].

2.3.2 Reaction times and optimal odor classification

Although the trajectories need about one second to reach the regions of stability, when they can be optimally separated, odors are already well discriminated after 300 ms (Fig. 2.4). This result leads to a testable prediction: Bees should be able to differentiate odors in behavioral tests with minimal reaction times that are significantly shorter than one second (the time to reach the steady plateau state). In addition, it would be interesting to investigate whether and to what extent the behavioral classification performance matches that obtained from the model.
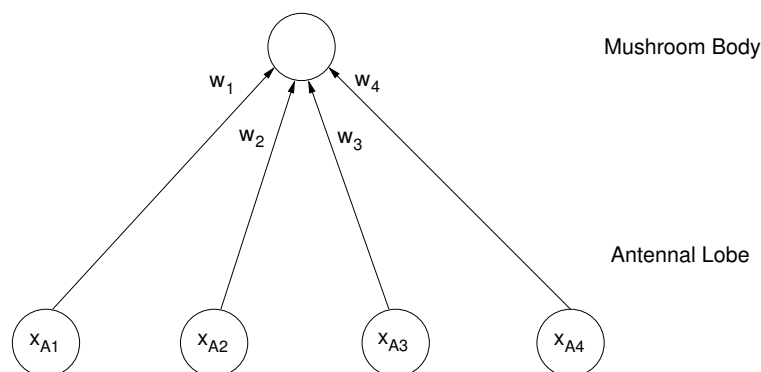
Figure 2.5: Perceptron-like architecture of the olfactory network in the honeybee. The algorithm used to analyze the imaging data can be implemented as a neural network, whose architecture is compatible with the anatomy of the bee brain. The units in the lower layer represent individual glomeruli in the antennal lobe. The unit in the upper layer represents a neuron of the mushroom body (Kenyon cell). This unit responses to a given odor A only if the whole activity of the lower units weighed by their synaptic strength $\sum_n^N x_{An} \cdot w_n$ exceeds a threshold b.

2.4 Robustness and invariances of the olfactory code

Natural stimuli are perceived in variable, noisy environments. Neural codes must therefore tolerate perturbations in the input channels. In particular, the recognition of an odor quality must be possible not only at a given concentration but over a range of concentrations. Bees, for example, must be able to recognize the aroma of a flower not only when they lick its nectar (very high concentration) but also when they fly nearby (low concentration). In this section we study the reliability of the olfactory code on the basis of our model by exploring the effects of odor concentration.

2.4.1 Neural dynamics change with odor concentration

Figures 2.6-2.9 show the changes of the averaged odor-specific trajectories with increasing concentration. All trials of the corresponding odor across bees were used for the average. Two effects are observed: i) the trajectories are monotonously stretched and ii) change their orientation monotonously.
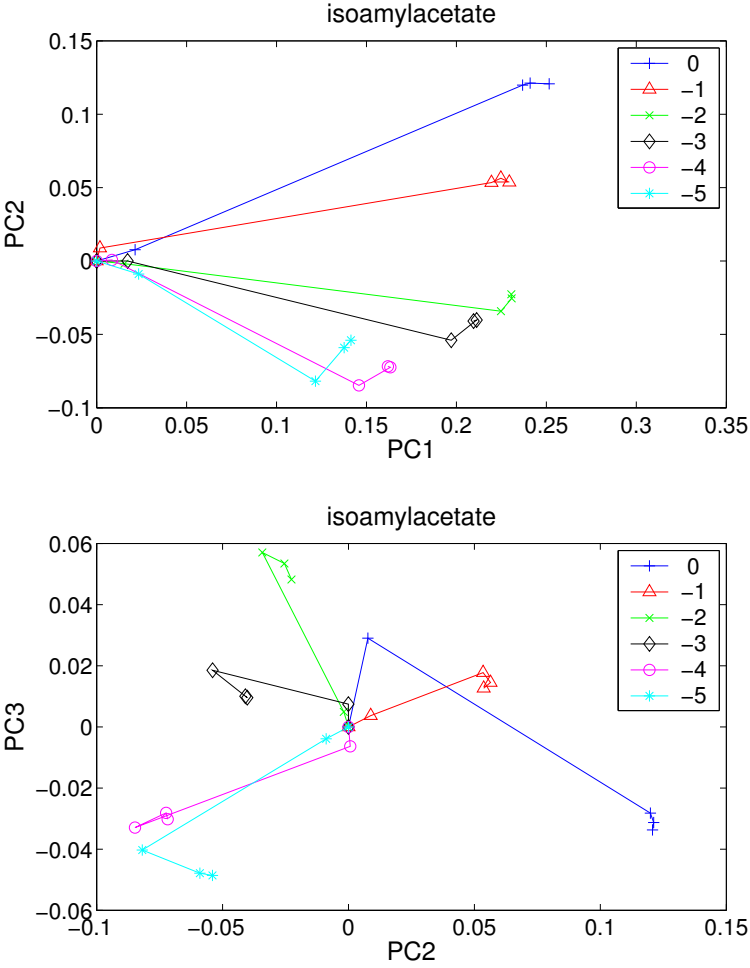
Figure 2.6: Effect of the odor concentration on the trajectories I: isoamylacetate. Average trajectories during stimulation across all trials of isoamylacetate in all bees at the logarithmic concentration indicated in the legend. The plotted trajectories have been projected onto principal components for optimal visualization. The first three principal components account for a 94% of the variance. With increasing concentration the average trajectories are stretched (top) and rotated (bottom).

2.4.2 An interesting invariant

Although a concentration increase deforms the odor-specific trajectories, they still preserve some kinematical properties. In particular, they require the same time to reach the maximum as well as the minimum velocity. In

Figure 2.7: Effect of the odor concentration on the trajectories II: hexanol. The first three principal components account for a 94% of the variance.

Fig. 2.10 the traces of the velocity at increasing concentrations are plotted. For a given concentration the variability across trials and bees was as large as between odors, so each velocity curve plotted is the mean of all odors presented in all bees.

We note a strong agreement between the curves. The maximum velocity is achieved in the same time-interval with respect to stimulus onset (around 500 ms) for all concentrations. Also the minimum velocity is reached at a fixed time-interval (approximately 800 ms) independent of the concentration. This means that, regardless of the odor concentration, the patterns of neural activity in the antennal lobe need approximately one second to stabilize.
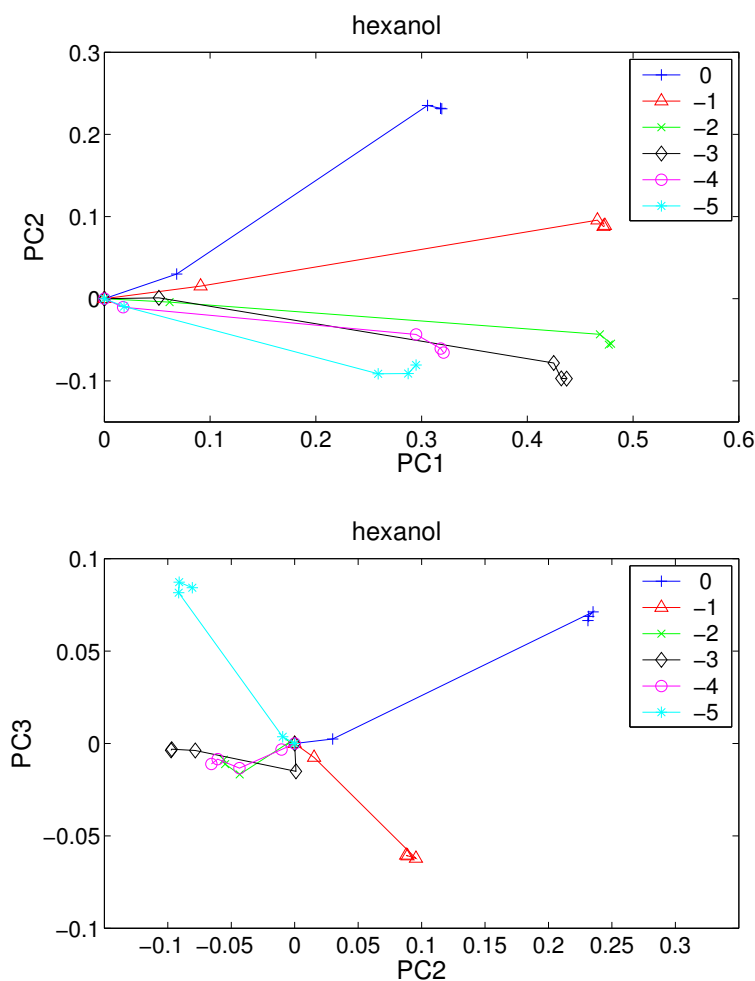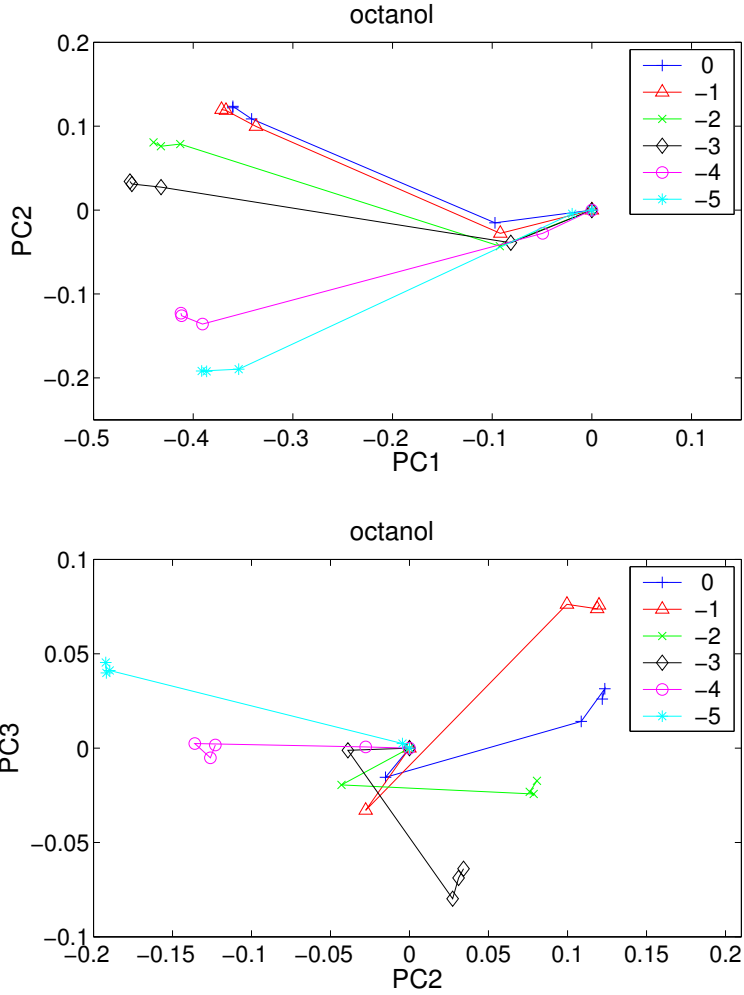
Figure 2.8: Effect of the odor concentration on the trajectories III: octanol. The first three principal components account for a 96% of the variance.

The only mismatch between different curves in Fig. 2.10 is the height of the velocity peak, which increases with increasing concentration. Figure 2.11 shows that such increase is linear in logarithmic concentration units. If the time interval to reach the attractors is the same but the velocity is higher at higher concentrations, the run path (see Appendix A) of the trajectories should be accordingly larger. And this is exactly what happens, as seen in Fig. 2.12. A longer path is a consequence of the stretching effect observed in Figs. 2.6-2.9.

Future research on the interaction between projection neurons should elu-
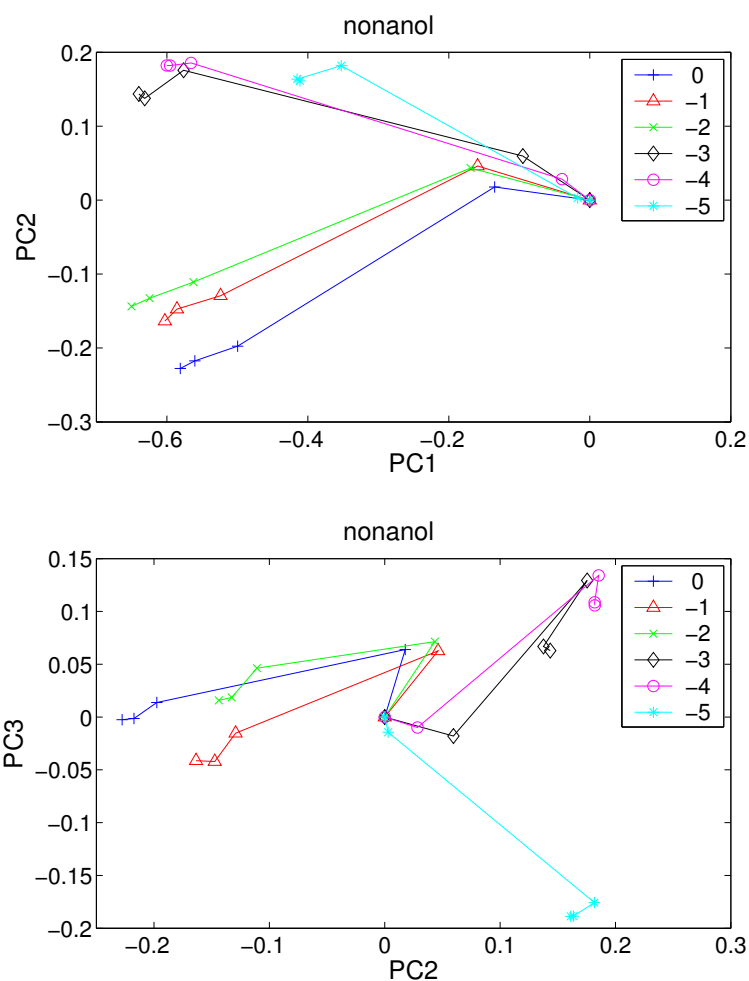
Figure 2.9: Effect of the odor concentration on the trajectories IV: nonanol. The first three principal components account for a 96% of the variance.

cidate the emergence of such invariant of the neural dynamics in the antennal lobe.

2.4.3 Effects of concentration on odor classification

The changes of the trajectories induced by increasing concentration may affect the classification performance of a downstream neuron. We now study this effect and relate it to experiments on behavior.

The perceptrons proposed in section 2.3 as a model of the interaction between the antennal lobe and the mushroom body identify odors by looking

Figure 2.10: Velocity plot at different concentrations. Each curve is the velocity averaged for all odors in all bees at the logarithmic concentration shown in the legend. The peaks of the velocity do not move with increasing concentration. The same occurs with the trough, which represents the stable state during stimulation. Thus, the neural activity in antennal lobe needs approximately 800 ms to reach the odor-specific attractors independently of the odor concentration. Black bar indicates stimulus duration
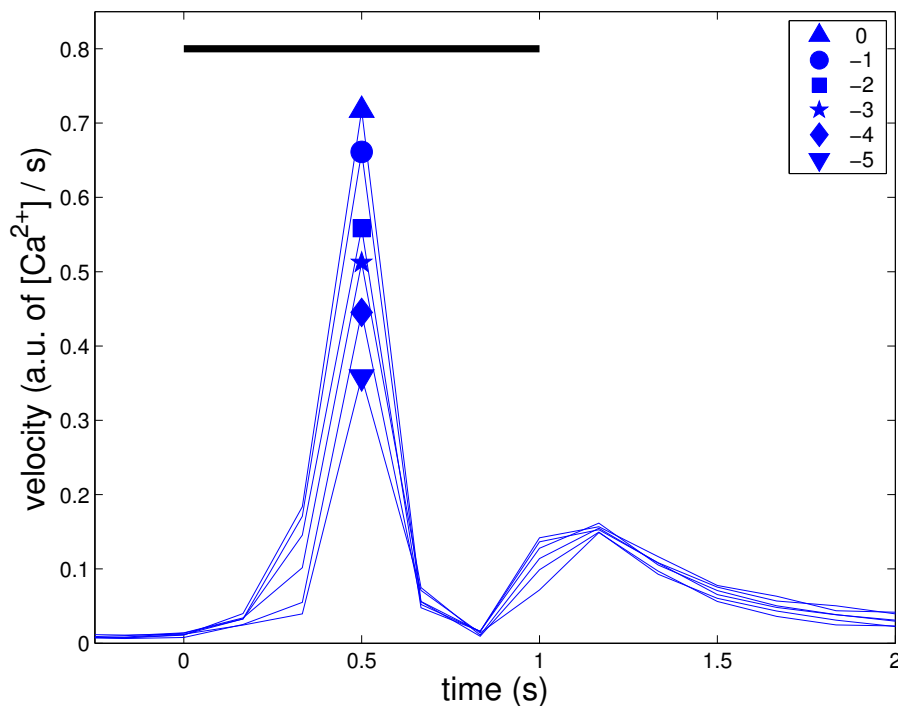
at the region the trajectories converge to. If the trajectories change with increasing concentration we expect the perceptrons to eventually change their response too. Let the hyperplane associated with a given perceptron (Kenyon cell, KC) divide the phase space into two regions, A and B. Imagine that odor X at lower concentration drives the antennal lobe into region A making the KC fire. Imagine now that odor X at higher concentrations drives the antennal lobe into region B. The KC will now not react to that odor. Analogously, a KC may react to a given odor at high concentrations but not at lower ones. It is also possible that a KC reacts to an odor in a broad concentration range. These cases correspond to our every-day-life experience: some odors and flavors change their quality with concentration; other odors and flavors smell and taste the same either diluted or concentrated.
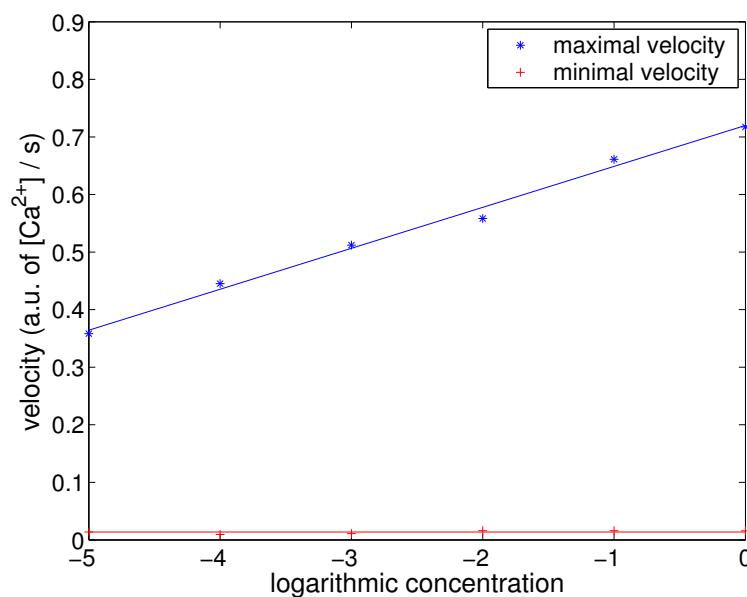
Figure 2.11: Effect of concentration on the extremal values of the velocity. The maximal velocity during stimulation increases linearly with the logarithm of concentration. The minimal velocity, which represents the level of fluctuations in the stable state, does not change with increasing concentration.

To train a perceptron to a given odor means calculating the optimal separating hyperplane of that odor (see Appendix A). When the perceptron has been trained to recognize a given odor at a given concentration, one can then study how its classification performace changes with concentration. In Figure 2.13 the change of classification performance with increasing concentration is studied for perceptrons associated with several odors.

It has been reported [Bhagavan and Smith, 1997] that honeybees can recognize odors learned at low concentrations when presented at high concentrations (generalization effect) but have difficulties recognizing odors learned at high concentrations when presented at low concentrations. In our model, learning is synonymous with being trained, i.e., we can make a perceptron learn an odor at a given concentration by calculating its associated separating hyperplane. We note (Fig. 2.13) that our model shows the generalization effect with isoamylacetate. A weaker trend of the effect is observed with nonanol. The effect is not observed with hexanol and octanol.
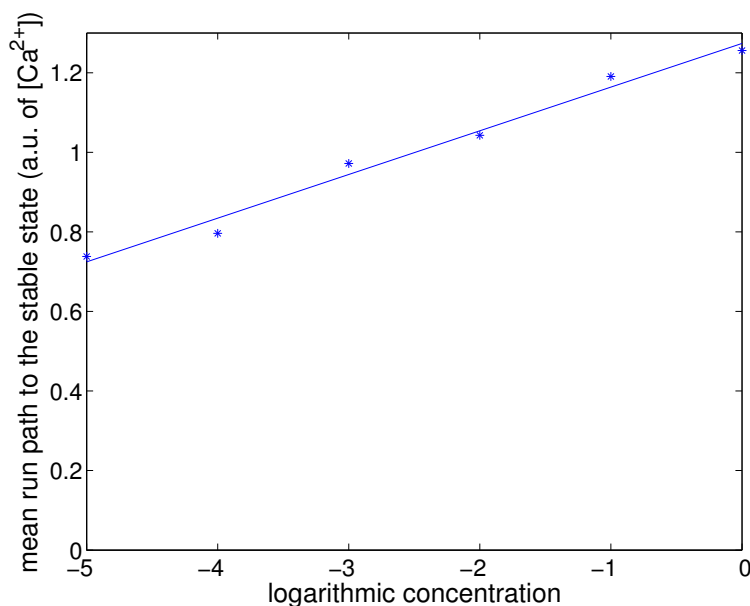
Figure 2.12: Effect of concentration on the run path. If the time-interval to reach the attractors does not change with concentration and the maximal velocity does, then the trajectories must describe a longer path with increasing concentration. This effect indeed occurs as shown in the plot. The mean run path (see text) increases with the logarithm of concentration in a roughly linear manner.

2.5 Discussion

From the study of the neural dynamics in the antennal lobe of honeybee with calcium imaging we conclude that the neural dynamics becomes stable approximately 800 ms after stimulus onset, independently of the identity and concentration of the odor presented. Different odors converge to different stable spatial patterns of neural activity. Although the activity patterns need over half a second to become stable, the time at which they can be optimally discriminated, some patterns can be recognized as soon as 300 ms.

These findings are incompatible with models of chaotic neural dynamics and also with a winnerless-competition network [Rabinovich et al., 2001, Laurent et al., 2001], since such a network encodes stimuli in complex trajectories on heteroclinic orbits. However, our results are in agreement with the findings on the dynamic representation of odors in the olfactory bulb of the zebrafish [Friedrich and Laurent, 2001], where the activity patterns also become increasingly odor specific during stimulation.

The experimental technique applied here permits us to accurately resolve the large-scale activity patterns in the antennal lobe. However, we cannot resolve fast events, such as 20 Hz network oscillation nor transient odor-specific synchronizations between the spikes of projection neurons [Laurent, 1996, Laurent et al., 1996, Laurent and Davidowitz, 1994]. This means that we cannot determine whether the olfactory code is based on sequences of oscillating projection neurons or whether it is based on the attractors of the slow temporal patterns reported here. As part of the ongoing controversy between spike-timing and firing-rate codes, this question remains open for further investigation.

Recent work on the moth's antennal lobe helps us understand the relation between the phenomena observed in electrophysiological and imaging techniques [Lei et al., 2002]. These authors have studied with intracellular recordings the activity of projection neurons enclosed in glomeruli which show an odor-specific response in imaging experiments. They found that projection neurons within the same glomerulus fire coherently during odor presentation and that the degree of synchrony is modulated by lateral inhibition between active neighboring glomeruli. Hence, the modulation of the odor-induced synchrony is translated into variations of the calcium concentration within the glomerulus, as observed with imaging techniques.

According to our results, the regions of stability, or correspondingly the associated stable calcium patterns, are a reliable mapping of the input onto the antennal lobe and they potentially provide a reliable output to the next neural structures: the mushroom body and the lateral protocerebrum. Within this framework, we have shown that the perceptron represents a simple biological model of the interaction between projection neurons in the antennal lobe and Kenyon cells in the mushroom body.

Our perceptron-based study of odor-recognition at different concentrations shows how a simple mechanism may account for concentration invariance of odor perception. Concentration invariance can also be achieved with a spike-timing-based computation, like the "many-are-equal" model of olfactory processing [Brody and Hopfield, 2003]. In this model, spiking neurons that are driven by a common network oscillation will phase-lock when they receive (approximately) equal inputs. The neurons of the model (representing projection neurons in the antennal lobe or mitral cells in the olfactory bulb) are assumed to have an intrinsic bias current, which is in general different in different neurons. If the sum of the input current from the receptors plus the intrinsic bias current is similiar in a group of neurons, these neurons will synchronize.

Since the input currents from the receptors logarithmicaly increase with increasing odor concentration, multiplying the concentration by a factor re-

sults in adding a constant (the logarithm of that factor) to the input currents. Thus, the neurons that received similar net input at the original concentration, will also receive similar net input at the new concentration and, therefore, they will also synchronize. According to the model, the phase of the synchronized assembly with respect to the network oscillation shifts to lower values with increasing concentration. However, recent experimental results in locusta have demonstrated that the projection neurons do not change their firing phase with respect to the network oscillation when the concentration changes [Stopfer et al., 2003].
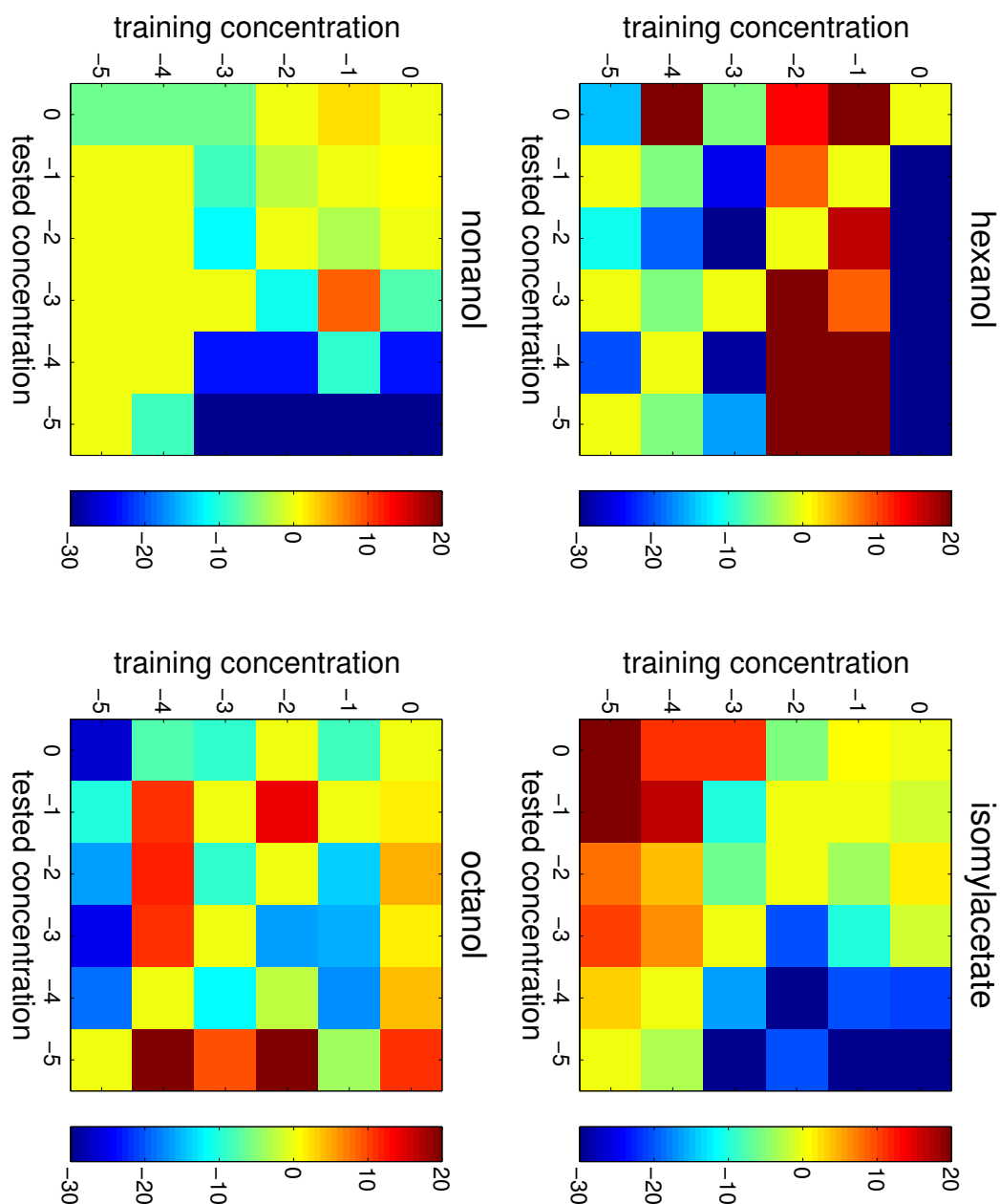
Figure 2.13: Simulation of a behavioral experiment. Based on our model one can simulate behavioral experiments on concentration effects. For each odor, a perceptron was trained at each concentration and tested at the rest. Colors represent the change of classification performance. According to the generalization effect observed with bees (see text) perceptrons trained to an odor at low concentrations should recognize that odor at higher concentrations but not the other way around. Thus, the matrices of the figure should have hot colors below the diagonal and cold colors above. This is observed for isoamylacetate. A weaker effect is also observed for nonanol. Hexanol and octanol show neither the generalization effect nor remarkable regularities.

Chapter 3

Sensory Memory and Hebbian Plasticity in the Antennal Lobe

Following a brief overview on olfactory memory in honeybees, the Hebbian postulate as a model of memory formation and learning is discussed. A mathematical approach is introduced to uncover traces of sensory memory in the spontaneous activity of the antennal lobe after a single and unrewarded odor presentation. The traces of memory consist of changes of pairwise correlations between glomeruli and provide evidence of a Hebbian mechanism at the network level. A mathematical technique inspired by the Hebbian postulate to retrieve the stimulus from the memory traces is described and applied.

The data analyzed in this chapter were recorded by Marcel Weidert at the Institute for Neurobiology of the Free University in Berlin. I am very thankful to him and also to Dr. Giovanni Galizia, former member of the same Institute, for their generous collaboration and the interesting discussions.

3.1 Olfactory memory in honeybees

It has long been known that honeybees are able to learn visual and olfactory stimuli [von Frisch, 1993] (first edition originally published in 1927). Although the biological mechanisms underlying memory formation remain unknown, great progress has been made in the last few years experimentally identifying several memory types and their putative neural correlates [Menzel, 1999], as well as the biochemistry involved [Menzel and Müller, 1996].

Most efforts have been devoted to studying associative memory and learning by reinforcement with a reward (typically sucrose). These approaches

disregard the possibility that a nonassociative component of memory may develop with stimulation alone (e.g. sensory memory). There may be two closely related reasons for this: i) Since the famous experiments of Pavlov [Pavlov, 1927] there has been a trend in ethology to reduce behavior to a collection of conditioned reflexes (see also [Klopfer, 1973] for a comparative exposition of this and other hypotheses). ii) In the laboratory, odor recognition is determined using the proboscis-extension paradigm: (ideally) the bee only extends her proboscis to lick the odor source she associates with the unconditioned stimulus (sucrose). Thus, experiments on odor recognition and memory with bees are constrained to a Pavlovian protocol, impeding the study of nonassociative memory.

One way to study nonassociative memory, such as sensory memory, is to look for lasting physiological changes specifically induced by a stimulus in its putative neural correlate. This is possible today using imaging techniques. Before presenting our approach based on the Hebbian postulate, we will briefly overview the types of associative memory found in honeybees, as well as their neural correlates.

3.1.1 Behavioral evidence of several memory types

A scout honeybee concentrates on one flower type as soon as she obtains sweet nectar from it, and different scout bees in general concentrate on different flower types [von Frisch, 1993]. This way, scout bees minimize exploration time and maximize the variety of visited flowers. In addition, by concentrating on only one flower type, a single bee increases the fertilization rate of that type and, as different scouts concentrate on different flower types, they increase the fertilization rate of all flower types they visit. This in turn ensures the bees a plentiful future harvest. Such an adapted behavior requires a memory that lasts as long as the foraging bout (time spent outside the hive), typically several minutes.

It has been observed with honeybees [Menzel, 1985] and more recently with bumblebees [Chittka et al., 1997] that the longer the animals scout, the more probable it is that they change flower type. This suggests that bees posses a short-term memory lasting several minutes which permits them to remember the chosen flower type. This memory decays when the foraging bout is likely to conclude.

Once bees are back to the hive they may spend several minutes, hours or even months (during the winter break) there. After this time bees can still remember specific feeding sources and identify flower types [von Frisch, 1993]. It can also be demonstrated in the laboratory that bees possess a long-term memory for odors [Hammer and Menzel, 1995]. Three or fewer presentations of the same reinforced odor suffice to induce memory consolidation: the bees will remember the odor after minutes, hours and days. Reinforcement (sucrose) is necessary for memory consolidation. This reveals the associative character of long-term memory in bees [Hammer, 1997].

3.1.2 Neural correlates of memory

Interestingly, it has been reported that if the sucrose reward is substituted with an octopamine injection in the brain, memory consolidation will also occur [Hammer and Menzel, 1998]. Octopamine is a neuromodulator released at several locations of the bee brain by a neuron referred to as VUMmx1 (ventral, unpaired, median neuron of the maxillary neuromere), [Hammer, 1993]. The VUMmx1 neuron therefore represents a reward pathway in the bee brain. The precise location at which octopamine injection is equivalent to the effect of the reward has also been determined [Hammer and Menzel, 1998]. It turns out that the mushroom body is the neural structure in which long-term memory is consolidated. This result corroborates what former experiments on induced retrograde amnesia by selective cooling had shown [Erber, 1976]. The same technique helped identify the antennal lobe as the putative neural correlate of a another type of associative memory: the short-term (lasting a few minutes) memory [Erber et al., 1980].

Thus, memory consolidation of interesting (reinforced) odors is shifted to a higher processing network (the mushroom body) for future retrieval and the interesting information for current use (working memory) is stored in the antennal lobe. We therefore chose the antennal lobe as the network in which seek sensory memory as well. To do so, we first needed a physiologically testable model of memory.

3.2 Hebbian model of memory: Learning through correlations

The idea that the conections between neurons are involved in learning and memory is due to Santiago Ramón y Cajal, who also discovered the synapses [Ramón y Cajal, 1891]. During a lecture at the Royal Society of London, Cajal claimed [Ramón y Cajal, 1894]:

> *Cerebral gymnastics are not capable of improving the organization of the brain by increasing the number of cells, because it is known that the nerve cells after the embryonic period have lost the property of proliferation; but it can be admitted as very probable that mental exercise leads to a greater development of the dendritic apparatus and of the system of axonal collaterals in the most utilized cerebral regions. In this way, associations already established among certain groups of cells would be notably reinforced by means of the multiplication of the small terminal branches of the dendritic appendages and axonal collaterals; but, in addition, completely new intercellular connections could be established thanks to the new formation of [axonal] collaterals and dendrites.* Quoted from the translation into English in [DeFelipe and Jones, 1988].

Over half a century after Cajal's lecture the psychologist Donald Hebb postulated how those "associations" among cells should be reinforced in order to encode information about stimuli.

> *Let us assume then that the persistence or repetition of a reverberatory activity (or **"trace"**) tends to induce lasting cellular changes that add to its stability. The assumption can be precisely stated as follows: When an axon of cell A is near enough to excite a cell B and repeatedly or persistently takes part in firing it, some growth process or metabolic change takes place in one or both cells such that A's efficiency, as one of the cells firing B, is increased.* Quoted from [Hebb, 1949]; (emphasis in bold is ours and its meaning will become clear later).

The Hebbian postulate is rephrased today in terms of correlated neural activity: modifications in the efficacy of synaptic transmission are driven by the correlation, C_{ij}, between the firing activity of the presynaptic neuron i and the postsynaptic neuron j (see also [Gerstner, 2002]). If a certain stimulus evokes a pattern of neural activity $\vec{u} = (u_1, u_2, ..., u_n)$, where u_i represents the activity level of the ith-neuron, the Hebbian postulate can be mathematically expressed as

$$\Delta C_{ij} = \alpha u_i u_j,$$

or in vector notation

$$\Delta C = \alpha \vec{u}\vec{u}^T, \tag{3.1}$$

where α is a proportionality constant and the pairwise changes of correlation between glomeruli, ΔC_{ij}, corresponds to the "trace" mentioned by Hebb, that eventually leads to synaptic modification. In neural-network modelling

(see e.g. [Hertz et al., 1991]), ΔC_{ij} itself is often directly identified with the synaptic changes. This is, however, an oversimplification of the Hebbian postulate.

According to (3.1), neuron (glomerular) pairs that are strongly excited during stimulation increase their correlation. Neuron (glomerular) pairs where one neuron (glomerulus) is excited and the other one inhibited, decrease their correlation. Neuron (glomerular) pairs that are inhibited during stimulation increase their correlation.

3.3 A novel approach to test the Hebbian hypothesis

The odor-evoked activity patterns in the antennal lobe can be used to infer interactions between the glomeruli belonging to the patterns. However, this is a difficult procedure to investigate the interactions between all (several) glomeruli, because it requires a large number of odors to stimulate as many glomeruli as possible. An alternative consists in using the activity patterns of the spontaneous activity. In calcium-imaging data, the spontaneous activity in the antennal lobe is typically 20% lower than the maximum activity recorded during stimulation. At different times during the spontaneous activity different sets of glomeruli are active allowing for the study of interactions between many more glomeruli.

The mechanism that drives the spontaneous activity in the antennal lobe is not known. It may rely on deterministic processes generating aperiodic self-sustained activity, like chaos. It may also be due to stochastic processes, like thermal noise: at finite temperature any electric circuit presents spontaneous random currents. The noise level is a measure of the circuit's temperature [Reif, 1965], provided that other parameters like the impedance remain constant. Also in neurons at a finite temperature random currents flow through the ion channels [Levitan and Kaczmarek, 1997], as observed with patch-clamp techniques [Sakmann and Neher, 1995].

A successful attempt to uncover the architecture of a neural network from the spontaneous activity has been reported by [Tsodyks et al., 1999]. The authors show with imaging techniques that cortical areas that are simultaneously active during stimulation also correlate during the spontaneous activity.

The procedure we apply here is similar to the so-called Reverse Engineering or System Identification Theory [Ljung and Ljung, 1998]. Reverse Engineering consists of considering an unknown system (e.g. electric device,

mechanical structure) as a black box with an input (driving force) and an output (response). Then, by studying the response to a known input (e.g. noise) some properties of the system (e.g. number of degrees of freedom, resonances, existence of feedback loops, self-sustained oscillations, etc.) can be inferred.

3.3.1 Network Structure and Spontaneous Activity

We regard the antennal-lobe during the spontaneous activity as a stochastic dynamical system whose statistical properties are determined by the probability distribution of glomerular activity measured with calcium imaging (see Appendix B):

$$p(\vec{x}) = p(x_1, x_2, ..., x_n),$$

where x_i refers to the activity in the ith-glomerulus. Once $p(\vec{x})$ is known, the interactions between glomeruli can in principle be estimated through joint and conditional probabilities. However, for high dimensional systems like neural networks $p(\vec{x})$ is difficult to handle. Therefore, it is preferable not to use $p(\vec{x})$ itself but rather the lower-dimensional associated quantities called moments [Honerkamp, 1993]. The moments of $p(\vec{x})$ can be obtained from the expansion of the formal Laplace transform of $p(\vec{x})$ [McCullagh, 1987]:

$$M(\vec{s}) = \int_{-\infty}^{\infty} p(\vec{x})e^{\vec{s}\vec{x}}d^n\vec{x} = 1 + \sum_i s_i \int_{-\infty}^{\infty} x_i p(\vec{x})d^n\vec{x} \ \ +$$

$$\sum_{i,j} s_i s_j/2! \int_{-\infty}^{\infty} x_i x_j p(\vec{x})d^n\vec{x} \ \ +$$

$$\sum_{i,j,k} s_i s_j s_k/3! \int_{-\infty}^{\infty} x_i x_j x_k p(\vec{x})d^n\vec{x} \ \ + \ \ ... \qquad (3.2)$$

being the m-th-order moment

$$\int_{-\infty}^{\infty} x_i x_j ... x_m p(\vec{x})d^n\vec{x}.$$

The expansion (3.2) reveals that moments of increasing order provide finer detail of $M(\vec{s})$ and hence of $p(\vec{x})$, as the Laplace transform is unique.

The calculation of $p(\vec{x})$ or its moments is mathematically consistent only if the signals are stationary [Priestley, 1996], i.e., if $p(\vec{x})$ does not explicitly depend on time. This is usually not the case with calcium-imaging signals because they have artifacts due to animal movements, calcium diffusion and bleaching. These artifacts can nevertheless be removed with an appropriate high-pass filter (see Appendix B). The filter also sets the first order moment (mean) to zero. Thus, after preprocessing, the lowest order description of the

statistics in $p(\vec{x})$ is given by the second-order moment, which for zero-mean data, is the covariance matrix.

Assuming that averaging over $p(\vec{x})$ is equivalent to averaging over the realizations of $\vec{x}$ in time (ergodicity), the covariance matrix C can be directly estimated from the spontaneous activity with

$$C_{ij} = \frac{1}{N} \sum_{t=1}^{N} x_i(t) x_j(t),$$

or in vector notation

$$C = \frac{1}{N} \sum_{t=1}^{N} \vec{x}(t)\vec{x}(t)^T. \tag{3.3}$$

To reduce finite-size effects in the estimation of C one can additionally use bootstrap methods (see Appendix B). If the spontaneous activity $x_i(t)$ of each glomerulus $i = 1, .., n$ is normalized to unitary variance

$$\sigma^2(x_i) = \frac{1}{N} \sum_{t=1}^{N} x_i^2(t) = 1, \tag{3.4}$$

then the covariance matrix is called the correlation matrix, as the element C_{ij} is the correlation coefficient between $x_i(t)$ and $x_j(t)$. From now on, we will consider the correlation matrix for two reasons: i) It equalizes intensity differences between glomeruli which have been caused by an inhomogeneous staining and a different location with respect to the focus of the microscope. ii) With the correlation matrix we can exclude that the memory effects we report below are due to a simple increase of variance in some glomeruli after stimulation.

3.3.2 Traces of sensory memory in the spontaneous activity

Having demonstrated how to uncover interactions between glomeruli from the spontaneous activity, the next step is to study whether those interactions change after stimulus presentation. In other words, we now look for traces of sensory memory following the Hebbian hypothesis.

The pairwise correlation changes between glomeruli can be calculated as:

$$\Delta C_{ij} = C_{ij}^{post} - C_{ij}^{pre}.$$

Such a straightforward calculation, however, does not give us the significance level of the changes. An estimator of ΔC that retains only significant

changes of correlation can be achieved with bootstrap methods (for details see Appendix B).

Each of the figures 3.1-3.9 shows the correlation matrix in a different bee before (top) and after (middle) a single odor presentation, as well as the correlation changes (bottom). The bees were presented one of the following odors: hexanol, octanol, limonene, limonene+linanol (see also Appendix B). Before stimulation some glomeruli correlate strongly as a result of the network architecture. The correlation matrix after stimulation is similar to the correlation matrix before but, for most of the bees remarkable changes in some glomeruli can be observed. The changes are quantified in the matrix ΔC below. In all matrices the glomeruli are ordered from left to right (x-axis) and top to bottom (y-axis) according to the activity level during stimulation (see respectively Figs. 3.10-3.18 at the bottom): those most excited glomeruli during stimulation lie at the bottom-right corner and the most inhibited at the top-left corner. This representation allows us to rapidly look for a Hebbian mechanism in the changes of correlation. Following the Hebbian postulate expressed in formula (3.1), we should find positive changes of correlation (hot colors) in the lower-right and upper-left corners of ΔC whereas we should find negative changes (cold colors) in the lower-left and upper-right corners. This trend is found in almost all bees investigated. These changes of correlation provide evidence of Hebbian-like plasticity and represent traces of a sensory memory in the antennal-lobe network after a single odor presentation.

3.3.3 Stimulus reconstruction from the spontaneous neural activity

The matrix of change of correlation between glomeruli contains information about the last odor presented. We now show how to retrieve this information.

The matrix ΔC can be expanded as a function of all its eigenvectors ξ_i^n and approximated by a function of the dominant one ξ_i^1 (i.e. the eigenvector whose eigenvalue is largest in magnitude):

$$\Delta C_{ij} = \sum_{p=1}^{n} \lambda_p \xi_i^p \xi_j^p \approx \lambda_1 \xi_i^1 \xi_j^1, \qquad (3.5)$$

where ξ_i^p is the i-th component of the p-th eigenvector and its corresponding eigenvalue. The number of recorded glomeruli is denoted by n. Since the size of the matrix ΔC_{ij} is $n \times n$, it has in general n eigenvectors of dimension n. The relative weight of the dominant eigenvalue, $|\lambda_1| / \sum_{p=1}^{n} |\lambda_p|$, ranges from 24% to 37%, depending on the bee.
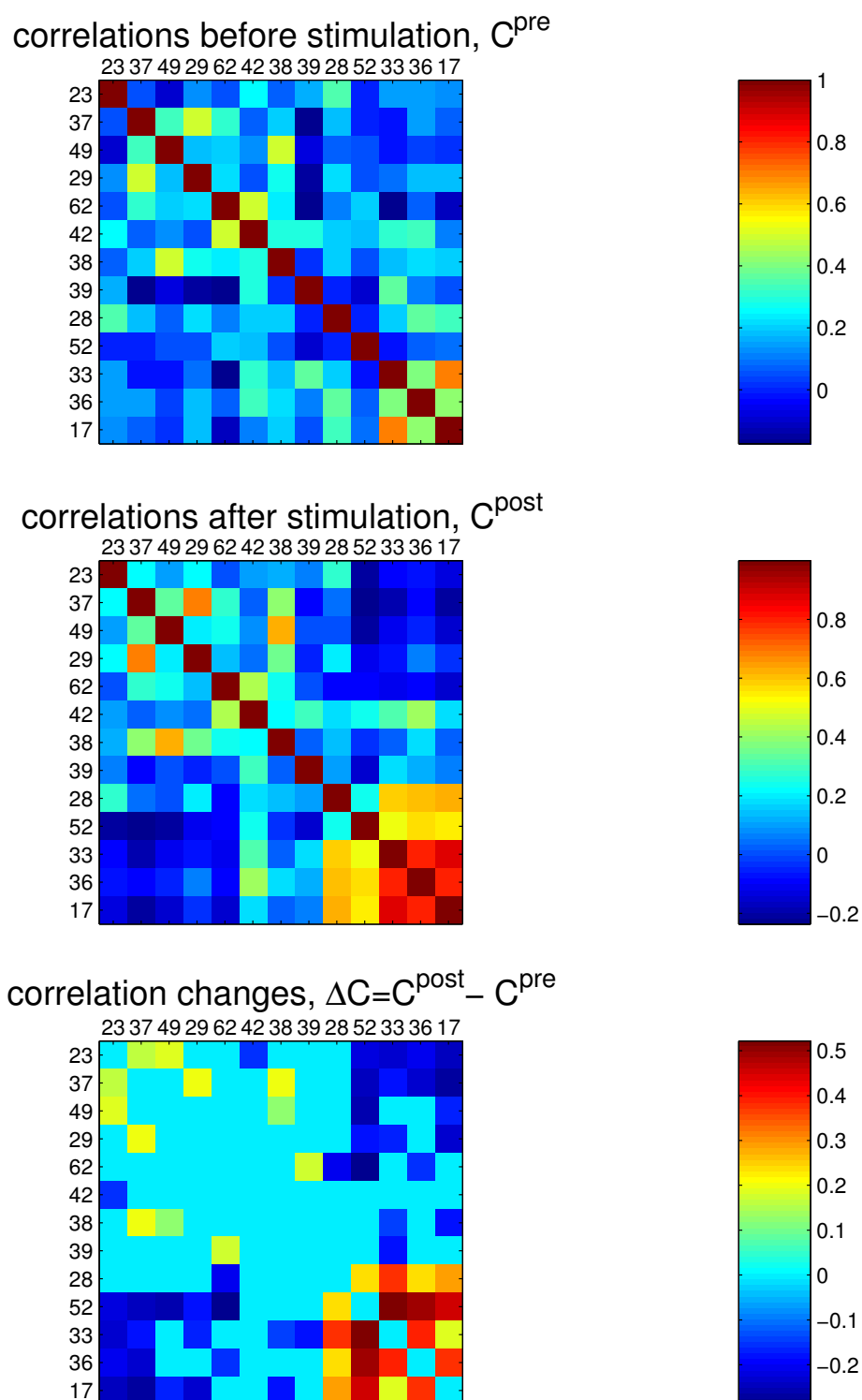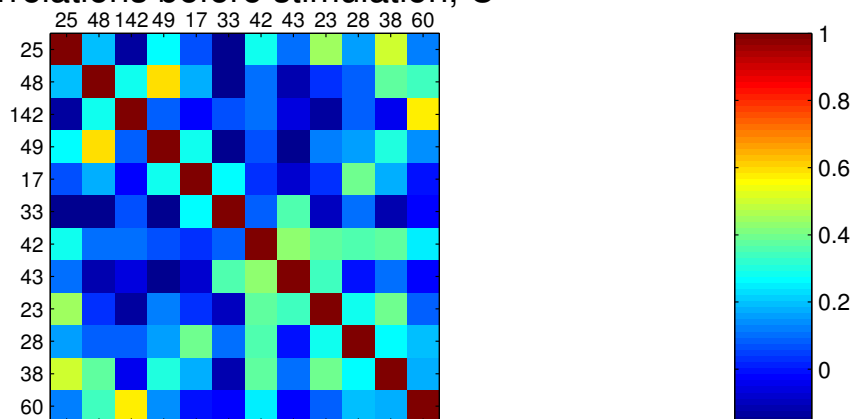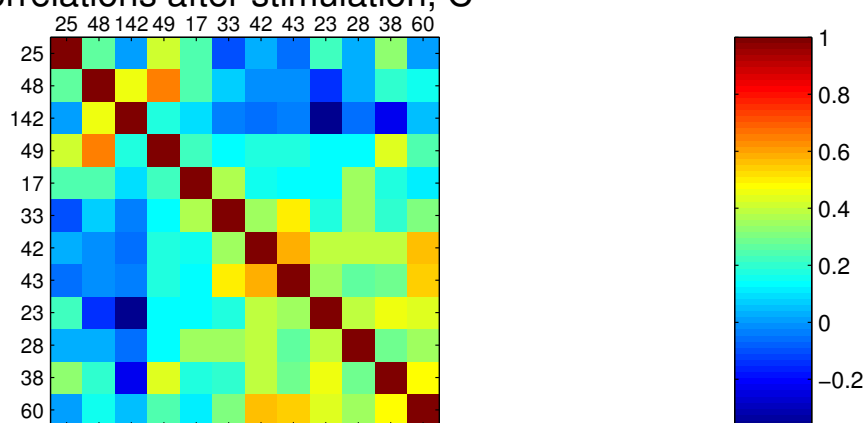
Figure 3.1: C^{pre}, C^{post} and ΔC in bee no. 1 (odor presented: octanol).
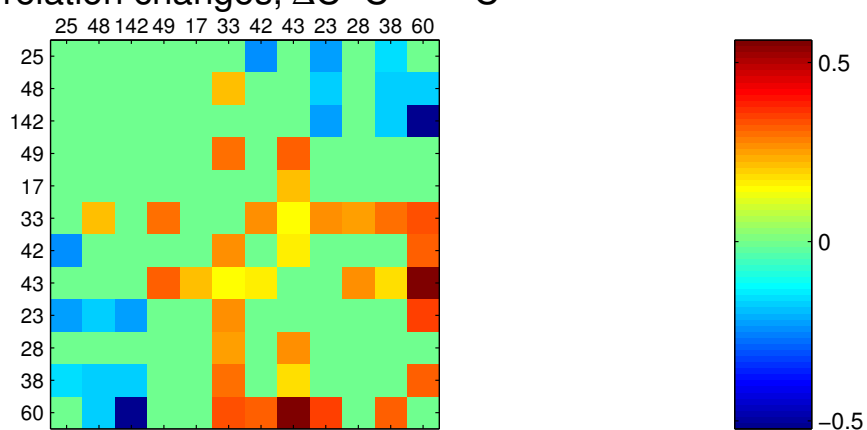
Figure 3.2: C^{pre}, C^{post} and ΔC in bee no. 2 (odor presented: limonene)
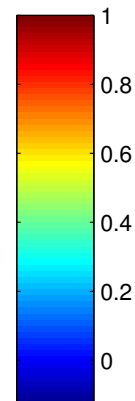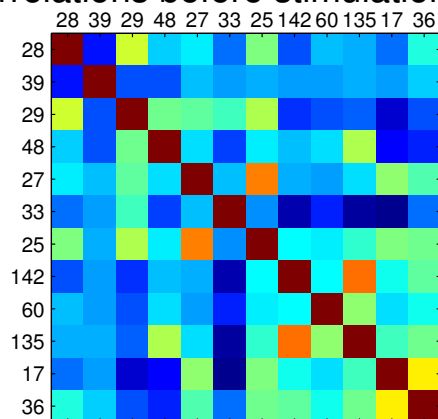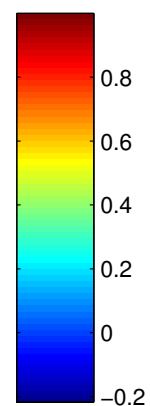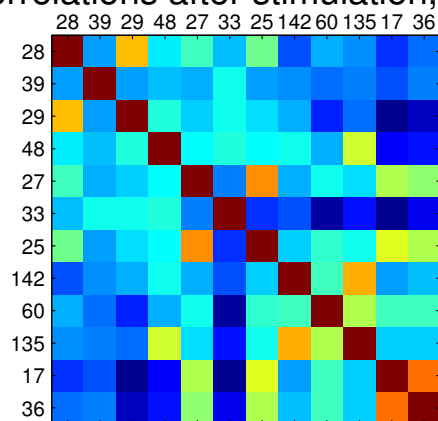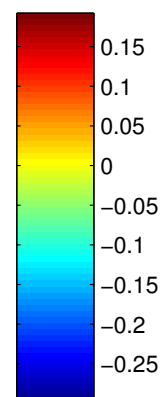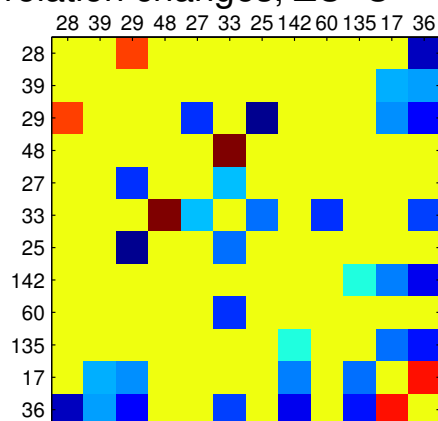
Figure 3.3: C^{pre}, C^{post} and ΔC in bee no. 3 (odor presented: hexanol)
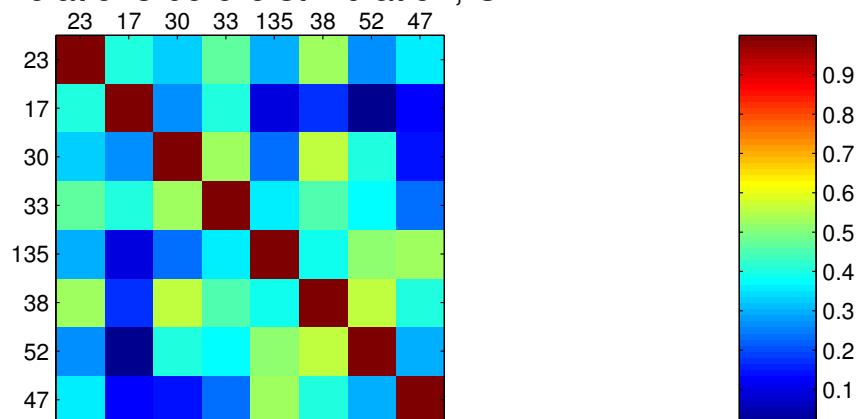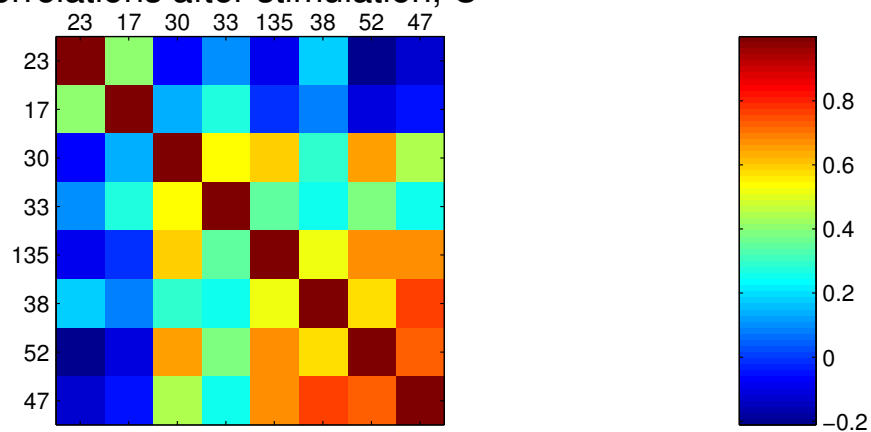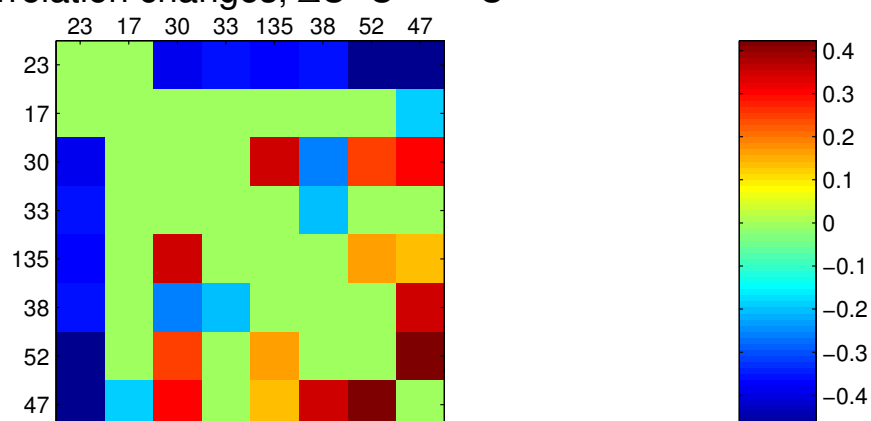
Figure 3.4: C^{pre}, C^{post} and ΔC in bee no. 4 (odor presented: octanol)
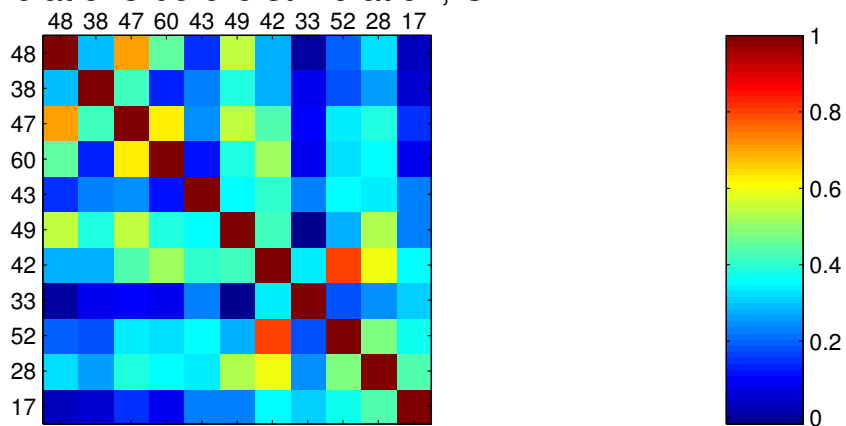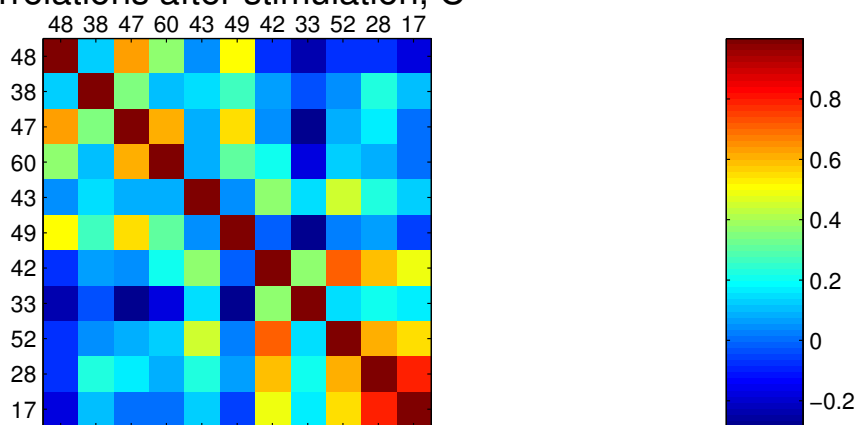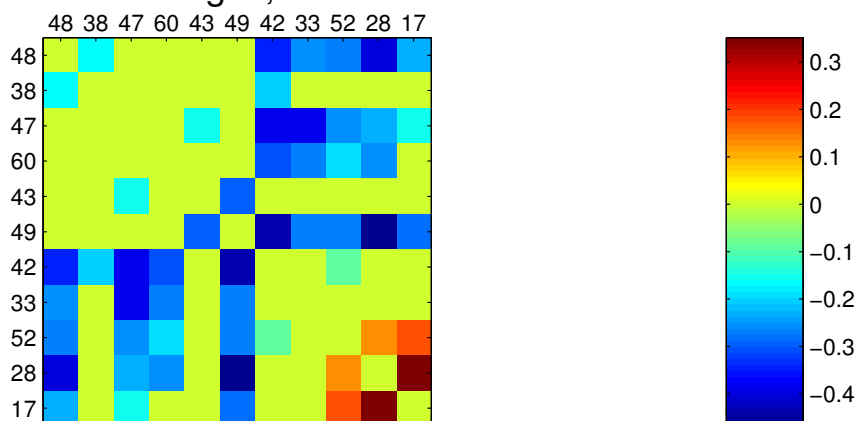
Figure 3.5: C^{pre}, C^{post} and ΔC in bee no. 5 (odor presented: octanol)
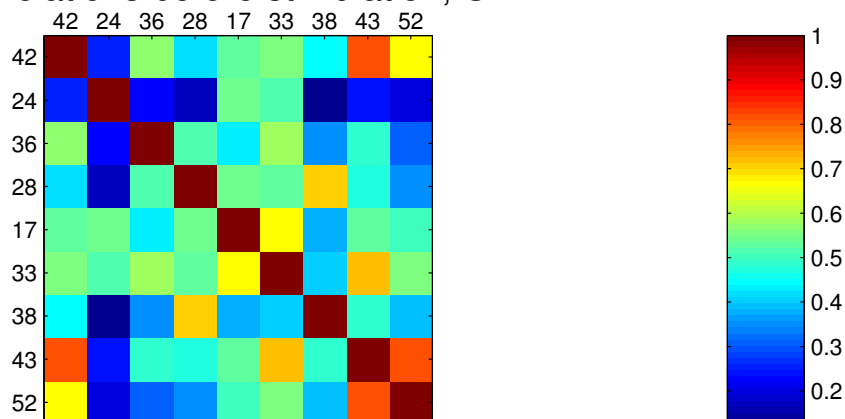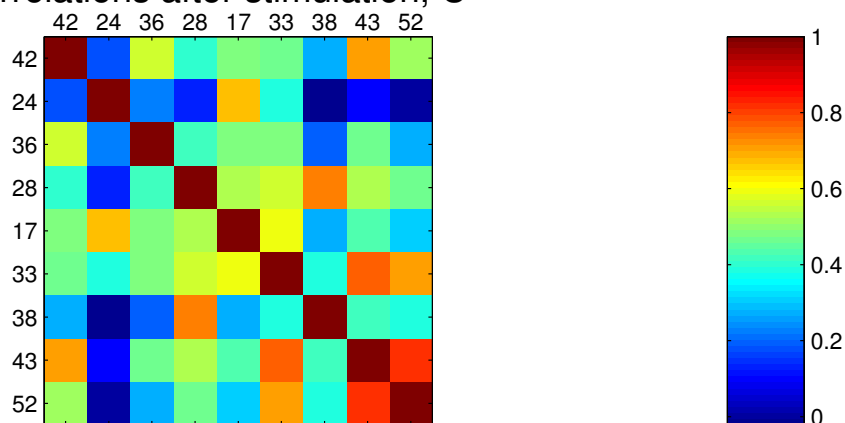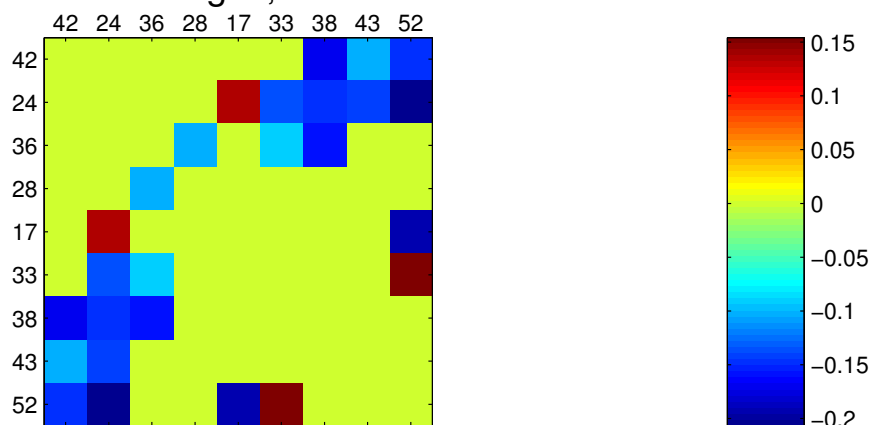
Figure 3.6: C^{pre}, C^{post} and ΔC in bee no. 6 (odor presented: limonene+linanol)
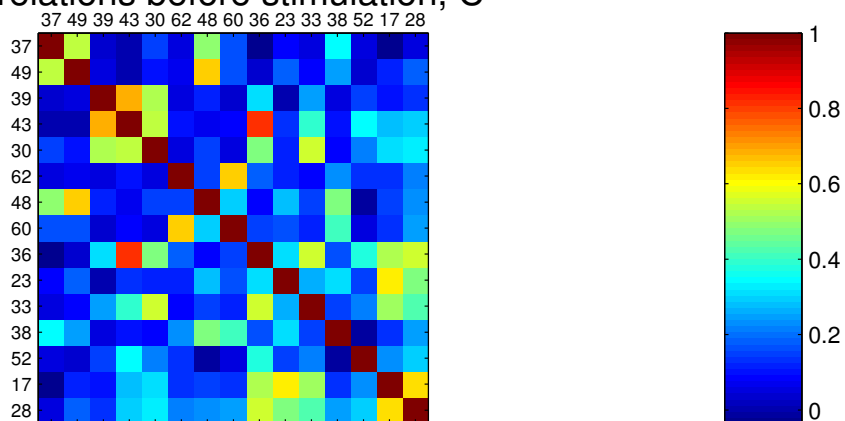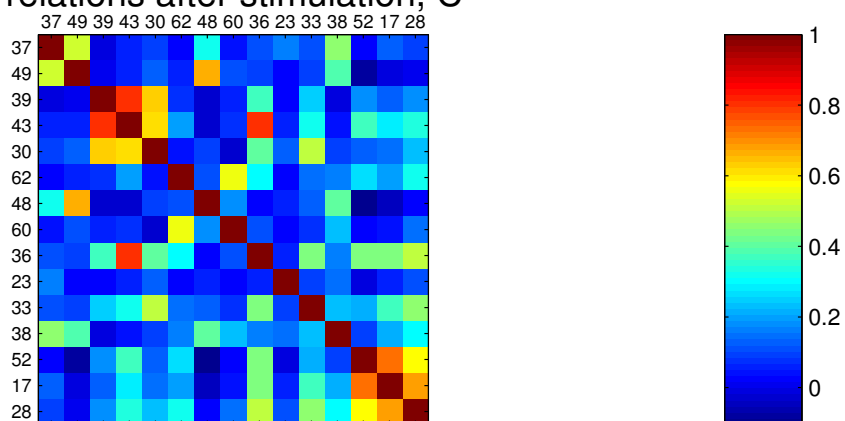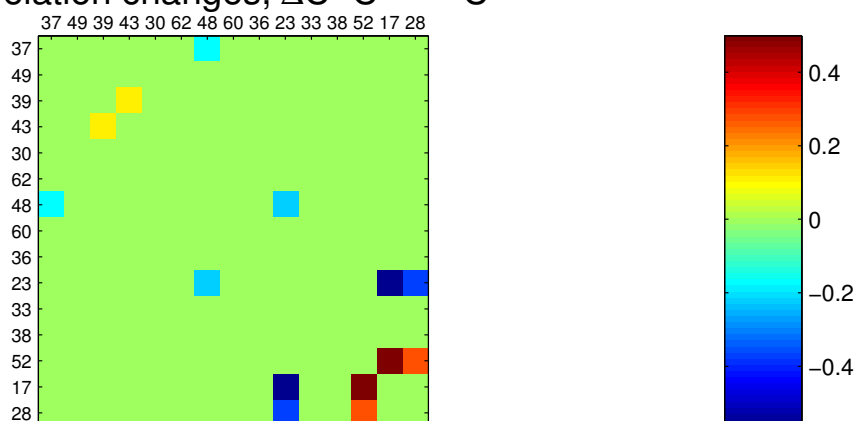
Figure 3.7: C^{pre}, C^{post} and ΔC in bee no. 7 (odor presented: octanol)
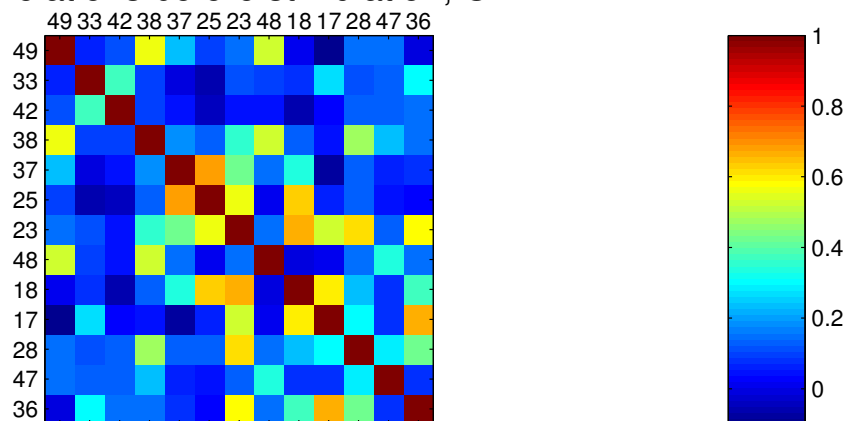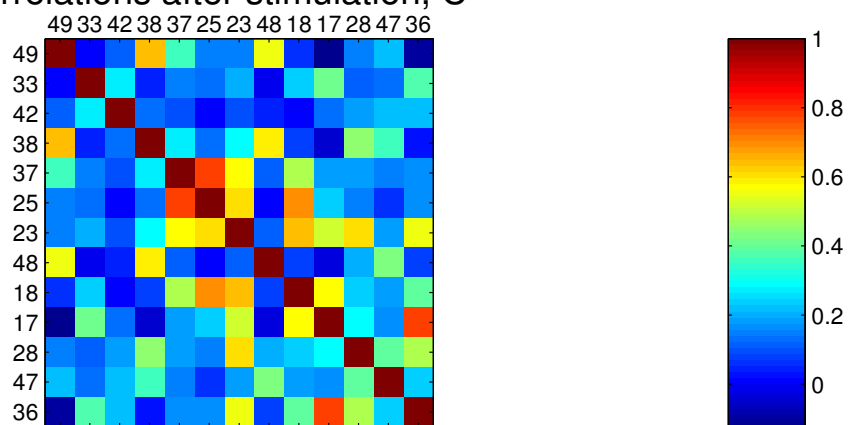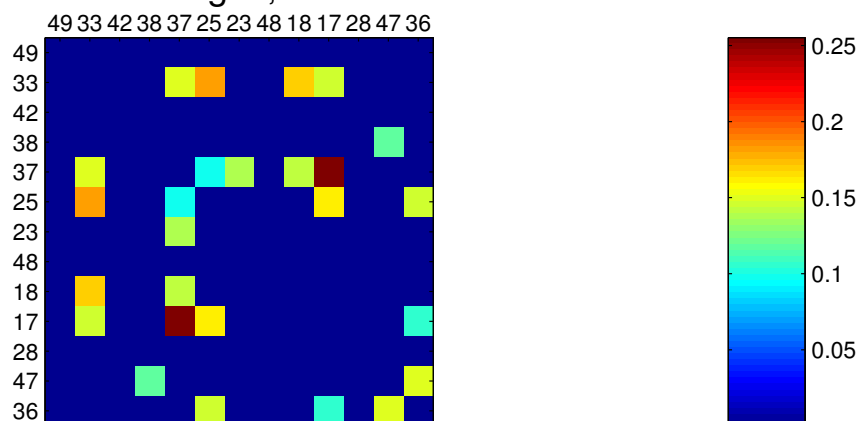
Figure 3.8: C^{pre}, C^{post} and ΔC in bee no. 8 (odor presented: hexanol)
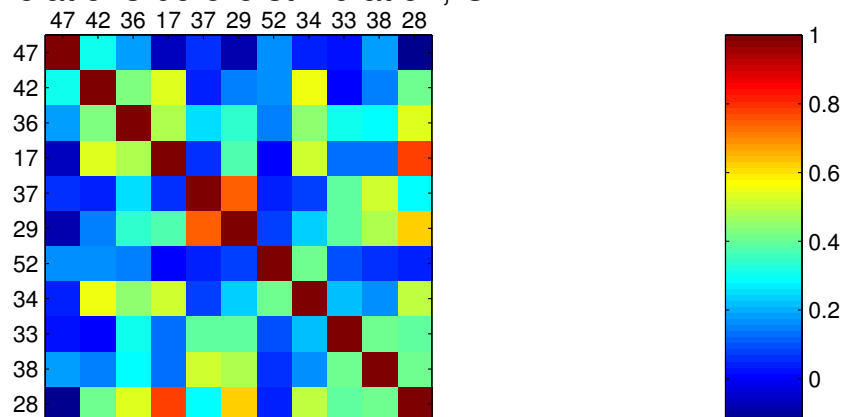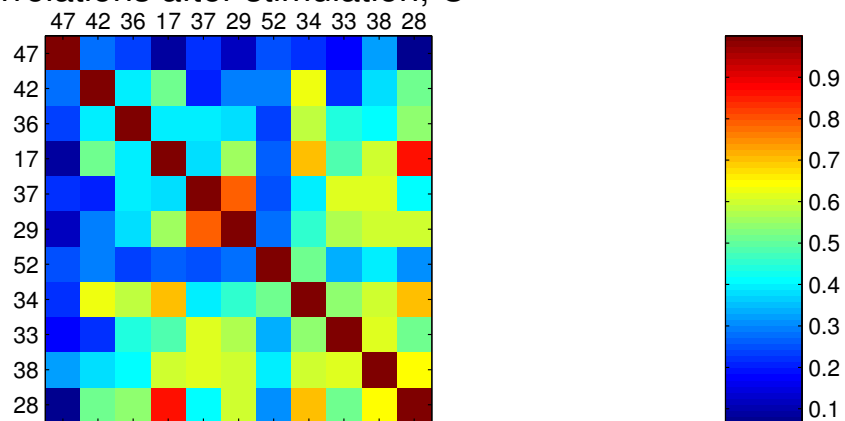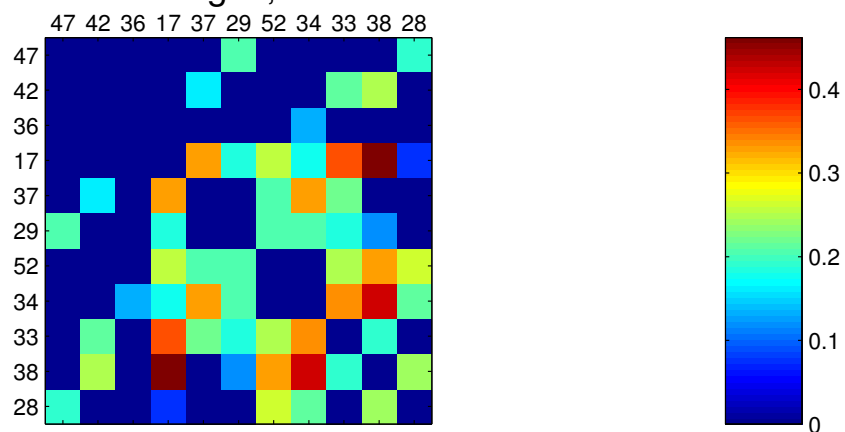
Figure 3.9: C^{pre}, C^{post} and ΔC in bee no. 9 (odor presented: hexanol)

In vector notation (3.5) reads

$$\Delta C = \sum_{p=1}^{n} \lambda_p \vec{\xi}_p \vec{\xi}_p^T \approx \lambda_1 \vec{\xi}_1 \vec{\xi}_1^T. \tag{3.6}$$

By comparing (3.6) with the Hebbian rule (3.1) we conclude

$$\vec{u} \approx \sqrt{\lambda_1/\alpha} \cdot \vec{\xi}_1, \tag{3.7}$$

which means that *the dominant eigenvector $\vec{\xi}_1$ of the matrix of changes of correlation resembles the activity pattern $\vec{u}$ evoked by the last experienced stimulus*, up to a scaling factor. Before we check the validity of this statement with the experimental data, we will first interpret the information extracted from C^{pre} and C^{post}.

The eigenvector expansion of ΔC in (3.6) permits us to optimally compress the information of the matrix within a single vector $\vec{\xi}_1$. The same analysis can also be applied to C^{pre} and C^{post}, in order to determine the largest weighed activity pattern in the network before and after stimulation, respectively. Such patterns are the dominant eigenvectors of C^{pre} and C^{post}, which are nothing but the first principal component of the spontaneous activity before and after odor presentation. The first principal component $\vec{\varphi}_1$ can be regarded as the dominant pattern of the network, as it is the spatial pattern $\vec{w}$ that maximizes the average squared projection onto the spontaneous activity:

$$\max_{|\vec{w}|=1} \frac{1}{N} \sum_{t=1}^{N} (\vec{x}(t)^T \vec{w})^2 = \frac{1}{N} \sum_{t=1}^{N} (\vec{x}(t)^T \vec{\varphi}_1)^2.$$

To prove this result (see also [Beckerman, 1995]), we first define the cost function $\mathcal{L}$ as the mean square projection of an unknown pattern $\vec{w}$ onto the spontaneous activity $\vec{x(t)}$:

$$\begin{aligned}
\mathcal{L} = \frac{1}{N} \sum_{t=1}^{N} (\vec{x}(t)^T \vec{w})^2 &= \frac{1}{N} \sum_{t=1}^{N} (\vec{w}^T \vec{x}(t))(\vec{x}(t)^T \vec{w}) \\
&= \vec{w}^T \left(\frac{1}{N} \sum_{t=1}^{N} \vec{x}(t)\vec{x}(t)^T \right) \vec{w} \\
&= \vec{w}^T C \vec{w},
\end{aligned}$$

where C is the correlation matrix. One constrains the maximization to patterns normalized to unity by introducing an additional term with a Lagrange multiplier λ

$$\mathcal{L} = \vec{w}^T C \vec{w} - \lambda(\vec{w}^T \vec{w} - 1).$$

The cost function $\mathcal{L}$ evaluated at the pattern that maximizes/minimizes it has gradient equal to zero

$$\frac{\partial \mathcal{L}}{\partial \vec{w}^T} = 0 \iff C\vec{w} = \lambda \vec{w}.$$

Thus the optimization of the cost function $\mathcal{L}$ is converted to the eigenvalue problem of the correlation matrix, i.e., the eigenvectors $\vec{w}_i = \vec{\varphi}_i$ of C, or equivalently the principal components of the spontaneous activity, optimize the cost function $\mathcal{L}$. In particular, the eigenvector $\vec{\varphi}_1$ with largest magnitude (dominant) eigenvalue λ_1 will maximize $\mathcal{L}$. The relative weight of the first eigenvalue ranges from 23% to 54% for C^{pre}, and from 28% to 51% for C^{post}, depending on the bee.

We now check which of the dominant eigenvectors of C^{pre}, C^{post} and ΔC permits us to best reconstruct the odor-evoked activity pattern. Figures 3.10-3.18 display the eigenvectors of the matrices shown in figures 3.1-3.9 respectively, as well as the actual odor-evoked patterns (bottom). The similarity between a given eigenvector and the odor-evoked pattern is quantified by their rank correlation r (see Appendix B). The rank correlation yields a value close to the correlation coefficient. However, for the rank correlation a significance level (p-value) can be easily computed without any assumption about the distribution of the data (see [Press et al., 1992]). The significance level p is given together with r in the plots. Values of p larger than 0.05 are considered as not significant. Values of p between 0.05 and 0.001 are considered as significant. Values of p less than 0.001 are considered as highly significant. Higher relative weights of the first eigenvalue, do not imply better retrieval of the stimulus presented.

Before stimulation the dominant pattern of the network does not contain significant information about the odor in any bee. In 6 out of 9 bees the dominant pattern of the network after stimulation is significantly correlated with the odor-evoked pattern. Also in 6 out of 9 bees the dominant eigenvector $\vec{\xi}_1$ of the matrix of changes of correlation significantly correlates with the odor-evoked pattern $\vec{u}$, confirming the theoretical result in equation (3.7). In general, when the dominant network pattern after stimulation carries significant information about the stimulus, so does the first eigenvector of ΔC. However, in one bee (Fig. 3.15) the stimulus inference from ΔC is significant but the inference from C^{post} is not. In another bee (Fig. 3.18), the stimulus inference from C^{post} is significant but the inference from ΔC is not, although the p-value is close to the significance level (p=0.0516).

Figure 3.10: Eigenvectors and odor-evoked pattern in bee no. 1. Amplitude in arbitrary units. All patterns have unitary norm. The relative weight of the dominant eigenvalue was 23% for C^{pre}, 29% for C^{post} and 36% for ΔC.

Figure 3.11: Eigenvectors and odor-evoked pattern in bee no. 2. Amplitude in arbitrary units. All patterns have unitary norm. The relative weight of the dominant eigenvalue was 25% for C^{pre}, 31% for C^{post} and 30% for ΔC.

Figure 3.12: Eigenvectors and odor-evoked pattern in bee no. 3. Amplitude in arbitrary units. All patterns have unitary norm. The relative weight of the dominant eigenvalue was 32% for C^{pre}, 27% for C^{post} and 24% for ΔC.

Figure 3.13: Eigenvectors and odor-evoked pattern in bee no. 4. Amplitude in arbitrary units. All patterns have unitary norm. The relative weight of the dominant eigenvalue was 44% for C^{pre}, 45% for C^{post} and 36% for ΔC.

Figure 3.14: Eigenvectors and odor-evoked pattern in bee no. 5. Amplitude in arbitrary units. All patterns have unitary norm. The relative weight of the dominant eigenvalue was 39% for C^{pre}, 29% for C^{post} and 31% for ΔC.
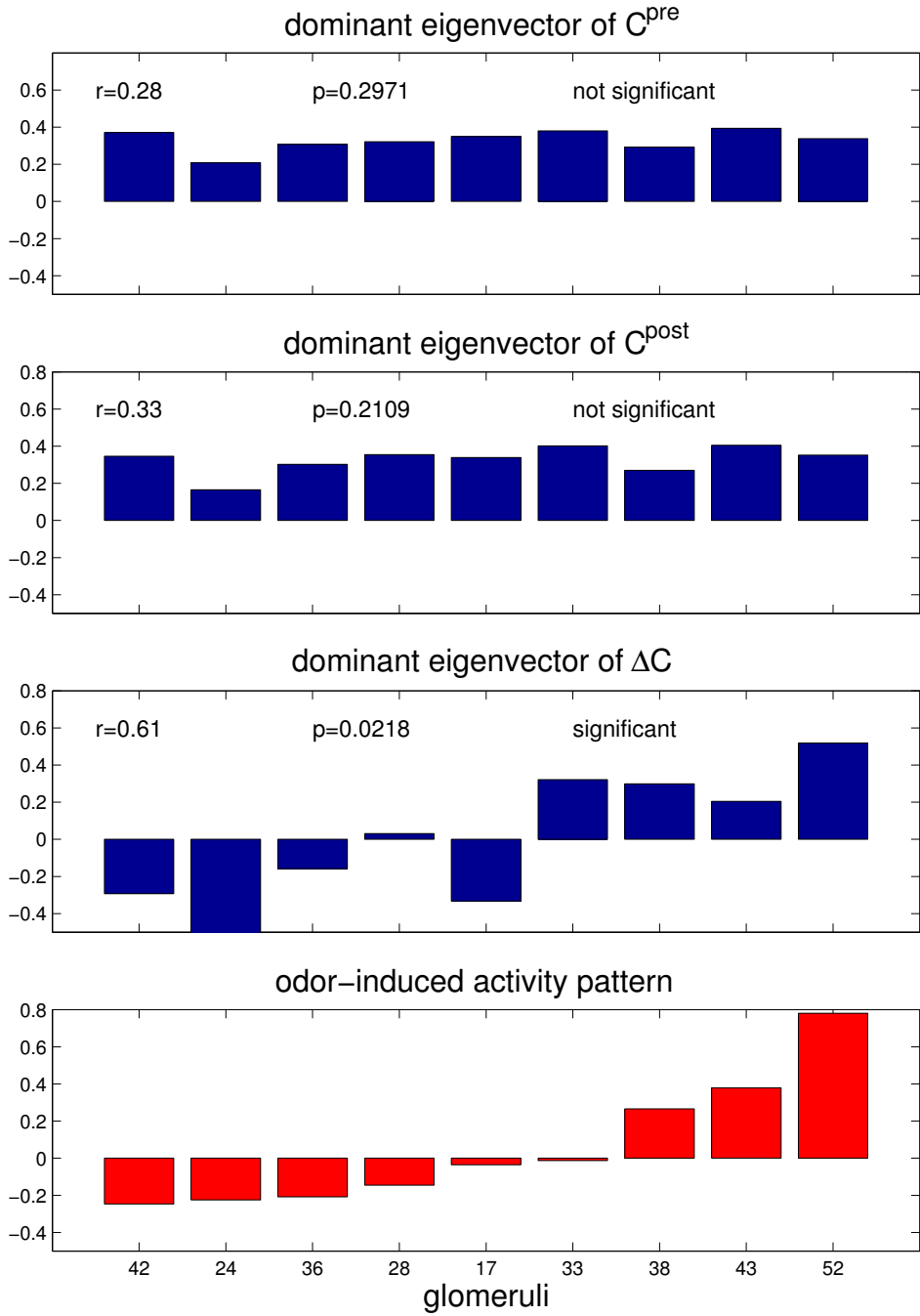
Figure 3.15: Eigenvectors and odor-evoked pattern in bee no. 6. Amplitude in arbitrary units. All patterns have unitary norm. The relative weight of the dominant eigenvalue was 54% for C^{pre}, 51% for C^{post} and 30% for ΔC.
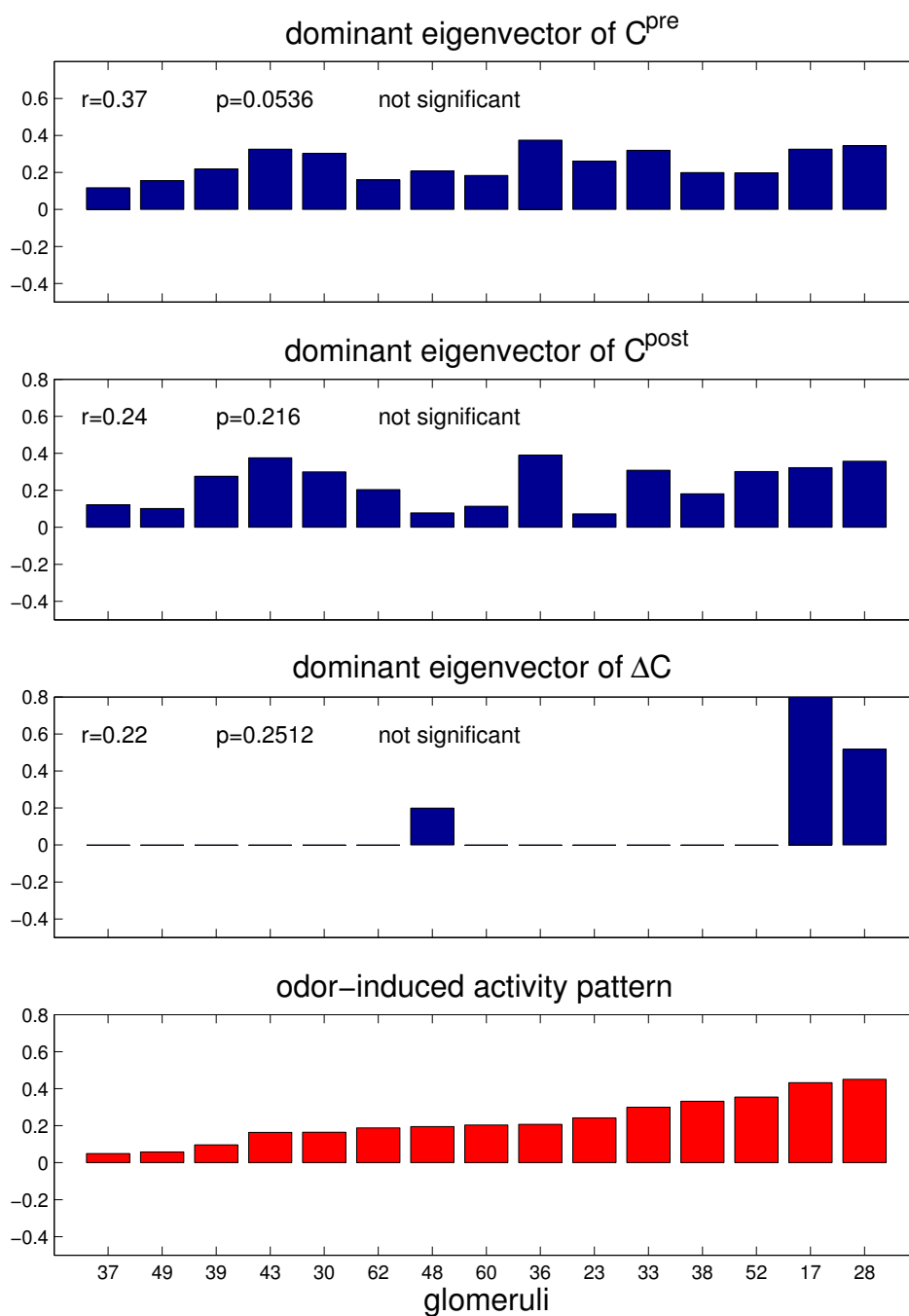
Figure 3.16: Eigenvectors and odor-evoked pattern in bee no. 7. Amplitude in arbitrary units. All patterns have unitary norm. The relative weight of the dominant eigenvalue was 30% for C^{pre}, 28% for C^{post} and 36% for ΔC.
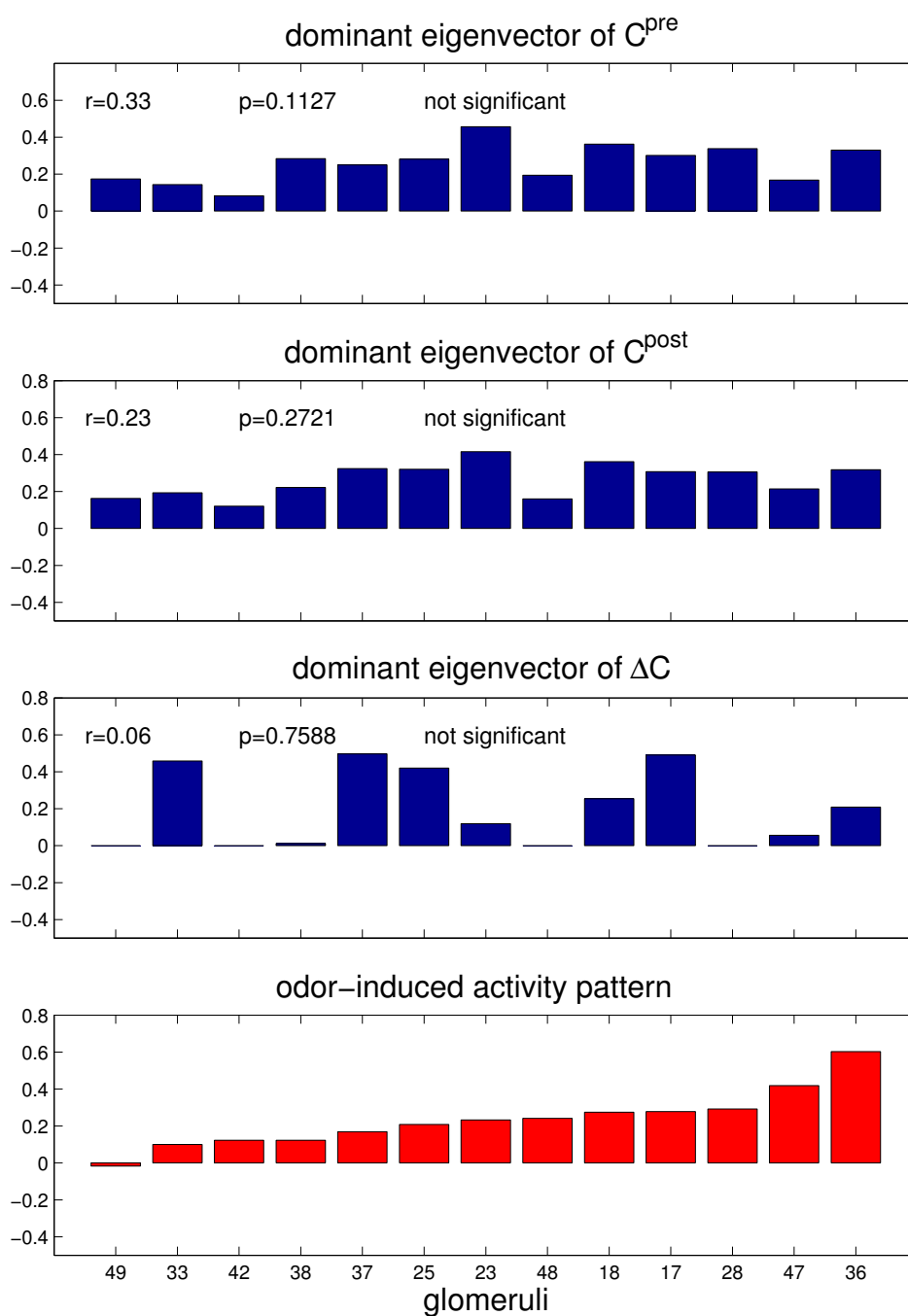
Figure 3.17: Eigenvectors and odor-evoked pattern in bee no. 8. Amplitude in arbitrary units. All patterns have unitary norm. The relative weight of the dominant eigenvalue was 29% for C^{pre}, 32% for C^{post} and 31% for ΔC.
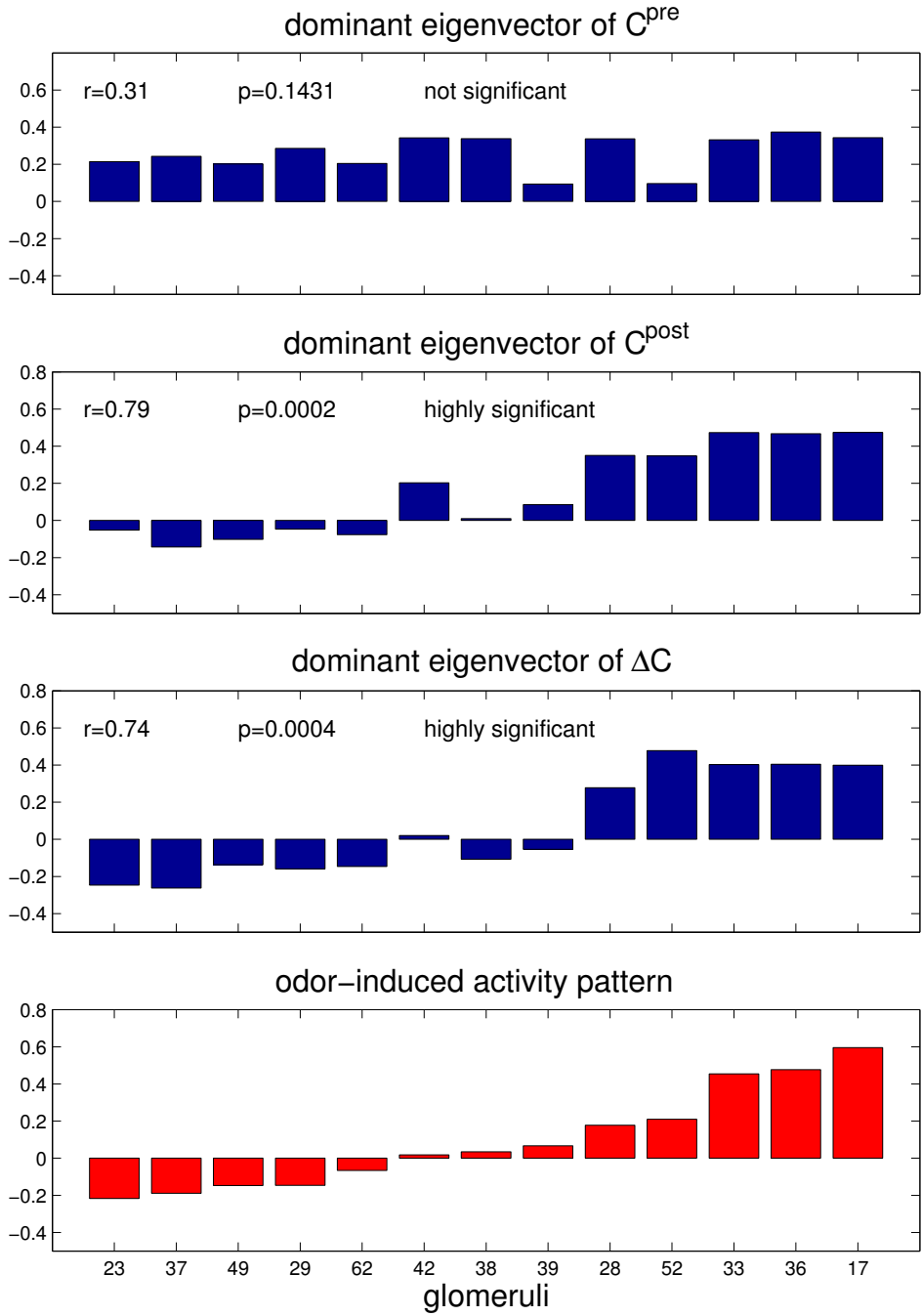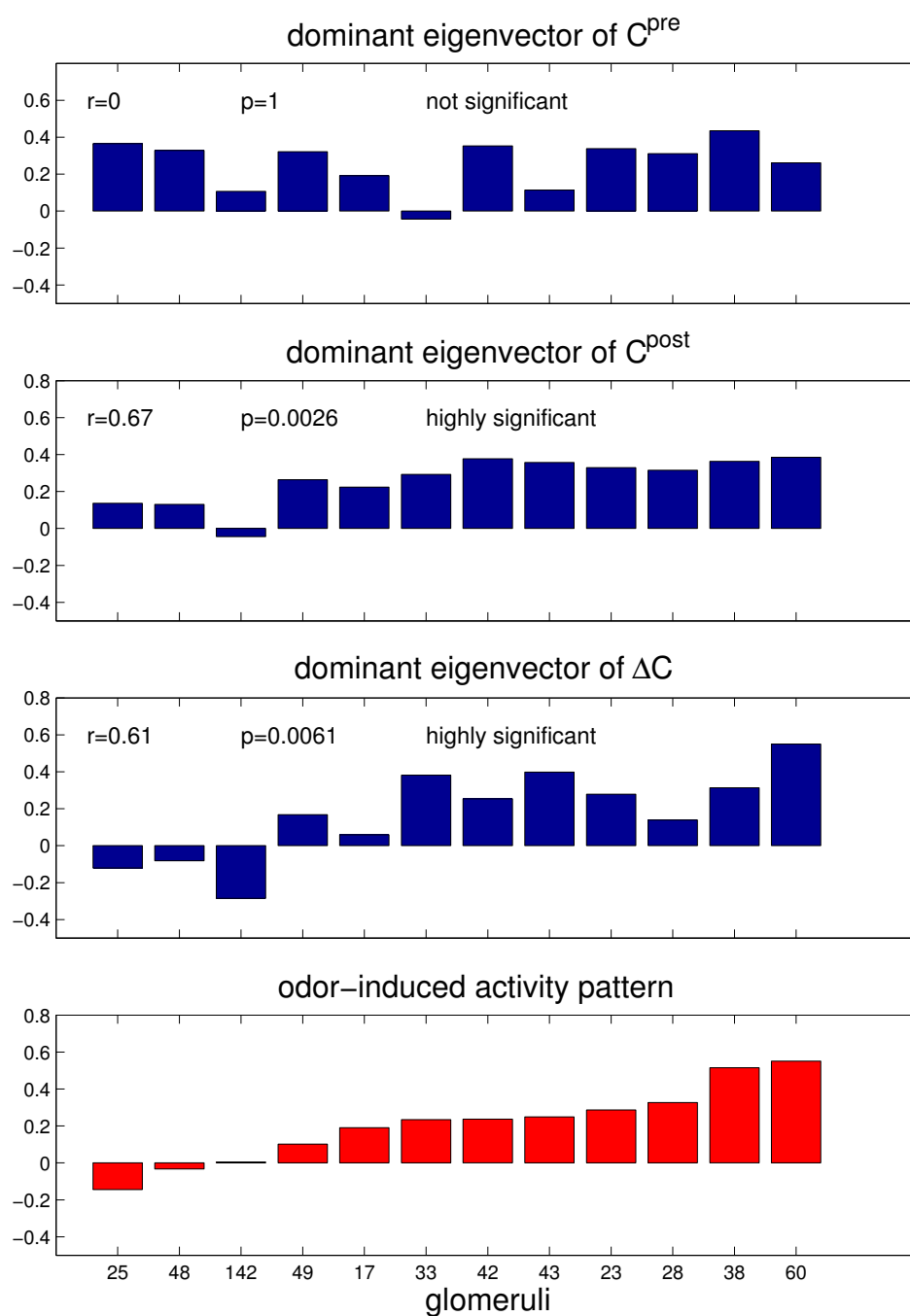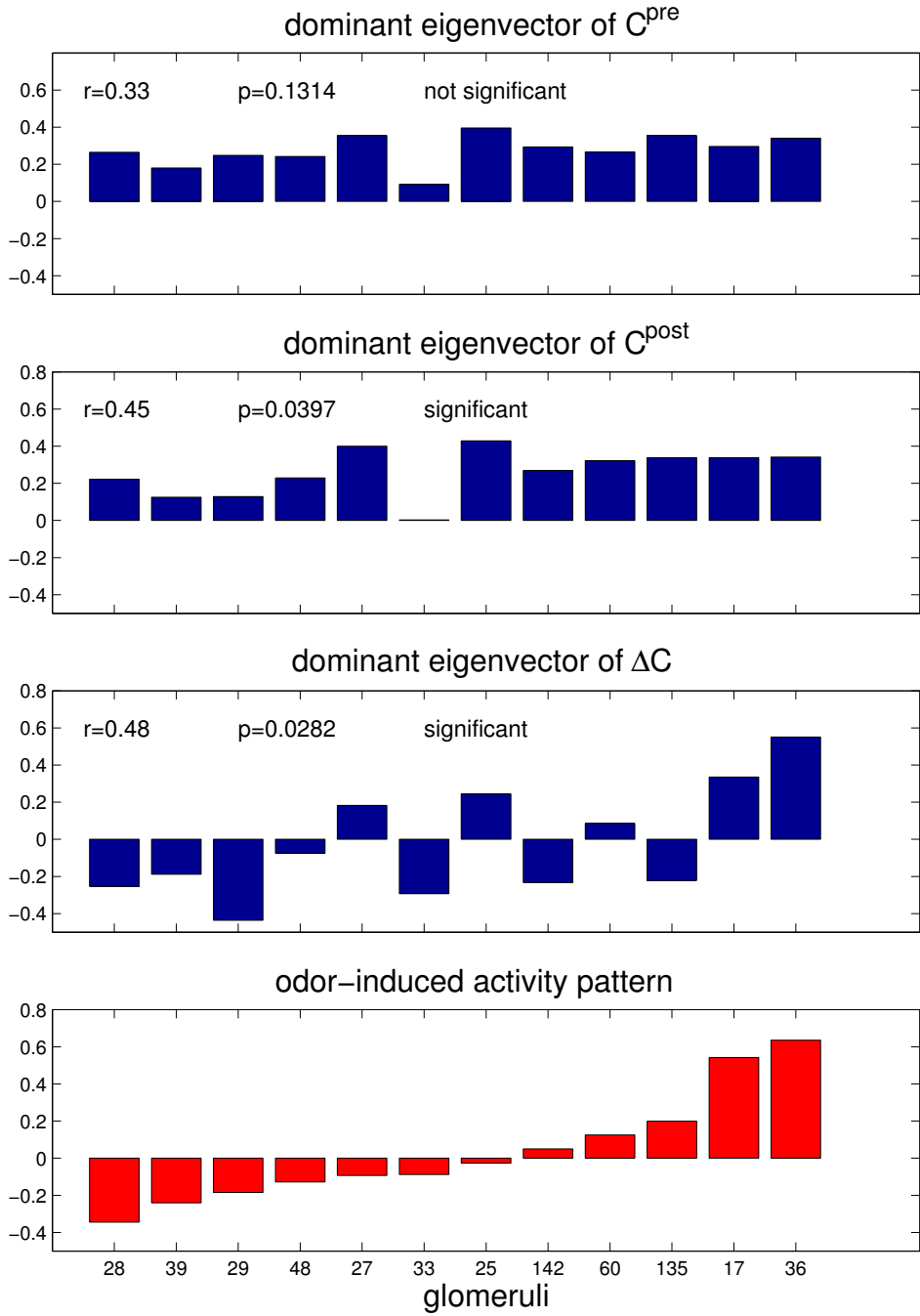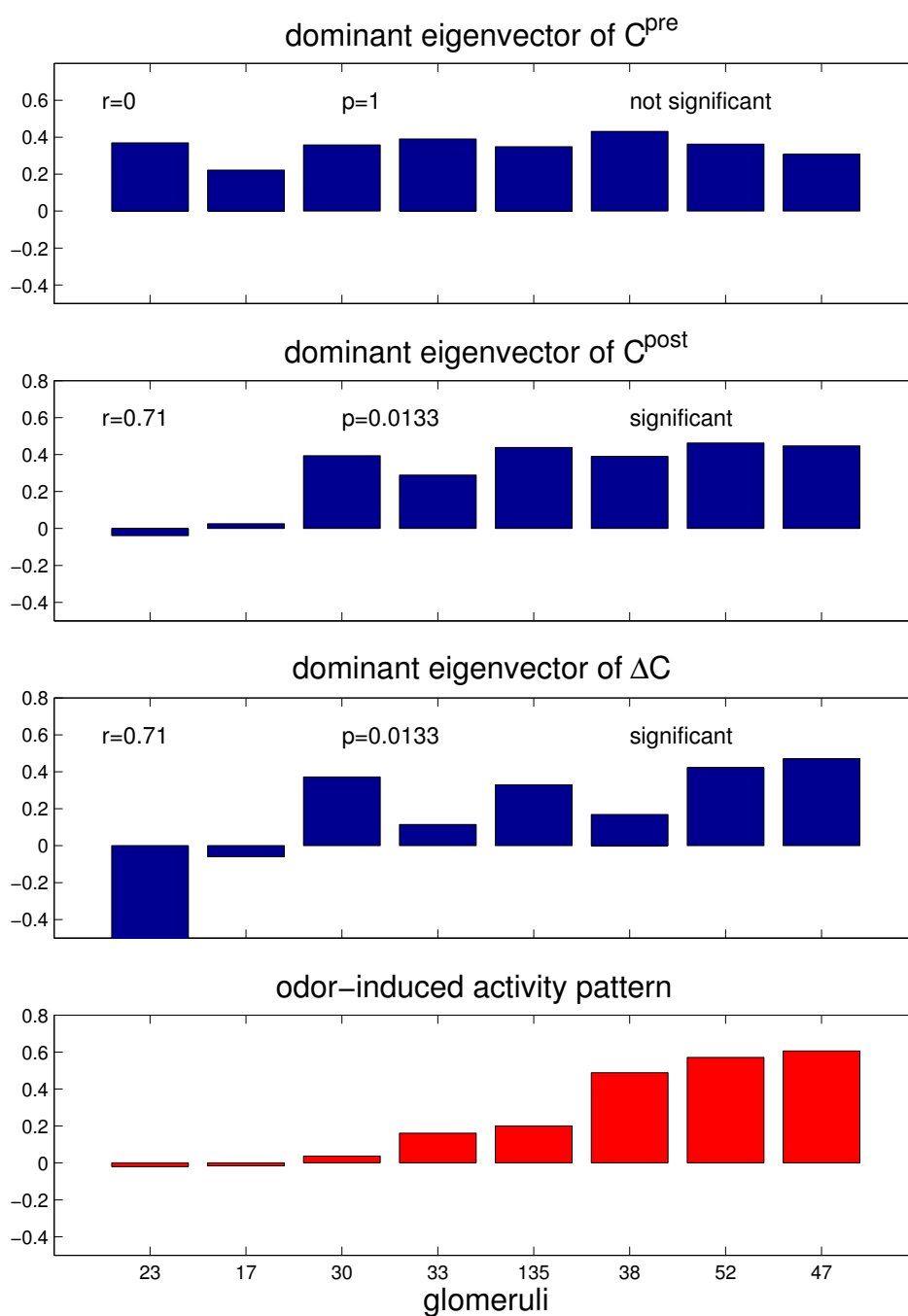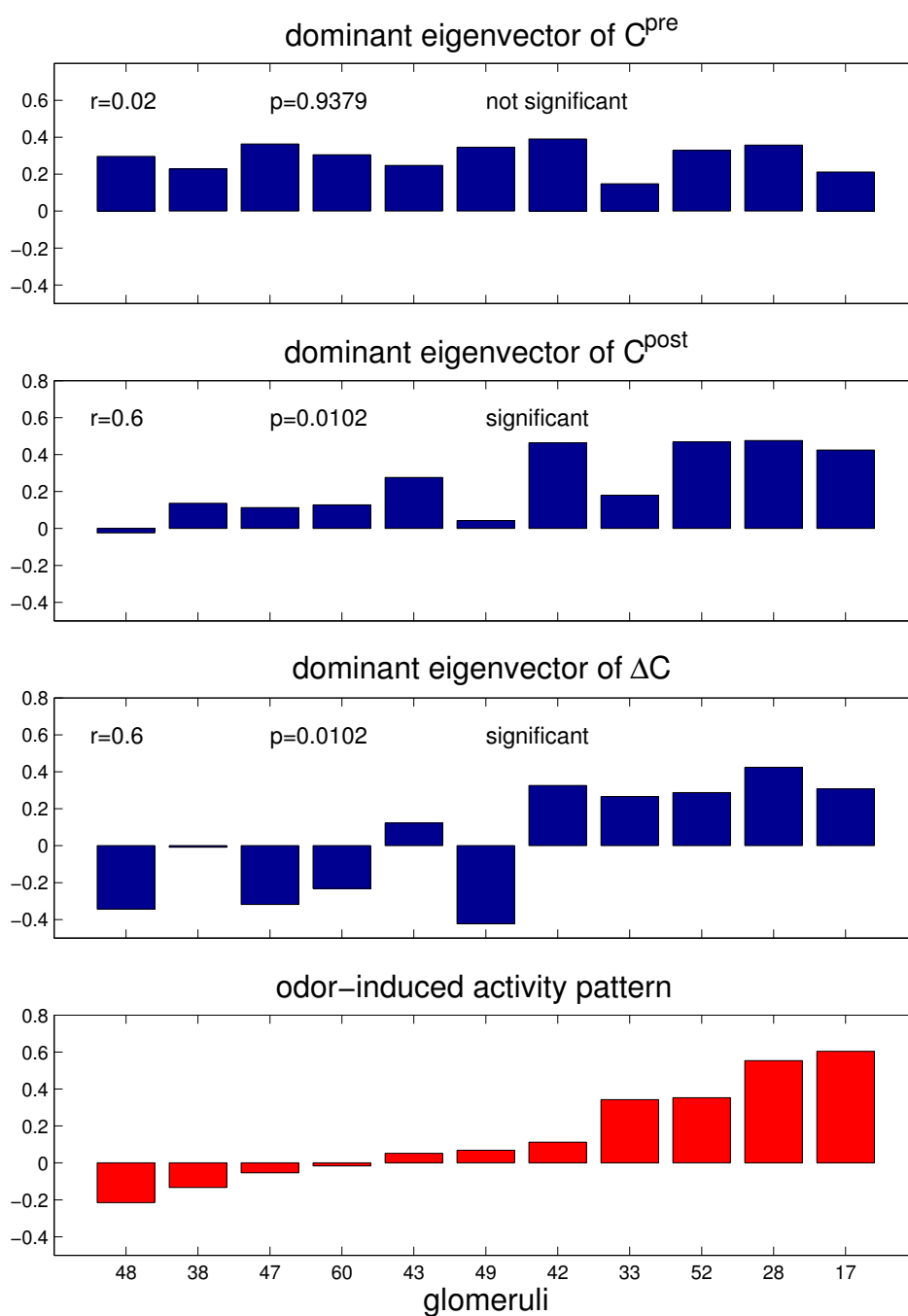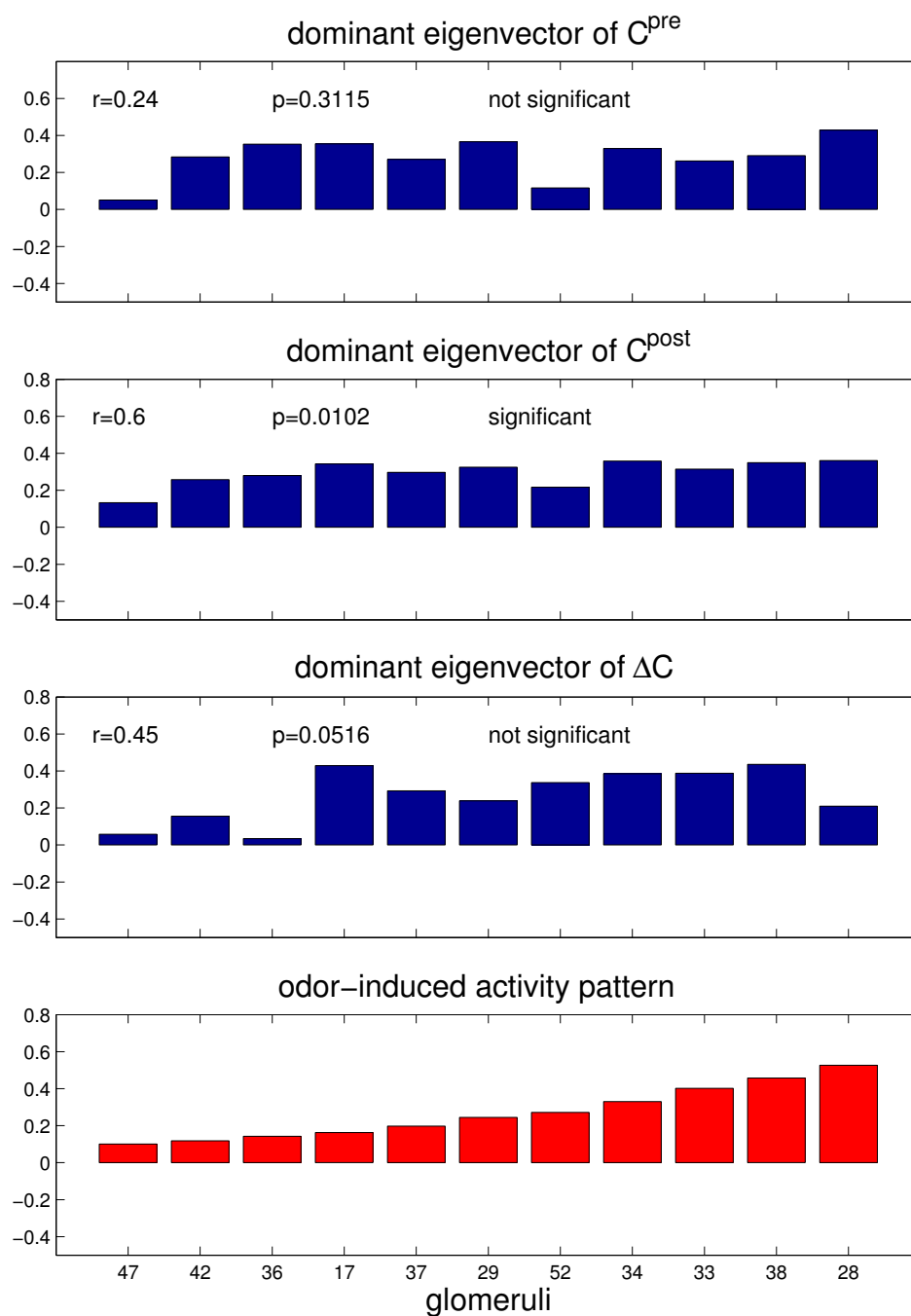
Figure 3.18: Eigenvectors and odor-evoked pattern in bee no. 9. Amplitude in arbitrary units. All patterns have unitary norm. The relative weight of the dominant eigenvalue was 36% for C^{pre}, 50% for C^{post} and 37% for ΔC.

3.3.4 Possible mechanisms underlying Hebbian-like plasticity

We now discuss what biological mechanisms might underly the changes of correlation between glomeruli. A recently reported phenomenon observed with electrophysiology in locusta [Stopfer and Laurent, 1999] may shed light on such mechanisms: after several presentations of the same odor there is a significant increase of synchrony between the spikes of projection neurons (PN) during stimulation. The effect lasts less than 12 minutes. The increase of synchrony is mediated by an enhancement of the inhibitory postsynaptic potentials from inhibitory local interneurons (ILN).

This phenomenon could also underly the Hebbian-like changes of correlation we observe with lower temporal (6 Hz) and spatial resolution (glomeruli, not single PN) after a single odor presentation in honeybees: The correlation between glomeruli would measure the degree of synchrony between their PNs or equivalently the level of common inhibitory input from ILN (correlation ⇔ synchrony ⇔ common inhibitory input). Thus, an increase of correlation between glomeruli after stimulation would result from an increase of common inhibitory input, whereas a decrease of correlation would be the consequence of a decrease of common inhibitory input, via inhibitory connections between ILNs (decrease of common inhibitory input ⇔ less synchrony ⇔ less correlation).

With calcium-imaging data we can also study how the correlations evolve in time. Since the spontaneous activity was recorded for two minutes before and two minutes after stimulation, we repeated the analysis for the first and the second minute separately, before and after stimulation (Fig. 3.19). The boxplots show, resolved in time, the distribution across bees of the Kendall's correlation between the dominant pattern of the spontaneous activity and the odor-induced pattern. The numbers above the boxplots indicate the fraction of bees (out of 9 bees studied) for which the stimulus inference was significantly correlated with the odor-evoked pattern. Before stimulation no prediction of the odor can be made from the spontaneous activity. After stimulation, the dominant pattern of the spontaneous activity during the first minute permits us to reliably infer the odor in 6 out of 9 bees, but the stimulus inference deteriorates by half (3 bees) in the second minute. These results are consistent with the decay within several minutes of the increase of spike synchrony [Stopfer and Laurent, 1999].

If the correlation changes were only due to changes in the timing between spikes of different PNs, the correlation changes should become weaker and eventually vanish at lower sampling rates, where no spikelets can be resolved. To test this we repeated the analysis after downsampling the original data

(Fig. 3.20). Interestingly, no dramatic deterioration of the stimulus inference is observed even down to 0.5 Hz.

Figure 3.21 shows the matrices C^{pre}, C^{post} and ΔC with a sampling rate of 1 Hz for the bee of Fig. 3.1, where the original sampling rate was 6 Hz. Although some information is lost after resampling, the Hebbian plasticity can still be detected. The stimulus retrieval from C^{post} and ΔC is also possible after resampling (compare Fig. 3.22 with Fig. 3.10). This contrasts with the fast time-scale (6 Hz) at which the increase of spiking synchrony between PNs has been reported. Further research should elucidate the biological mechanims underlying the traces of memory shown here. How these mechanisms may lead to memory consolidation will be discussed next.

3.3.5   Biological relevance of a sensory memory

The sensory memory may act as a filter that enhances the last presented odor with respect to the background. It may also prepare the system for a reward that would facilitate memory consolidation in a downstream network (the mushroom body). This could be achieved in the following manner. It is known that the Kenyon cells in the mushroom body behave as coincidence detectors [Pérez-Orive et al., 2002]. An increase of correlation (synchronization) between glomeruli (projection neurons) that encode a certain odor would make the odor pattern more salient during the spontaneous activity with respect to the noisy background. According to the Hebbian postulate, this may lead to a synaptic modification between the neurons in those gomeruli, that would account for a short-term memory in the antennal lobe, provided that sucrose is also given. Analogously, the salient pattern could be interpreted by those Kenyon cells that reacted to the odor as a signal to strengthen their synapses with the salient glomeruli. Such a mechanism would lead to memory consolidation in the mushroom body.

This mechanism is also supported by the experimental findings on synaptic potentiation between the projection neurons in the antennal lobe and the Kenyon cells in the mushroom body [Oleskevich et al., 1997]. Synaptic potentiation can be induced by electrically stimulating the antennal lobe with frequencies of 1 Hz and lower. This time scale is comparable with the time scale of the Hebbian mechanism reported here with calcium-imaging data.

62
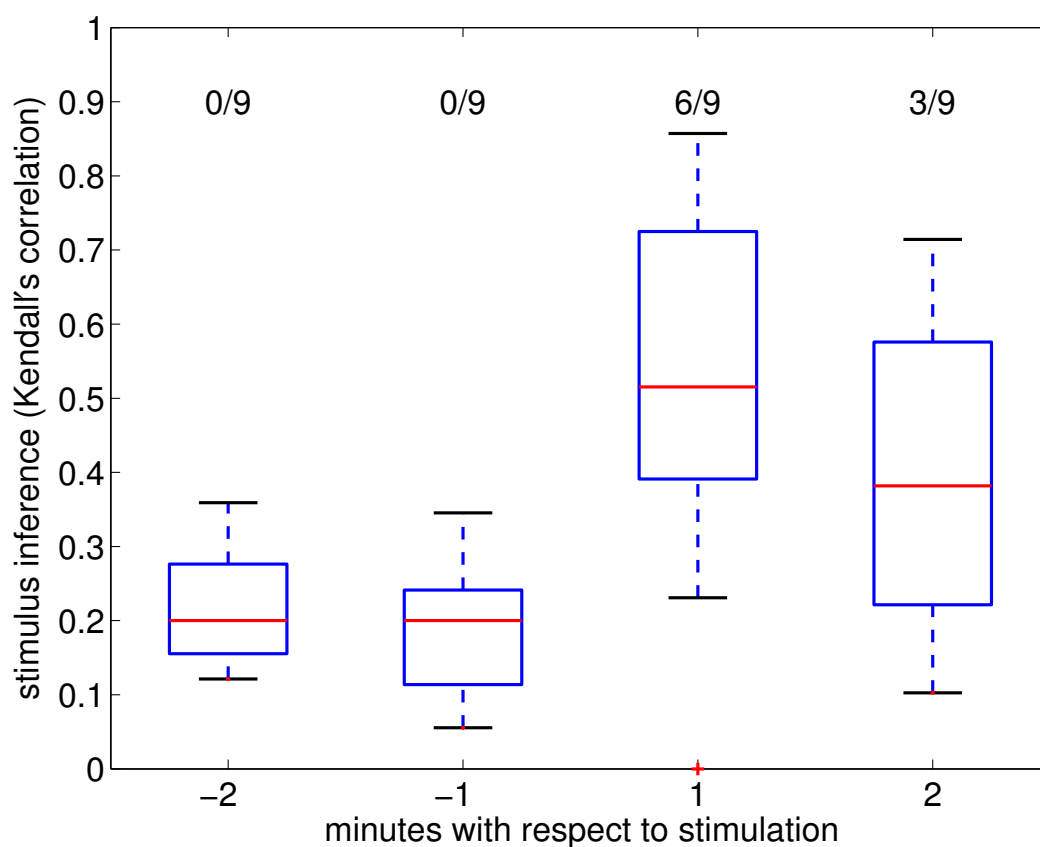
Figure 3.19: Temporal decay of sensory-memory traces. The boxplots represent the distributions across bees at successive time intervals of the Kendall's correlation between the dominant pattern of the spontaneous activity and the odor-evoked pattern. The boxes' height delimits the interquartile range. The line within the boxes indicates the median value. The whiskers indicate the extremal values. The fraction of bees for which the dominant pattern of the spontaneous activity was significantly correlated with the odor-evoked pattern is given above each distribution. Data were sampled at 6 Hz.
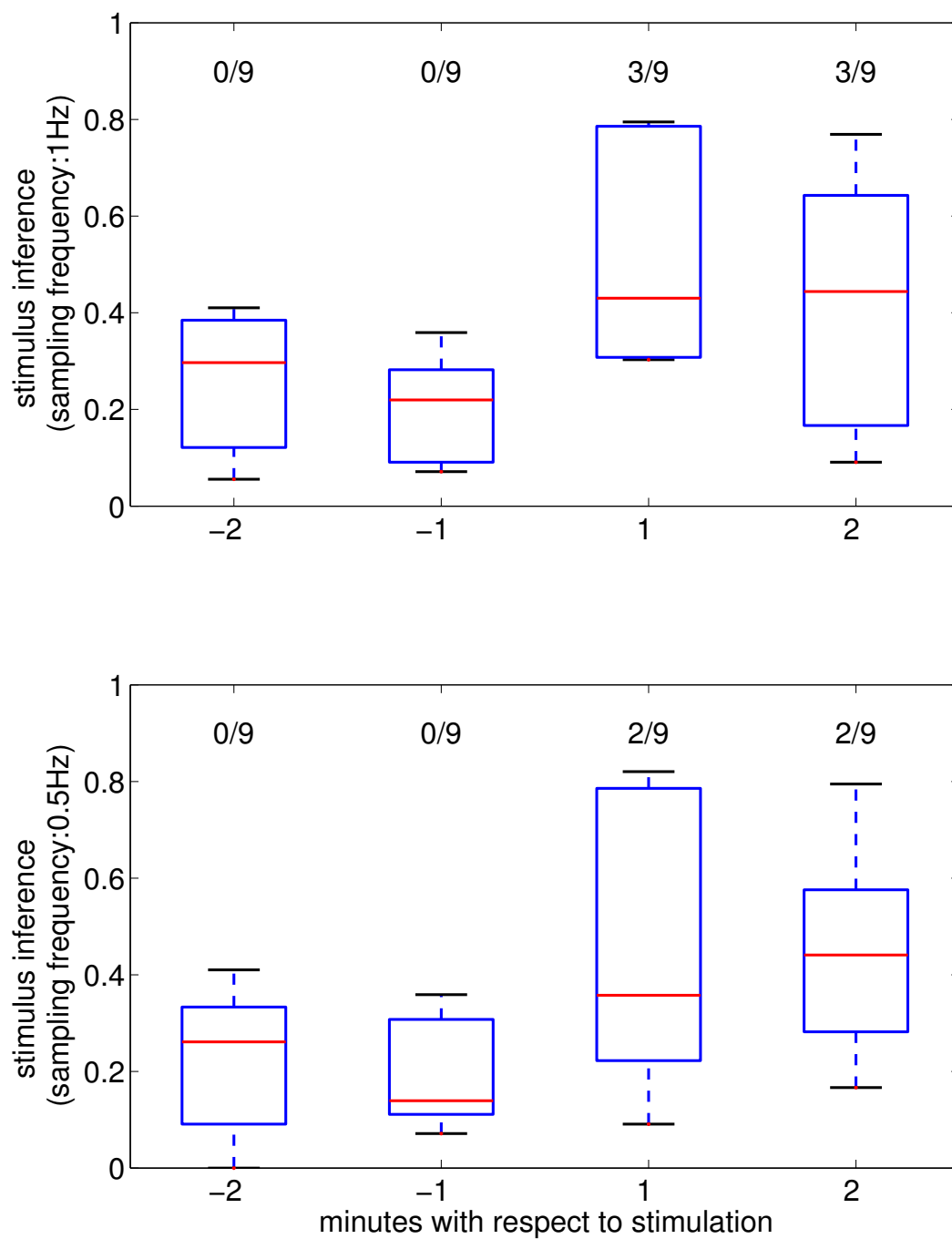
Figure 3.20: Time scale of the Hebbian mechanisms. Similar representation to Fig. 3.19 but here with downsampled data (top: 1 Hz; bottom: 0.5 Hz). The stimulus inference after stimulation decreases with lower temporal resolution
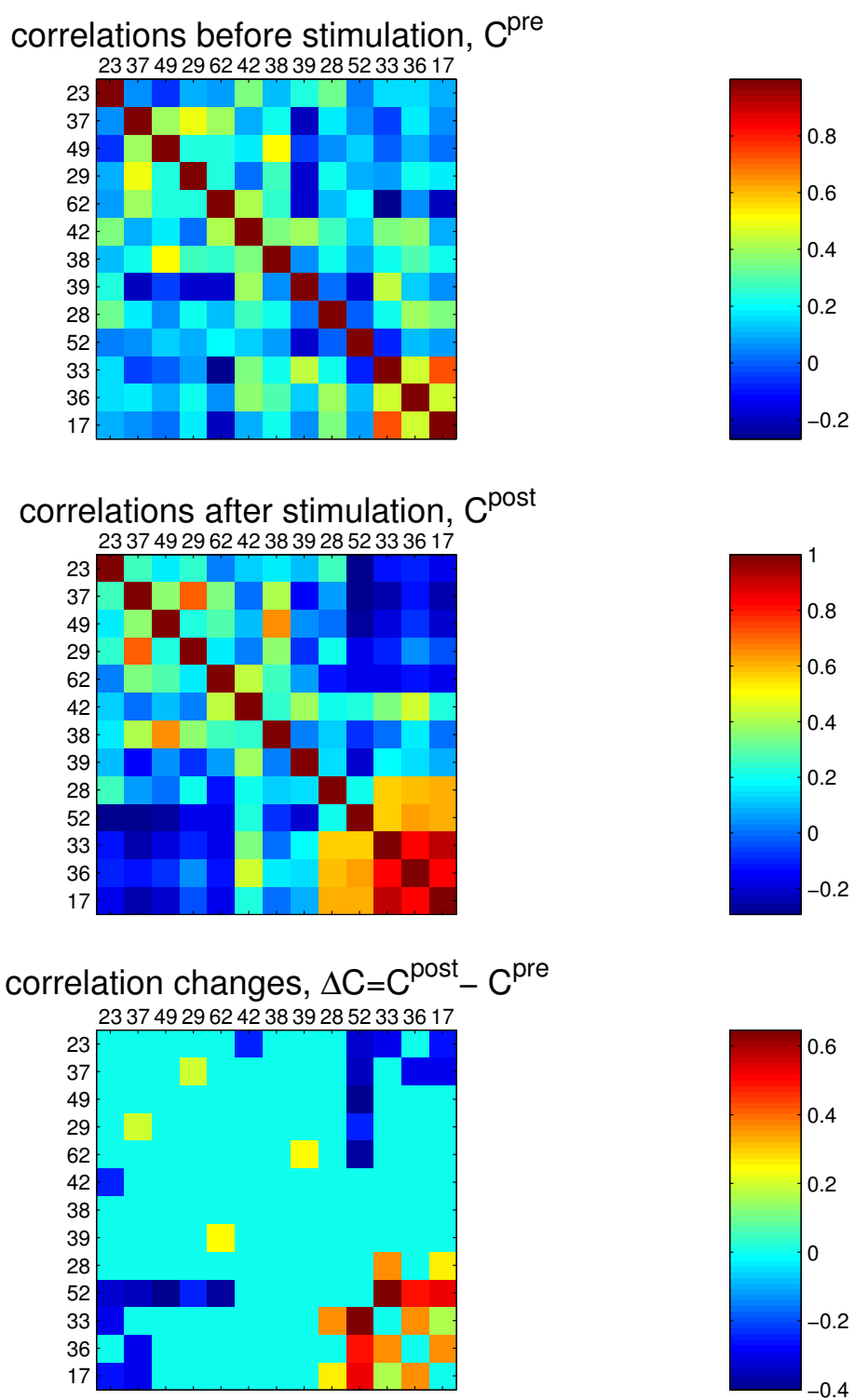
Figure 3.21: C^{pre}, C^{post} and ΔC in bee no. 1 with downsampled data at 0.5 Hz. Compare with Fig. 3.1, where the data were sampled at 6 Hz.
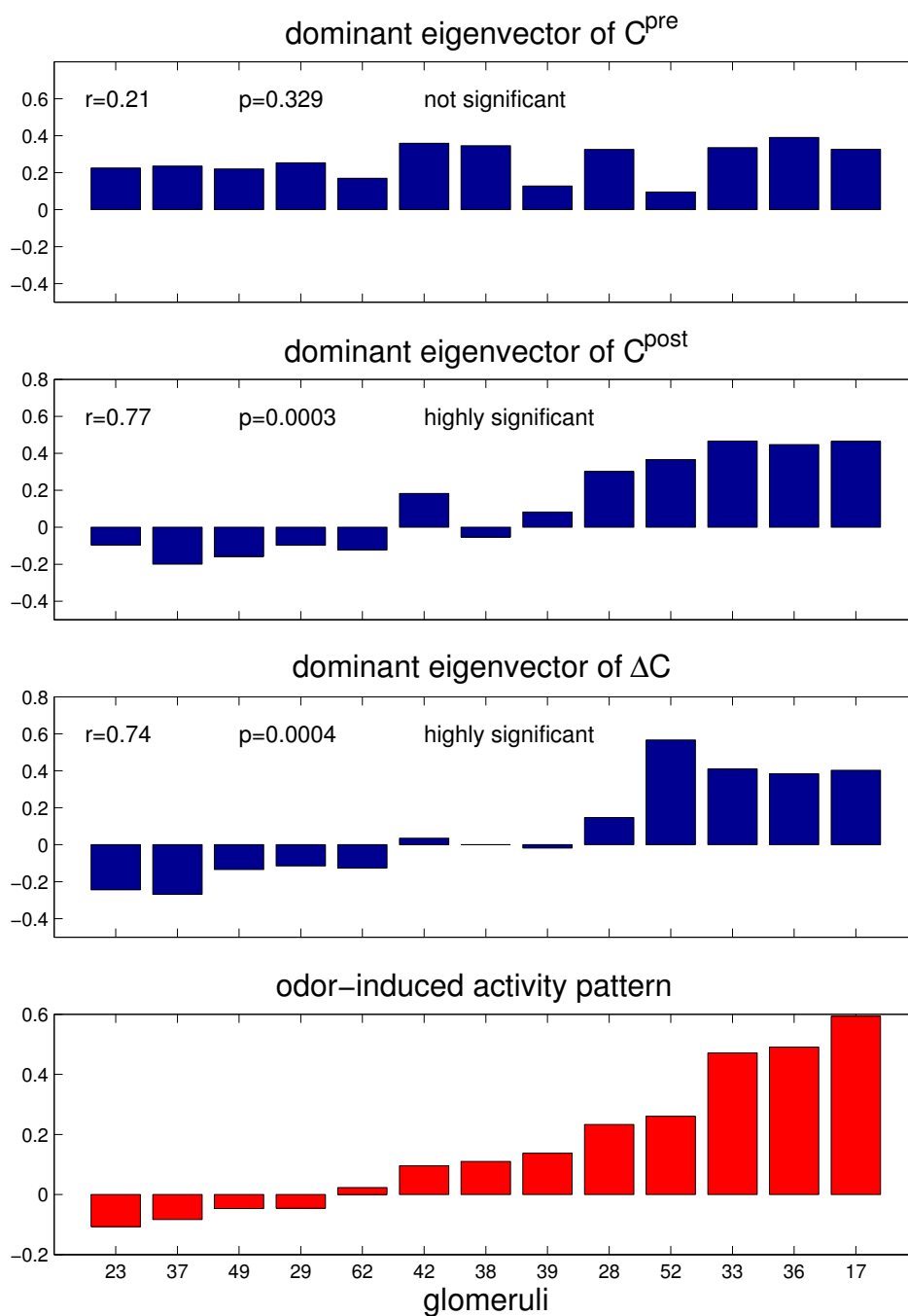
Figure 3.22: Eigenvectors and odor-evoked pattern in bee no. 1 with down-sampled data at 0.5 Hz. Compare with Fig. 3.10, where the data were sampled at 6 Hz. All patterns have unitary norm. The relative weight of the dominant eigenvalue was 25% for C^{pre}, 30% for C^{post} and 32% for ΔC.

3.4 Discussion

We have provided experimental evidence of the Hebbian hypothesis at the network level. We have shown that the information stored in the odor-induced changes of correlation between glomeruli suffices to retrieve the presented odors in 2/3 of the animals. The first principal component of the spontaneous activity after, but not before, stimulation also permits us to reconstruct the odor-evoked pattern. The quality of the reconstruction decreases in time. After one minute a succesful reconstruction is possible in only 1/3 of the bees.

Part of the information about the odor stored in the correlation, and changes of correlation between glomeruli, is also present at slow time-scales (0.5 Hz). The mechanism underlying the Hebbian effects we observe could rely on spike-timing changes along spike-trains or on variations of firing-rate synchrony.

We suggest that the pairwise changes of correlation between glomeruli reported here represent traces of a sensory memory that may result in a short-term memory in the antennal lobe and be consolidated as a long-term memory in the mushroom body, if the odor is paired with sucrose. These memory traces can be thought of as the "reverberations" postulated by Hebb (see section 3.2).

Following the experiments on working memory with monkeys reported in [Fuster and Alexander, 1971] and [Kubota and Niki, 1971], persistent neural activity after stimulation (delay activity) has been implicitly considered in neuroscience as *the* trace of working memory. Yet, as we have demontrated, a delay activity is not the only "reverberation" possible. In fact, according to Hebb, it is not an increase of activity what eventually leads to synaptic modification, but rather an increase of correlated activity.

Classical approaches have been limited to two, or at most a few, neurons. In contrast, the calcium-imaging data analyzed here contain information of projection neurons in several glomeruli. This has permitted us to provide evidence of the Hebbian hypothesis at the network level.

Chapter 4

Summary and Outlook

Two major novel results have been reported in this work. The first concerns olfactory coding and the second concerns sensory memory.

Considering olfactory coding we have demonstrated that the neural dynamics in the antennal lobe describe odor-specific trajectories during stimulation that converge to odor-specific attractors. The time interval to reach these attractors is, regardless of odor identity and concentration, approximately 800 ms. We have shown that support-vector machines, and in particular perceptrons provide a realistic and biological model of the interaction between the antennal lobe (coder) and the mushroom body (decoder). This model can also account for reaction-times of about 300 ms and for concentration invariance of odor perception.

Future research should expand our results on odor coding in at least two directions: First, it should be studied how odor-mixtures are encoded in the antennal lobe and how they are related to the encoded components of the mixture. Second, it is highly interesting to understand the relation between our findings with calcium-imaging data and the transient synchronization of oscillating neural assemblies reported by other authors in electrophysiological studies (see review in [Laurent et al., 2001]). The effort devoted to this question could also elucidate whether the olfactory code is a spike-based or a firing-rate-based neural code.

Regarding sensory memory we have shown that a single stimulation without reward induces changes of pairwise correlation between glomeruli in a Hebbian-like manner. We have demonstrated that those changes of correlation suffice to retrieve the last stimulus presented in 2/3 of the bees studied. Succesful retrieval decays to 1/3 of the bees within the second minute after stimulation. In addition, a principal-component analysis of the spontaneous activity revealed that the dominant pattern of the network during the spontaneous activity after, but not before stimulation, resembles the odor-induced

activity pattern in 2/3 of the bees studied. One can therefore consider the odor-induced (changes of) correlation as traces of a sensory memory or as Hebbian "reverberations".

There are at least two natural continuations of our studies on sensory memory: First, it should be tested whether a reinforced stimulus (stimulus + reward) allows for a higher ratio of successful retrieval. Second, it should be studied how a sequence of stimuli is stored in the antennal-lobe network. In particular, it would be interesting to check whether a considerable overlap between stored patterns impairs retrieval, as it is the case in a Hopfield network (see e.g. [Hertz et al., 1991]).

Appendix A

Experimental and Analytical Methods for Neural Dynamics and Odor Coding

Animal preparation and data recording

The preparation and calcium imaging of PNs was performed as described in [Sachse and Galizia, 2002]. Briefly, adult worker honeybees were caught and fixed in a plexiglas stage. Projection neurons were backfilled from the protocerebrum with the calcium-sensitive dye fura-dextran (potassium salt, 3000 MW, Molecular Probes, Eugene, USA). Imaging was done using a T.I.L.L. Photonics imaging system (Gräfelfing, Germany). For each measurement, a series of 60 double frames was taken at a sampling frequency of 6 Hz. The inter-stimulus interval was 40 s. Stimulation lasted 2 s in the experiments at fixed odor-concentration and 1 s in the experiments with varying concentration. Odors were delivered to the antennae using a custom-made and computer-controlled olfactometer. Odors tested: isoamylacetate, 1-hexanol, 1-octanol and 1-nonanol (Sigma-Aldrich, Deisenhofen, Germany). Neural responses were calculated as absolute changes of fluorescence ratio between 340 nm and 380 nm excitation light. Signals were attributed to identified glomeruli by reconstructing the glomerular structure in the fura ratio images. Glomeruli were identified on the basis of their morphological borderlines using a digital atlas of the antennal lobe of honeybee [Galizia et al., 1999]. In total 7 bees were studied in the experiments at constant concentration and 9 additional bees were studied in the experiments at varying concentration.

Data Analysis

At each point in time t the activity pattern of the AL-network is represented by a point in a multidimensional space in which each dimension corresponds to the calcium signal from one glomerulus. Depending on the bee, between 18 to 23 glomeruli could be identified. For the sake of simplicity, we will refer to this glomerular subspace as the AL-space. During an odor presentation the AL-activity draws an open curve in this multidimensional space. We firstly study the system's evolution along these trajectories. Since the data were sampled at a frequency of 6 Hz, the temporal resolution is $\Delta t = 0.167$ seconds. We denote as $\vec{r}_A(t)$ the trajectory triggered by odor A. To quantify the rate of activity changes, the velocity $v_A(t)$ of the activity state along the trajectories is used,

$$v_A(t) = \left| \frac{\Delta \vec{r}(t)}{\Delta t} \right| = \frac{|\vec{r}_A(t + \Delta t) - \vec{r}_A(t)|}{\Delta t}.$$

As a measure of the force causing changes of the neural activity patterns, we introduce the magnitude $a_A(t)$ of the acceleration vector,

$$a_A(t) = \frac{|\vec{v}_A(t + \Delta t) - \vec{v}_A(t)|}{\Delta t}.$$

The acceleration vector can be decomposed into a tangential component $a_{tA}(t)$ and a normal component $a_{nA}(t)$ relative to the trajectory. These two components are given by

$$a_{tA}(t) = \frac{|\vec{v}_A(t + \Delta t)| - |\vec{v}_A(t)|}{\Delta t}$$

and

$$a_{nA}(t) = \sqrt{|a_A(t)|^2 - |a_{tA}(t)|^2}.$$

The first component provides information about the amount of force parallel to the current trajectory, preserving the movement direction but changing the movement velocity. The second component measures the amount of force that leads to changes in the direction of the trajectory.

When analyzing the effects of odor-concentration on odor coding we use the mean run-path, which is defined as the mean length of the trajectories during stimulation, averaged across trials and bees at a given concentration. The length of a single trajectory is calculated as:

$$\text{run path} \equiv \sum_t |\Delta \vec{r}(t)|.$$

In addition to their detailed dynamical properties, we also study the reproducibility and specifity of the odor-driven trajectories. To this end we use perceptrons, which are a special case of support-vector machines (SVMs). A SVM [Vapnik, 1998, Burges, 1998, Boser et al., 1992] is an algorithm to calculate a certain manifold (hyperplane in the case of perceptrons) that divides a multidimensional space into two regions: the first region contains all points of a specified data set within the given data; the other region contains the remaining points. Let us call these regions I and II, respectively. A hyperplane is completely determined by a normalized orthogonal vector $\vec{w}$ and the distance $|b|$ to the origin. In fact, every point $\vec{x}_{hp}$ on the hyperplane satisfies:

$$\vec{w} \cdot \vec{x}_{hp} = b. \tag{A.1}$$

The optimal separating hyperplane between the two datasets is calculated by maximizing the margin with respect to the points of both regions. This mathematical problem can be turned into the minimization of a quadratic form in the positive quadrant. A separating hyperplane exists only if both datasets do not overlap. However, the minimization problem can be reformulated to tolerate some overlap and the calculation of an optimal separating hyperplane is also possible.

According to SVM-theory [Vapnik, 1998, Burges, 1998, Boser et al., 1992], the vector $\vec{w}$ that characterizes the separating hyperplane can always be expressed as a linear combination of the points which lie on the margin: the so-called "support vectors". Once $\vec{w}$ and b of the optimal hyperplane are known, it is straightforward to cast new data $\vec{x}$ into I or II according to the following criterion:

$$\text{if } \vec{w} \cdot \vec{x} > b, \ \vec{x} \text{ belongs to I}$$
$$\text{otherwise } \vec{x} \text{ belongs to II.} \tag{A.2}$$

As already mentioned, the SVM-algorithm can be extended to separating manifolds different from the hyperplane. This is done by applying appropriate coordinate transformations (expressed as kernel functions) which are equivalent to a change in the metric of the space under consideration, in our case the AL-space. The scalar product, whose associated separating manifold is the hyperplane, was among the tested kernels (scalar product, 2nd and 3rd order polynomial, gaussian and sigmoidal) the one that provided the best separation of odors. In other words, the perceptron was the most efficient SVM tested and is the one we chose for the analysis.

To quantify the ability of the SVM to classify an odor correctly, we use a measure called "classification performance". This measure is defined as the fraction of points cast into the correct region expressed as a percentage. It

yields 100% when the data set of a given odor does not overlap with the rest and yields less when it does.

When two datasets overlap the optimal separating hyperplane lies at the intersection and its orientation is very sensitive to the particular distribution of points there. In this case it is interesting to quantify the stability of the plane through the "generalization performance", defined as the relative number of points that can be singly removed without affecting the classification performance. A lower-bound estimator of the generalization performance is obviously the fraction of points that do not belong to the intersection (unambiguous patterns). The exact value of the generalization performance is calculated based on its definition, which represents a bootstrap or "leave-one-out" method [Efron and Tibshirani, 1993] commonly used to test SVMs [Boser et al., 1992]: Let A be the set of n points we want to separate from the rest. Let us now remove one point P of the set A and compute the separating hyperplane. We then check whether P falls into the correct region, i.e. the region where the other $n-1$ points of A lie. We repeat this procedure for all n points of A. The fraction of points successfully classified is expressed as a percentage and measures the generalization performance of an hyperplane. The average of the generalization performance for all odors (all separating hyperplanes) quantifies the reliability of the partition of the AL-space into odor-specific regions. We call this measure the "separability" of odors.

Separating any set of points from the rest of a given ensemble becomes a trivial task in a space of many dimensions. As the number of dimensions increases, it becomes easier to separate the data points. Equivalently, any subset of a small ensemble of points can typically be separated from the rest, even in a low-dimensional space. Therefore, before carrying out all SVM-analyses (classification performance, generalization performance and separability) we pool the data of the seven bees investigated. By doing this we do not only study the robustness of the olfactory code across trials but also across individuals.

In the experiments at fixed concentration 70 points were available in total, corresponding to the 4 different odors. Up to 8 common glomeruli could be identified in the 7 bees studied. Thus, the AL-space used for the SVM-analysis at fixed concentration has 8 dimensions.

In the experiments with varying concentration 156 points were available at each concentration, corresponding to the 4 different odors. Up to 7 common glomeruli could be identified in the 16 bees studied (7-dimensional AL-space).

Appendix B

Experimental and Analytical Methods for Sensory Memory and Hebbian Plasticity

Experimental Methods

Animal preparations, selective staining of projection neurons in the antennal lobe, signal estimation with calcium-imaging and glomerular identification were performed as described in Appendix A. Here, the spontaneous activity in the antennal lobe was recorded (sampling frequency: 6 Hz) during 2 minutes before and after one single, unrewarded odor presentation. The response of the antennal lobe to the odor was also recorded. Odor presentation lasted 4 seconds. The 4 seconds just before and just after odor presentation were cut out from the spontaneous activity to assure that the spontaneous activity does not contain any response to the odor. Stimuli used were 1-octanol 1-hexanol, limonene and a mixture of limonene and linanol (Sigma-Aldrich, Deisenhofen, Germany). In total 9 bees were studied.

Data Analysis

The raw data of the spontaneous activity presented non-reproducible drifts, mainly due to movement artifacts and calcium diffusion, that were removed with an off-line, high-pass filter (cutoff: 0.025 Hz). The filter also set the mean value of the spontaneous activity to zero.

The matrices C^{pre}, C^{post} and ΔC were calculated by applying bootstrap methods. The bootstrap is a computational technique to detect finite-size effects in estimated statistical quantities [Efron and Tibshirani, 1993]. Here,

it is applied as follows: we first estimate the probability distribution $p(\vec{x})$ of the recorded data and use it to generate 2000 new data sets with the same statistical properties (surrogate data). From each surrogate data set the correlation matrix is calculated according to (3.3) and (3.4). The distribution of each element C_{ij} is constructed and the median value is taken as the bootstrapped estimator of the C_{ij}. The calculation is done for the spontaneous activity before (C_{ij}^{pre}) and after (C_{ij}^{post}) stimulation. If the distributions of C_{ij}^{pre} and C_{ij}^{post} overlap 2.5% or less, then this change of correlation is considered as significant (95% significance level) and computed as:

$$\Delta C_{ij} = \mathrm{median}(C_{ij}^{post}) - \mathrm{median}(C_{ij}^{pre}).$$

Otherwise it is not considered as a significant change and we set $\Delta C_{ij} = 0$.

The quality of the stimulus retrieval is measured as the non-parametric Kendall's correlation coefficient r between the actual odor-evoked stimulus and the respective eigenvector. Kendall's correlation quantifies the agreement between the ranks of the values in both vectors. The rank is the occupied position after sorting the elements of each vector in increasing order. Following the "Numerical Recipes in C" [Press et al., 1992], to define r we start with the n data points (x_i, y_i). Now consider all $n(n-1)/2$ pairs of data points, where a data point cannot be paired with itself, and where the points in either order count as one pair. A pair is called concordant (con) if the relative ordering of the ranks of the two $x's$ is the same as the relative ordering of the ranks of the two $y's$. A pair is called discordant (dis) if the relative ordering of the ranks of the two $x's$ is opposite from the relative ordering of the ranks of the two $y's$. If the ranks of the two $x's$ or the ranks of the two $y's$ are equal, then we do not call the pair neither concordant nor discordant. If the $x's$ have equal ranks, we will call the pair an extra-y pair. If the ranks of the two $y's$ are equal, we will call the pair an extra-x pair. If ranks of the two $x's$ and the two $y's$ are equal, we do not consider this pair. Kendall's correlation is then calculated from these various counts as:

$$r = \frac{\mathrm{con} - \mathrm{dis}}{\sqrt{\mathrm{con} + \mathrm{dis} + \text{extra-}y} \cdot \sqrt{\mathrm{con} + \mathrm{dis} + \text{extra-}x}},$$

Kendall's correlation and the correlation coefficient yield close values. We chose Kendall's correlation because, contrary to the correlation coefficient, it allows us to give a significance level of the correlation. The p-value is given by

$$p = \mathrm{erfc}\left(\frac{|r|}{\sigma\sqrt{2}}\right), \quad \text{with} \quad \sigma^2 = \frac{4n + 10}{9n(n-1)},$$

where $\mathrm{erfc}(x)$ is the complementary error function.

Bibliography

[Beckerman, 1995] Beckerman, M. (1995). *Adaptive cooperative systems.* John Wiley & Sons.

[Bhagavan and Smith, 1997] Bhagavan, S. and Smith, B. (1997). Olfactory conditioning in the honeybee, *apis mellifera*: Effects of odor intensity. *Physiology & Behavior*, 61:107–117.

[Bliss and Lomo, 1973] Bliss, T. and Lomo, T. (1973). Long-lasting potentiation of synaptic transmission in the dentate area of the anaesthetized rabbit following stimulation of the perforant path. *J. Physiol.*, 232(2):331–56.

[Boser et al., 1992] Boser, B. E., Guyon, I., and Vapnik, V. (1992). A training algorithm for optimal margin classifiers. In *Computational Learing Theory*, pages 144–152. Available at http://citeseer.nj.nec.com/boser92training.html.

[Brody and Hopfield, 2003] Brody, C. and Hopfield, J. (2003). Simple networks for spike-timing-based computation, with application to olfactory processing. *Neuron*, 37:847–852.

[Burges, 1998] Burges, C. J. C. (1998). A tutorial on support vector machines for pattern recognition. *Data Mining and Knowledge Discovery*, 2(2):121–167. Available at http://citeseer.nj.nec.com/burges98tutorial.html.

[Chittka et al., 1997] Chittka, L., Gumbert, A., and Kinze, J. (1997). Foraging dynamics of bumblebees: correlates of movements within and between plant species. *Behav. Ecol*, 8:239–249.

[DeFelipe and Jones, 1988] DeFelipe, J. and Jones, E. (1988). *Cajal on the Cerebral Cortex*. Oxford University Press.

[Dujardin, 1850] Dujardin, F. (1850). Mémoire sur le système nerveux des insectes. *Ann. Sci. Nat. Zool.*, 14:195–206.

[Efron and Tibshirani, 1993] Efron, B. and Tibshirani, R. (1993). *An Introduction to the Bootstrap*. Chapman and Hall.

[Eisthen, 2002] Eisthen, H. (2002). Why are olfactory systems of different animals so similar. *Brain, Behavior and Evolution*, 59:273–293.

[Erber, 1976] Erber, J. (1976). Retrograde amnesia in honeybees (*apis mellifera carnica*). *J Comp Physiol*, 99:231–242.

[Erber et al., 1980] Erber, J., Masuhr, T., and Menzel, R. (1980). Localization of short-term memory in the brain of the bee, *apis mellifera. Physiol Entomol*, 5:343–358.

[Freeman, 1988] Freeman, W. J. (1988). Strange attractors that govern mammalian brain dynamics shown by trajectories of electroencephalographic (eeg) potential. *IEEE Transactions on Circuits and Systems*, 35(7).

[Freeman, 1991] Freeman, W. J. (1991). The physiology of perception. *Scientific American*, 264(2)(2):78–85.

[Freeman, 1994] Freeman, W. J. (1994). Neural networks and chaos. *J. Theoretical Biology*, 171:13–18.

[Friedrich and Laurent, 2001] Friedrich, R. W. and Laurent, G. (2001). Dynamic optimization of odor representations by slow temporal patterning of mitral cell activity. *Science*, 291:889–894.

[Fuster and Alexander, 1971] Fuster, J. and Alexander, G. (1971). Neuron activity related to short-term memory. *Science*, 173:652–654.

[Galizia et al., 1999] Galizia, C. G., McIlwrath, S. L., and Menzel, R. (1999). A digital three-dimensional atlas of the honeybee antennal lobe glomeruli based on optical sections acquired using confocal microscopy. *Cell and Tissue Research*, 295:383–394.

[Gao et al., 2000] Gao, Q., Yuan, B., and Chess, A. (2000). Convergent projections of drosophila olfactory neurons to specific glomeruli in the antennal lobe. *Nature Neurosci.*, 3(8):780–785.

[Gerstner, 2002] Gerstner, W. (2002). Mathematical formulations of hebbian learning. *Biol. Cybern.*, 87:404–415.

[Grassberger and Procaccia, 1983] Grassberger, P. and Procaccia, I. (1983). Characterization of strange attractors. *Phys. Rev. Lett.*, 50:346–349.

[Hammer, 1993] Hammer, M. (1993). An identified neuron mediates the unconditioned stimulus in associative olfactory learning in honeybees. *Nature*, 366:59–63.

[Hammer, 1997] Hammer, M. (1997). The neural basis of associative reward learning in honeybees. *Trends. Neurosci.*, 20:245–252.

[Hammer and Menzel, 1995] Hammer, M. and Menzel, R. (1995). Learning and memory in the honeybee. *J. Neurosci.*, 15(3):1617–1630.

[Hammer and Menzel, 1998] Hammer, M. and Menzel, R. (1998). Multiple sites of associative odor learning as revealed by local brain microinjections of octopamine in honeybees. *Learn. Mem.*, 5:146–156.

[Hebb, 1949] Hebb, D. (1949). *The organization of behavior: A neuropsychological theory.* John Wiley & sons.

[Hegger et al., 1998] Hegger, R., Kantz, H., and Olbrich, E. (1998). Problems in the reconstruction of highdimensional deterministic dynamics from time series. In H.Kantz, Kurths, J., and G.Mayer-Kress, editors, *Nonlinear Analysis of Physiological Data*, pages 23–47. Springer.

[Heisenberg, 1998] Heisenberg, M. (1998). What do the mushroom bodies do for the insect brain? *Learn. Mem.*, 5:1–10.

[Hertz et al., 1991] Hertz, J., Krogh, A., and Palmer, R. G. (1991). *Introduction to the Theory of Neural Computation.* A Lecture Notes Volume in the Santa Fe Institute Studies in the Science of Complexity. Perseus Books.

[Hildebrand and Shepherd, 1997] Hildebrand, J. G. and Shepherd, G. M. (1997). Mechanisms of olfactory discrimination: Converging evidence for common principles across phyla. *Annu. Rev. Neurosci.*, 20:595–631.

[Honerkamp, 1993] Honerkamp, J. (1993). *Stochastic Dynamical Systems. Concepts, Numerical Methods, Data Analysis.* VCH Publishers.

[Joerges et al., 1997] Joerges, J., Küttner, A., Galizia, C. G., and Menzel, R. (1997). Representation of odours and odour mixtures visualized in the honeybee brain. *Nature*, 387:285–288.

[Klopfer, 1973] Klopfer, P. H. (1973). *An introduction to animal behavior.* Prentice-Hall.

[Korsching, 2002] Korsching, S. (2002). Olfactory maps and odor images. *Curr Opin Neurobiol*, 12(4):387–392.

[Kubota and Niki, 1971] Kubota, K. and Niki, H. (1971). Prefrontal cortical unit activity and delayed alternation performance in monkeys. *J. Neurophysiol.*, 34(3):337–47.

[Laurent, 1996] Laurent, G. (1996). Dynamical representation of odors by oscillating and evolving neural assemblies. *Trends Neurosci.*, 19:489–496.

[Laurent, 2002] Laurent, G. (2002). Olfactory network dynamics and the coding of multidimensional signals. *Nat Rev Neurosci*, 3(11):884–895.

[Laurent and Davidowitz, 1994] Laurent, G. and Davidowitz, H. (1994). Encoding of olfactory information with oscillating neural assemblies. *Science*, 265:1872–1875.

[Laurent et al., 2001] Laurent, G., Stopfer, M., Friedriech, R. W., Rabinovich, M. I., Volkovskii, A., and Abarbanel, H. D. (2001). Odor encoding as an active, dynamical process: Experiments, computation and theory. *Annu. Rev. Neurosci.*, 24:263–97.

[Laurent et al., 1996] Laurent, G., Wehr, M., and Davidowitz, H. (1996). Temporal representations of odors in an olfactory network. *J. Neurosci.*, 16:3837–3847.

[Lei et al., 2002] Lei, H., Christensen, T. A., and Hildebrand, J. G. (2002). Local inhibition modulates odor evoked synchronization of glomerulus specific output neurons. *Nature Neuroscience*, 5(6):557–565.

[Levitan and Kaczmarek, 1997] Levitan, I. B. and Kaczmarek, L. K. (1997). *The Neuron. Cell and Molecular Biology.* Oxford University Press, 2nd edition.

[Li and Hertz, 2000] Li, Z. and Hertz, J. (2000). Odor recognition and segmentation by a model olfactory bulb and cortex. *Computation in Neural Systems*, 11:83–102.

[Ljung and Ljung, 1998] Ljung, L. and Ljung, E. (1998). *System Identification: Theory for the User.* Prentice Hall Information and System Science Series. Pearson Education, 2nd edition.

[McCullagh, 1987] McCullagh, P. (1987). *Tensor Methods in Statistics.* Monographs on statistics and applied probability. Chapman and Hall.

[Menzel, 1985] Menzel, R. (1985). Learning in honeybees in an ecological and behavioral context. In Höldobler, B. and Lindauer, M., editors, *Experimental behavioral ecology*, pages 55–77. Fischer, Stutugart.

[Menzel, 1999] Menzel, R. (1999). Memory dynamics in the honeybee. *J Comp Physiol A*, 185:323–340.

[Menzel and Müller, 1996] Menzel, R. and Müller, U. (1996). Learning and memory in honeybee: from behavior to neural substrates. *Annu. Rev. Neurosci.*, 19:379–404.

[Oleskevich et al., 1997] Oleskevich, S., Clements, J., and Srinivasan, M. (1997). Long-term synaptic plasticity in the honeybee. *J. Neurophysiol.*, 78:528–532.

[Packard et al., 1979] Packard, N. H., Crutchfield, J. P., Farmer, J. D., and Shaw, R. S. (1979). Geometry from a time series. *Phys. Rev. Lett.*, 45:712–716.

[Pavlov, 1927] Pavlov, I. P. (1927). *Conditioned Reflexes: An investigation of the physiological activity of the cerebral cortex.* Oxford University Press.

[Pérez-Orive et al., 2002] Pérez-Orive, J., Mazor, O., Turner, G. C., Cassenaer, S., Wilson, R. I., and Laurent, G. (2002). Oscillations and sparsening of odor representations in the mushroom body. *Science*, 297:359–365.

[Press et al., 1992] Press, W. H., Teukolsky, S. A., Vetterling, W. T., and Flannery, B. P. (1992). *Numerical Recipes in C. The Art of Scientific Cumputing. Second Edition.* Cambridge University Press.

[Priestley, 1996] Priestley, M. B. (1996). *Spectral Analysis and Time Series.* Probability and Mathematical Statistics. Academic Press.

[Rabinovich et al., 2001] Rabinovich, M., Volkovskii, A., Lecanda, P., Huerta, R., Abarbanel, H., and Laurent, G. (2001). Dynamical encoding by networks of competing neuron groups: Winnerless competition. *Phys. Rev. Lett.*, 87(6):68102.

[Ramón y Cajal, 1890] Ramón y Cajal, S. (1890). Origen y terminación de las fibras nerviosas olfatorias. *Gaz. Sanit. Barcelona*, pages 1–21.

[Ramón y Cajal, 1891] Ramón y Cajal, S. (1891). Significación fisiológica de las expansiones protoplasmáticas y nerviosas de la sustancia gris. *Revista de Ciencias Médicas de Barcelona*, 22:23.

[Ramón y Cajal, 1894] Ramón y Cajal, S. (1894). La fine structure de centres nerveux. *The Croonian Lecture, Proc. Roy. Soc. Lond.*, 55:443–468.

[Reif, 1965] Reif, F. (1965). *Fundamentals of Statistical and Thermal Physics*. McGraw-Hill.

[Rosenblatt, 1962] Rosenblatt, F. (1962). *Principles of Neurodynamics*. New York: Spartan.

[Rumelhart and McClelland, 1986] Rumelhart, D. E. and McClelland, J. L. (1986). *Parallel Distributed Processing. Explorations in the Microstructure of Cognition*, volume 1: Foundations. The MIT Press.

[Sachse and Galizia, 2002] Sachse, S. and Galizia, C. G. (2002). Role of inhibition for temporal and spatial odor representation in olfactory output neurons: A calcium imaging study. *Journal of Neurophysiology*, 87:1106–1117.

[Sakmann and Neher, 1995] Sakmann, B. and Neher, E. (1995). *Single-Channel Recordings*. New York: Plenum, 2nd edition.

[Seung, 2000] Seung, H. S. (2000). Half a century of hebb. *Nat. Neurosci.*, 3:1166.

[Stopfer et al., 2003] Stopfer, M., Jayaraman, V., and Laurent, G. (2003). Intensity versus identity coding in an olfactory system. *Neuron*, 39:991–1004.

[Stopfer and Laurent, 1999] Stopfer, M. and Laurent, G. (1999). Short-term memory in olfactory network dynamics. *Nature*, 402:664–668.

[Strausfeld, 1976] Strausfeld, N. (1976). *Atlas of an insect brain*. Springer.

[Strausfeld et al., 1998] Strausfeld, N., Hansen, L., Li, Y., Gómez, R., and K.Ito (1998). Evolution, discovery, and interpretations of arthropod mushroom bodies. *Learn. Mem.*, 5:11–37.

[Szyszka, 1999] Szyszka, P. (1999). *Extrazelluläre Doppelableitungen im Gehirn der Biene: Oszillatorische und synchrone Erregungsmuster in den Pilzkörpern*. Institut für Neurobiologie. Freie Universität Berlin.

[Takens, 1981] Takens, F. (1981). Detecting strange attractors in turbulence. *Lecture Notes in Math.*, 898.

[Tsodyks et al., 1999] Tsodyks, M., Kenet, T., Grinvald, A., and Arieli, A. (1999). Linking spontaneous activity of single cortical neurons and the underlying functional architecture. *Science*, 286:1943.

[Turin, 1996] Turin, L. (1996). A spectroscopic mechanism for primary olfactory reception. *Chemical Senses*, 21(6):773–791.

[Turin, 2002] Turin, L. (2002). A method for the calculation of odor character from molecular strucutre. *J. theor. Biol.*, 216:367–385.

[Vapnik, 1998] Vapnik, V. (1998). *Statistical Learning Theory*. John Wiley & Sons.

[von Frisch, 1993] von Frisch, K. (1993). *Aus dem Leben der Bienen*. Springer, 10th edition.

[Wehr, 1999] Wehr, M. (1999). *Oscillatory sequences of firing in the locust olfactory system: mechanisms and functional significance*. PhD thesis, California Institute of Technology. Available at http://www.cns.caltech.edu/∼mike/thesis.html.

[Wehr and Laurent, 1996] Wehr, M. and Laurent, G. (1996). Odor encoding by temporal sequences of firing in oscillating neural assemblies. *Nature*, 384:162–166.

[Wilson and Cowan, 1972] Wilson, H. and Cowan, J. (1972). Excitatory and inhibitory interaction in localized population of model neurons. *Biophys J*, 12:1–24.

Acknowledgements

I am very thankful to Prof. Andreas Herz for making possible my research and training at the Institute for Theoretical Biology of the Humboldt University. I am also very grateful to Dr. Giovanni Galizia who was the promotor of the collaborations with Dr. Silke Sachse and Dipl.-Biol. Marcel Weidert at the Institute for Neurobiology of the Free University that led to the results reported in this work. It has been a great pleasure to work with all of them.

I proudly thank the land of Berlin for having supported my research with a NaFöG-grant for two years.

During the time I have been working at the Institute for Theoretical Biology I have met many colleagues with whom I spent many good moments. I will miss the exciting lunch-time discussions, ranging from politics to the theory of evolution, with the Mensa-Nord connection: Arndt Telschow, Edward Hagen, Roland Schaette, Samuel Glauser, Tim Opperman, Florian Geier and Matthias Flor. I will also happily remember Susanne Schreiber, Martin Stemmler, Szymon Kiełbasa, Maciej Swat and Raphael Ritz who were there from the very beginning for scientific discussions as well as for a coffee or cake. My colleagues Martin Stemmler and Edward Hagen helpfully discussed with me an early version of this manuscript.

Now that my time in Berlin is running out, I fondly remember the many cheerful evenings in the warm company of the Familie Rose-Maaß. I hope we will have many more in the future.

In these moments, when I am about to finish a period of my life and start a new one, I specially think of my parents, who encouraged and trusted me also in the distance.

Finally, I want to express my gratitude to Elke Binder, my wife-to-be, who I first met when she was writing her Diploma-Thesis at the Institute for Theoretical Biology. She is the reason why this work came to an end.

Deutsche Zusammenfassung

In dieser Arbeit werden die neuronale sensorische Kodierung und die sensorische Gedächtnisbildung am Beispiel des olfaktorischen Systems der Honigbiene erforscht. Die dargestellten Befunde basieren auf der Auswertung und Interpretation von Calcium-Imaging Daten, die von Dr. Silke Sachse und Dipl.-Biol. Marcel Weidert am Institut für Neurobiologie der Freien Universität Berlin abgeleitet wurden.

Im ersten Kapitel wird eine für die Neurowissenschaften interessante Eigenschaft des Riechsystems vorgestellt: Die auffallend ähnliche Struktur des Riechsystems in mehreren Zweigen der Phylogenie - u.a. bei den Säugetieren und den Arthropoden - deutet darauf hin, dass die Duftinformation nach einem universellen Verfahren von Neuronen ver- und entschlüsselt wird. Daneben wird das olfaktorische System der Honigbiene als Prototyp eines neuronalen Netzwerkes dargestellt, in dem die globale neuronale Dynamik erforscht werden kann.

Im zweiten Kapitel wird untersucht, wie olfaktorische Reize in neuronale Aktivität umgesetzt werden. Anhand der Auswertung experimenteller Daten wird festgestellt, dass die neuronale Aktivität im primären olfaktorischen Netzwerk (Antennal Lobus) der Honigbiene nach ca. 800 ms ein stabiles räumliches Muster bildet, das duftspezifisch ist. Solche Muster sind nicht nur bei der selben Biene reproduzierbar, sondern bei allen Bienen. Darüber hinaus wird gezeigt, dass die räumlichen Muster der neuronalen Aktivität nicht nur unabhängig vom Duft, sondern auch von der Konzentration nach ca. 800 ms bis zum Ende der Stimulation stabil bleiben. Die Muster sind duftspezifisch, obwohl sie sich für einen bestimmten Duft mit steigender Konzentration kontinuierlich ändern. Diese zuverlässige Abbildung der Düfte in räumliche neuronale Aktivität im Antennal Lobus könnte der olfaktorischen Kodierung zugrunde liegen.

Anhand einer auf Support-Vector-Machines basierenden Analysemethode ist es auch möglich zu erklären, wie die im Antennal Lobus verschlüsselte Information von benachbarten neuronalen Netzwerken (insbesondere dem Pilzkörper) entschlüsselt werden kann. Die Support-Vector Machine ist mathematisch betrachtet ein Algorithmus zur Datenklassifizierung, der sich auch als Netzwerk zweier Neuronenschichten implementieren lässt. Biologisch betrachtet entsprechen solche Schichten beim Riechsystem der Insekten dem Antennal Lobus und dem Pilzkörper.

Im dritten Kapitel wird mit Hilfe einer Korrelationsanalyse der spontanen Aktivität im Antennal Lobus ein Hebbscher Mechanismus bewiesen, der zur Gedächtnisbildung führen kann. Insbesondere wird gezeigt, dass sich die paarweisen Korrelationen zwischen Glomeruli nach der Duftstimulation dem Hebbschen Postulat folgend verändern. Solche duftinduzierten Korrelationsveränderungen können als Spuren der "Erinnerung an den Duft" betrachtet werden, da sie allein genügen, um das letzte duftinduzierte Aktivitätsmuster innerhalb von zwei Minuten nach der Duftgabe nachzubilden. Dies ist bei 2/3 der untersuchten Bienen reproduzierbar. Darüber hinaus wird gezeigt, dass die erste Hauptkomponente der spontanen Aktivität nach, aber nicht vor der Stimulation, das duftinduzierte Aktivitätsmuster bei 2/3 der untersuchten Bienen nachbildet.

Lebenslauf

1975	Geboren am 26. März in Madrid.
1979 - 1989	Grundschule "El Porvenir", Madrid.
1989 - 1993	Gymnasium "Lope de Vega", Madrid.
1993 - 1998	Studium der deutschen Sprache und Landeskunde am Goethe-Institut in Madrid.
1993 - 1999	Physikstudium an der Universidad Autónoma de Madrid.
1997	Praktikum am Deutschen Elektronen-Synchrotron (DESY) in Hamburg.
1998	Sommerschule zur Theorie Neuronaler Netzwerke an der Universidad Nacional a Distancia (UNED) in Ávila, Spanien.
1998	Workshop zur modernen Optik am "Consejo Superior de Investigaciones Científicas" (CSIC), in Madrid.
1998 - 1999	Aufbaustudium zu Theorie und Anwendungen der Methode Finiter Elemente an der Universidad Autónoma de Madrid.
1999 - 2000	Erasmus Stipendiat in Berlin. Anfertigung einer schriftlichen Arbeit ("Statistische Analyse von lokalen Feldpotentialen im olfaktorischen System der Honigbiene") am Institut für Biologie der Humboldt Universität zu Berlin für die Zulassung zur Promotion.
2000	Workshop "Analysis of Neural Data" (WAND 2000) am Marine Biological Laboratory in Woods Hole MA.
2001	Workshop "Dynamics of Neural Networks" an der University of California, Santa Barbara (UCSB)
Seit 2000	Doktorand am Institut für Theoretische Biologie der Humboldt Universität zu Berlin in der Arbeitsgruppe von Prof. Dr. Andreas V. M. Herz.

Veröffentlichungen

Journals

Roberto Fdez. Galán, Silke Sachse, C. Giovanni Galizia and A. V. M. Herz (2004). Odor-Driven Attractor Dynamics in the Antennal Lobe Allow for Simple and Rapid Odor Classification. *Neural Computation* 16, p.1-14.

R. Fdez. Galán, R. Ritz, P. Szyszka and A. V. M. Herz (im Druck). Uncovering short-time correlations between multichannel recordings of brain activity. *International Journal of Bifurcations and Chaos*, Vol. 14(2).

R. Ritz, R. Fdez. Galán, P. Szyszka and A. V. M. Herz (2001). Analysis of odor processing in the mushroom bodies of the honeybee. *Neurocomputing* 38-40, p.313-318.

Abstracts und Tagungsbeiträge

R. Fdez. Galán, M. Weidert, A. V. M. Herz, R. Menzel and C. G. Galizia (2003). Dissecting the olfactory code: A working memory trace in the bee antennal lobe. *Zweites Symposium der Volkswagenstiftung über "Dynamics and Adaptivity of Neuronal Systems. Integrative Approaches to Analyzing Cognitive Functions".*

R. Fdez. Galán, S. Sachse, C. G. Galizia and A. V. M. Herz (2003). Odor-driven Calcium Dynamics in the Antennal Lobe of Honeybee: A Hypothesis about the Olfactory Code. *Proceedings of the 29th Göttingen Neurobiology Conference.*

M. Weidert, R. Fdez. Galán, C. G. Galizia, A. V. M. Herz and R. Menzel (2003). Odor stimulation induces changes of correlation between glomeruli in the Antennal Lobe of the Honeybee. *Proceedings of the 29th Göttingen Neurobiology Conference.*

R. Fdez. Galán, R. Ritz, P. Szyszka and A. V. M. Herz (2002). Detecting Correlations in Multisite Recordings of Nonstationary Brain Activity. *Attractors, Signals and Synergetics: Proceedings of the 1st European Interdisciplinary School on Nonlinear Dynamics for System and Signal Analysis (Euroattractor 2000).* W. Klonowski (Editor). Pabst Science Publishers.

R. Fdez. Galán, R. Ritz, P. Szyszka and A.V.M. Herz (2001). Detecting Correlations between Nonstationary Brain Signals. *Proceedings of the 28th Göttingen Neurobiology Conference.*

Selbständigkeitserklärung

Hiermit erkläre ich, die vorliegende Arbeit selbständig ohne fremde Hilfe verfaßt und nur die angegebene Literatur und Hilfsmittel verwendet zu haben.

Roberto Fernández Galán
6. Oktober 2003